



1997

## Ionic Interaction Studies of Bovine Copper, Zinc-Superoxide Dismutase

Hanan A. Hasan  
*Loyola University Chicago*

Follow this and additional works at: [https://ecommons.luc.edu/luc\\_diss](https://ecommons.luc.edu/luc_diss)

 Part of the [Chemistry Commons](#)

---

### Recommended Citation

Hasan, Hanan A., "Ionic Interaction Studies of Bovine Copper, Zinc-Superoxide Dismutase" (1997).  
*Dissertations*. 3711.  
[https://ecommons.luc.edu/luc\\_diss/3711](https://ecommons.luc.edu/luc_diss/3711)

This Dissertation is brought to you for free and open access by the Theses and Dissertations at Loyola eCommons. It has been accepted for inclusion in Dissertations by an authorized administrator of Loyola eCommons. For more information, please contact [ecommons@luc.edu](mailto:ecommons@luc.edu).



This work is licensed under a [Creative Commons Attribution-Noncommercial-No Derivative Works 3.0 License](#).  
Copyright © 1997 Hanan A. Hasan

LOYOLA UNIVERSITY OF CHICAGO

**IONIC INTERACTION STUDIES OF BOVINE  
COPPER, ZINC-SUPEROXIDE DISMUTASE**

A DISSERTATION SUBMITTED TO  
THE FACULTY OF THE GRADUATE SCHOOL  
IN CANDIDACY FOR THE DEGREE OF  
DOCTOR OF PHILOSOPHY

DEPARTMENT OF CHEMISTRY

BY

HANAN A. HASAN

CHICAGO, ILLINOIS

MAY 1997

*Copyright by Hanan Hasan, 1997*

*All Rights Reserved*

## ACKNOWLEDGMENTS

I am extremely grateful to my mentor Dr. Duarte Mota de Freitas for his excellent and brilliant guidance and generous financial support. I am also thankful to Dr. de Freitas for his patience and encouragement during this study.

My sincere gratitude to our collaborator Dr. William E. Antholine (Medical College of Wisconsin, Milwaukee) for his help and guidance with EPR experiments and data analysis. I would also like to thank Dr. Chris Felix (Medical College of Wisconsin, Milwaukee) for his help with the same experiments.

I am grateful to my committee members, Dr. Patrick Henry, Dr. David Crumrine and Dr. Mir Shamsuddin for their time and suggestions during the course of this work. I would like to thank Dr. Alanah Fitch and Dr. Yunlong Wang for their assistance with cyclic voltammetry experiments. I would also like to thank Dr. Kenneth Olsen for allowing me to use the electrophoresis equipment in his laboratory.

My sincere gratitude to my precious husband Arab for his encouragement, support, and patience during this study. I would also like to thank my twin brother Dr. Mohammad Hasan (Jordan University of Science and Technology) who I stayed with for several years in the United States for his positive contribution to my life during the period of research. I would like to thank my family in Jordan who have waited patiently until I

finished my dissertation. Special thanks to my uncle Mahmoud Bazzi for his generous financial support and encouragement.

I sincerely thank my lab mates Joyce Nikolakopoulos, Cherian Zachariah, Louis Amari, Wanrong Lin, Yuling Chi, Chandra Srinivasan, Qinfen Rong for their cooperation and suggestions. My sincere gratitude to Joyce Nikolakopoulos and Cherian Zachariah for their helpful cooperation in the lab.

I would like to thank my colleagues in the Department of Chemistry, Joseph Brunzelle, Dr. Naser Qutaishat, Dr. Nick Menhart, Dr. Othman Hamed, and John Rost for their help.

*TO MY LOVELY HUSBAND ARAB,  
MY PARENTS, BROTHERS, SISTERS  
and UNCLE MAHMOUD BAZZI*

## TABLE OF CONTENTS

<b>ACKNOWLEDGEMENTS</b>	<b>.....iii</b>
<b>LIST OF FIGURES</b>	<b>.....xi</b>
<b>LIST OF TABLES</b>	<b>.....xiii</b>
<b>LIST OF ABBREVIATIONS</b>	<b>.....xv</b>
<b>CHAPTER</b>	
<b>I. INTRODUCTION</b>	<b>.....1</b>
I.1. Background on Cu, Zn-SOD	.....1
I.2. Structure of Cu, Zn-SOD	.....3
I.3. Function of Cu, Zn-SOD	.....10
I.4. SOD Activity Assay Methods	.....12
I.5. Roles of Negatively and Positively Charged Residues in Cu, Zn-SOD	.....13
I.6. Anion Binding to Cu, Zn-SOD	.....17
I.7. Cation Binding to Cu, Zn-SOD	.....21
I.8. Stability of Cu, Zn-SOD	.....22
I.9. Metal-Substituted Derivatives of Cu, Zn-SOD	.....23
I.10. Modification of Carboxylate Groups in Proteins	.....24
I.11. Vanadium in Biological Systems	.....26

<b>II. STATEMENT OF THE PROBLEMS .....</b>	<b>32</b>
<b>III. EXPERIMENTAL APPROACH .....</b>	<b>36</b>
III.1. Materials .....	36
III.1.1. Reagents .....	36
III.1.2. Enzymes .....	37
III.2. Sample Preparation.....	37
III.2.1. Preparation of Apoprotein and Zinc-Only Derivative Forms of Bovine Cu, Zn-SOD.....	37
III.2.2. Preparation and Purification of Glu-modified Cu, Zn-SOD .....	38
III.2.3. Preparation of Vanadyl-SOD Derivative.....	39
III.2.4. NMR Measurements of Sodium, Lithium, Phosphate, and Vanadate Binding to Cu, Zn-SOD .....	40
III.2.5. EPR Measurements .....	40
III.2.6. Fluorescence Measurements.....	41
III.2.7. Alkaline Agarose Gel Electrophoresis .....	41
III.2.8. Activity Assay .....	42
III.2.9. Protein Concentration Determination.....	42
III.3. Instrumentation .....	43
III.3.1. Fast Protein Liquid Chromatography (FPLC) .....	43
III.3.2. Electrophoresis .....	43
III.3.3. UV/Visible Spectrophotometer .....	43



III.3.4. Nuclear Magnetic Resonance (NMR) Spectrometer .....	43
III.3.5. Electron Paramagnetic Resonance (EPR) Spectrometers .....	44
III.3.6. Fluorimeter .....	44
III.3.7. Cyclic Voltammetry Equipment.....	44
III.3.8. Atomic Absorption Spectrophotometer .....	46
III.3.9. Centrifuge and Amicon Equipment.....	46
III.3.10. Chloride Electrode.....	46
III.3.11. Densitometer .....	47
III.3.12. Viscometer .....	47
III.4. Data Analysis.....	47
III.4.1. Determination of Azide and Cyanide Binding Constants to Cu, Zn-SOD Derivatives.....	47
III.4.2. Determination of Phosphate Binding Constants to Cu, Zn-SOD Derivatives.....	48
III.4.3. Determination of Binding Constant of $\text{VO}^{2+}$ to Apo-SOD .....	49
III.4.4. Determination of Dissociation Constants of $\text{Ca}^{2+}$ and $\text{Mg}^{2+}$ from Apo-SOD .....	49
III.4.5. Chloride Concentration Determination .....	53
<b>IV. RESULTS .....</b>	<b>54</b>
IV.1. Preparation and Characterization of Glu-modified Cu, Zn-SOD.....	54
IV.1.1. Preparation of Glu-modified Cu, Zn-SOD.....	54
IV. 1. 2. Purification of Glu-modified Cu, Zn-SOD .....	59

IV.1.3. Determination of the Charge of Glu-modified Cu, Zn-SOD .....	65
IV.1.4. UV/visible Studies of the Interactions of Azide and Cyanide with Glu-modified and Native Cu, Zn-SOD .....	68
IV.1.5. $^{31}\text{P}$ NMR Studies of the Interaction of Phosphate with Glu-modified and Native Cu, Zn-SOD .....	74
IV.1.6. $^{51}\text{V}$ NMR Studies of the Interaction of Vanadate with Glu-modified and Native Cu, Zn-SOD .....	74
IV.1.7. Activity Assay for Glu-modified and Native Cu, Zn-SOD .....	84
IV.2. Preparation and Characterization of the Vanadyl-SOD derivative .....	84
IV.2.1. Preparation and EPR Spectra and Parameters of the Vanadyl-SOD derivative .....	84
IV.2.2. Activity Assay of the Vanadyl-SOD derivative .....	96
IV.2.3. Cyclic Voltammetry of Native and Vanadyl-SOD derivatives .....	96
IV.3. Cationic Interactions with SOD Derivatives .....	102
IV.3.1. Fluorescence Studies of the Interactions of $\text{Ca}^{2+}$ and $\text{Mg}^{2+}$ with Native Cu, Zn-SOD and Apo-SOD .....	102
IV.3.2. $^7\text{Li}$ and $^{23}\text{Na}$ NMR Studies of $\text{Li}^+$ and $\text{Na}^+$ Interactions with Native Cu, Zn-SOD .....	109
<b>V. DISCUSSION .....</b>	<b>118</b>
V.1. Preparation and Characterization of Glu-Modified Cu, Zn-SOD .....	118
V.1.1. Preparation and Determination of the Number of Glu-Modified Residues in Glu-Modified Cu, Zn-SOD .....	118
V.1.2. Anionic Interactions with Glu-Modified Cu, Zn-SOD and Native Cu, Zn-SOD .....	119

V.2. Preparation and Characterization of the Vanadyl-SOD Derivative.....	125
V.2.1. Preparation and EPR Spectra of Vanadyl-SOD Derivative. ....	125
V.2.2. Activity Assay of the Vanadyl-SOD Derivative .....	130
V.2.3. Cyclic Voltammetry of Vanadyl-SOD Derivative and of Native Cu, Zn-SOD .....	130
V.3. Cationic Interactions with Glu-Modified Cu, Zn-SOD, Native Cu, Zn-SOD and Apo-SOD.....	132
V.4. Conclusions.....	133
REFERENCES.....	135
VITA .....	151

## LIST OF FIGURES

Figure	Page
1. Schematic drawing of the metal binding region of one subunit of bovine Cu, Zn-SOD .....	5
2. Schematic diagram of the solvent channel of bovine Cu, Zn-SOD indicating the relative positions of charged amino acid residues .....	7
3. Peak height of experimentally-measured EPR and of theoretical 100% bound $\text{VO}^{2+}$ versus $[\text{VO}^{2+}]$ added .....	50
4. Agarose gel electrophoresis of the coupling reaction of EDC to bovine Cu, Zn-SOD at different ratios .....	57
5. Purification of Glu-modified Cu, Zn-SOD with an FPLC system .....	61
6. Agarose gel electrophoresis of native Cu, Zn-SOD, of the Glu-modified Cu, Zn-SOD reaction mixture, and of the effluents from FPLC .....	63
7. Plot of the overall net charges of bovine Cu, Zn-SOD derivatives .....	66
8. UV/visible titration of Glu-modified and of native Cu, Zn-SOD with $\text{NaN}_3$ .....	69
9. UV/visible titration of native Cu, Zn-SOD with KCN .....	72
10. $^{31}\text{P}$ NMR $T_1$ relaxation values for native and Glu-modified Cu, Zn-SOD .....	75
11. $^{51}\text{V}$ NMR spectra of vanadate in the absence and in the presence of native Cu, Zn-SOD or Glu-modified Cu, Zn-SOD .....	77
12. $^{51}\text{V}$ NMR spectra of 2.0 mM vanadate in the absence and in the presence of increasing concentrations of Glu-modified Cu, Zn-SOD .....	81
13. X-band EPR spectrum of $\text{VO}^{2+}$ in a frozen solution of apo protein .....	86

14.	EPR titration of apo protein with $\text{VO}^{2+}$ .....	88
15.	X-band EPR spectrum of a frozen solution of the zinc-only derivative with $\text{VO}^{2+}$ .....	92
16.	X-band EPR spectrum of a frozen solution of native Cu, Zn-SOD in the presence of $\text{VO}^{2+}$ .....	94
17.	Air stability of the $\text{VO}^{2+}$ -SOD derivative as determined by the spectral features of the 77 K EPR spectrum .....	97
18.	Cyclic voltammograms of native Cu, Zn-SOD and of $\text{VO}^{2+}$ -SOD .....	100
19.	Fluorescence excitation spectra of fura-2 in the absence and in the presence of native Cu, Zn-SOD or apo-SOD titrated with $\text{Ca}^{2+}$ .....	103
20.	Fluorescence excitation spectra of fura-2 in the presence of apo-SOD at two protein concentrations .....	106
21.	Fluorescence excitation spectra of furaptra in the absence and in the presence of apo-SOD titrated with $\text{Mg}^{2+}$ .....	111
22.	Correlation between $g_{\parallel}$ and $A_{\parallel}$ values for various vanadyl(IV) complexes .....	128

## LIST OF TABLES

Table	Page
1. Amino acid compositions of single subunits of bovine, human, and yeast Cu, Zn-SOD proteins .....	2
2. Distances from copper or Lys-134 to positively- and negatively-charged residues at the active site of bovine Cu, Zn-SOD .....	9
3. NMR parameters of nuclei investigated at 7.0 T .....	45
4. <sup>35</sup> Cl NMR measurements .....	55
5. Chloride electrode measurements .....	56
6. Densitometer results of gel electrophoresis .....	60
7. Binding constant values of anions to native and Glu-modified Cu, Zn-SOD .....	71
8. <sup>51</sup> V chemical shift and line width values of different vanadate species with various concentrations of Glu-modified Cu, Zn-SOD .....	80
9. Concentrations of different vanadate species in various concentrations of Glu-modified Cu, Zn-SOD .....	83
10. SOD activity of native and Glu-modified Cu, Zn-SOD in various buffers .....	85
11. EPR parameters of the vanadyl-SOD derivative and model compounds .....	91
12. SOD activity of the vanadyl-SOD derivative .....	99
13. Fluorescence excitation ratios of fura-2 in the absence and presence of native Cu, Zn-SOD, and apo-SOD as a function of Ca <sup>2+</sup> .....	108

## LIST OF ABBREVIATIONS

$A_{\parallel}$	EPR parameter; the parallel hyperfine splitting constant
$A_{\perp}$	EPR parameter; the perpendicular hyperfine splitting constant
AA	Atomic Absorption
Ala	Alanine
Arg	Arginine
Asp	Aspartate
AT	Acquisition time
$^{35}\text{Cl}$	Chlorine-35 isotope
Cu, Zn-SOD	Copper, zinc-superoxide dismutase
$\delta$	Chemical shift in ppm
$\Delta\nu_{1/2}$	Line width of NMR resonance at half height in Hz
DEA	Diethanolamine
E	Empty (in SOD derivatives)
EDC	1-Ethyl-3-[3-(dimethylamino)propyl]carbodiimide
EDTA	Ethylenediamine tetraacetate
E, E-SOD	Apo protein derivative of Cu, Zn-SOD

EGTA	Ethyleneglycol bis-( $\beta$ -aminoethyl ether)-N,N'-tetraetic acid
EPR	Electron paramagnetic resonance
E, Zn-SOD	Zinc-only derivative of Cu, Zn-SOD
FPLC	Fast protein liquid chromatography
$g_{\parallel}$	EPR parameter; the parallel g-factor
$g_{\perp}$	EPR parameter; the perpendicular g-factor
HEPES	4-(2-Hydroxyethyl)-1-piperazine-ethanesulfonic acid
His	Histidine
Ile	Isoleucine
Gln	Glutamine
Glu	Glutamate
$^7\text{Li}$	Lithium-7 isotope
Leu	Leucine
Lys	Lysine
$^{23}\text{Na}$	Sodium-23 isotope
NMR	Nuclear magnetic resonance
$^{31}\text{P}$	Phosphorous-31 isotope
PW	Pulse width
SW	Spectral width
Tris-Cl	Tris[hydroxymethyl]aminomethanehydrochloride



T	Tesla
T <sub>1</sub>	Spin-lattice relaxation time
<sup>51</sup> V	Vanadium-51 isotope
V <sub>1</sub>	Vanadate monomer species (HVO <sub>4</sub> <sup>2-</sup> )
V <sub>2</sub>	Vanadate dimer species (HV <sub>2</sub> O <sub>7</sub> <sup>3-</sup> )
V <sub>4</sub>	Vanadate tetramer species (V <sub>4</sub> O <sub>12</sub> <sup>4-</sup> )
V <sub>5</sub>	Vanadate pentamer species (V <sub>5</sub> O <sub>15</sub> <sup>5-</sup> )
VO <sup>2+</sup> -SOD	Vanadyl-SOD derivative

## **ABSTRACT**

### **IONIC INTERACTION STUDIES OF BOVINE COPPER, ZINC-SUPEROXIDE DISMUTASE**

Chemical modification of carboxylate groups of the essential glutamate residues in bovine copper, zinc superoxide dismutase (Cu, Zn-SOD) was carried out at room temperature by using 1-ethyl-3-[3-(dimethylamino)propyl]carbodiimide hydrochloride (EDC) in the ratio of 2:1 of EDC:protein, in the presence of 5.5 M ammonium chloride at pH 5.0. The carboxylate modified Cu, Zn-SOD was purified by using a fast protein liquid chromatography system equipped with a mono-Q column. The modified protein was characterized by activity assay measurements and by investigating its interactions with the anions azide, cyanide, phosphate, and vanadate. The binding of azide and cyanide to native and modified Cu, Zn-SOD were followed by the changes in the absorbance of the azide- and cyanide-adducts measured by optical spectroscopy. The interactions of phosphate and vanadate with native and modified Cu, Zn-SOD were followed by  $^{31}\text{P}$  nuclear magnetic resonance (NMR) relaxation measurements, and by changes in the intensities of the  $^{51}\text{V}$  NMR resonances. The results of these anion binding studies indicated that there was stronger anion binding to the glutamate-modified derivative than

to native Cu, Zn-SOD. The number of modified glutamate residues was estimated to be two residues per monomer of Cu, Zn-SOD. Based on the crystal structure information, we concluded that carboxylate groups located at or near the entrance of the solvent channel of the protein were modified. A decrease in the negative charge on the protein resulted in an increase in the electrostatic interactions between the modified protein and the anions azide, cyanide, phosphate, and vanadate; no significant increase in the SOD activity was, however, detected for the glutamate-modified derivative.

Vanadyl,  $\text{VO}^{2+}$ , was used as an electron paramagnetic resonance (EPR) spin label to study the metal-binding properties of bovine Cu, Zn-SOD. The  $\text{VO}^{2+}$ -SOD derivative was prepared in 0.10 M HEPES, pH 7.4, at the ratio of 2:4:1 of  $\text{VO}^{2+}$ :dithionite: Apo-SOD (E, E-SOD, E = Empty), and under nitrogen atmosphere. X-band EPR titrations indicated that two  $\text{VO}^{2+}$  ions bound strongly to the protein dimer establishing a 1:1 complex per subunit. EPR parameters indicated that the  $\text{VO}^{2+}$  is bound at the native copper site. Exposure of  $\text{VO}^{2+}$ -SOD to air for 90 minutes showed a decrease of approximately 35% in the peak intensity of the EPR spectrum. X-band EPR titrations of the zinc-only derivative (E, Zn-SOD) with  $\text{VO}^{2+}$  showed that the occupation of the native zinc site weakens the binding of  $\text{VO}^{2+}$  to the native copper site. Addition of  $\text{VO}^{2+}$  to native protein under similar experimental conditions gave a characteristic  $\text{Cu}^{2+}$  EPR spectrum which ruled out the binding of  $\text{VO}^{2+}$  to the negatively-charged residues not at the active site in bovine Cu, Zn-SOD. The activity of  $\text{VO}^{2+}$ -SOD was examined by using

the indirect xanthine oxidase/cytochrome c assay method and the derivative was found to be inactive. The peak potential values measured by cyclic voltammetry at pH 4.0 for  $\text{VO}^{2+}$ -SOD and native Cu, Zn-SOD were + 425 mV and + 300 mV, respectively.

Fluorescence measurements were conducted to investigate the interactions of  $\text{Mg}^{2+}$  and  $\text{Ca}^{2+}$  with Cu, Zn-SOD derivatives using furaptra and fura-2 as fluorophores, respectively. The studies indicated that the interactions between either  $\text{Mg}^{2+}$  or  $\text{Ca}^{2+}$  and apo-SOD were very weak.  $^7\text{Li}$  and  $^{23}\text{Na}$  NMR  $T_1$  measurements indicated that the interactions of  $\text{Na}^+$  and  $\text{Li}^+$  with native Cu, Zn-SOD were not significant.

## CHAPTER I

### INTRODUCTION

#### I.1. Background on Cu, Zn-SOD

Copper, Zinc superoxide dismutase (Cu, Zn-SOD) [E.C.1.15.1.] is a metalloprotein present in almost all oxygen-tolerant organisms and bacteria. The most common form of the enzyme is present in the cytosol of the cell; more recently, an extracellular Cu, Zn-SOD has been found (Carlsson et al., 1996). The enzyme isolation was first reported in 1938 by Mann and Keilin (Mann & Keilin, 1938). Though the pale blue-green color of Cu, Zn-SOD strongly suggested that the protein contained  $\text{Cu}^{2+}$  ion, the presence of the colorless  $\text{Zn}^{2+}$  was not discovered until 1970 (Carrico & Deutsch, 1970). Shortly after the superoxide dismutase (SOD) function of the bovine Cu, Zn-SOD protein was discovered by McCord and Fridovich in 1969 (McCord & Fridovich, 1969). The amino acid composition (Table 1) and sequence, and the x-ray structure of the oxidized and reduced forms of the bovine enzyme, which is a relatively small (Mol Wt 31200) globular protein, then became known (Evans et al., 1974; Steinman et al., 1974; Abernethy et al., 1974; Tainer et al., 1982; Banci et al., 1994a; Rypniewski et al., 1995). The x-ray structures were determined for the oxidized form of SOD enzymes from different species, such as spinach, yeast, human, and *Xenopus laevis* (Kitagawa et al., 1991; Djinovic et al., 1992a; Parge et al., 1992;

**Table 1.** Amino acid compositions of single subunits of bovine, human, and yeast Cu, Zn-SOD proteins calculated from their amino acid sequences (adapted from Valentine & Pantoliano, 1981).

	<i>Bovine</i>	<i>Human</i>	<i>Yeast</i>
Glycine	25	25	22
Alanine	9	10	13
Valine	15	15	17
Leucine	8	9	6
Isoleucine	9	8	6
Proline	6	5	8
Phenylalanine	4	4	6
Tyrosine	1	0	1
Serine	8	10	11
Threonine	12	8	10
Aspartic Acid	11	12	9
Glutamic Acid	8	9	10
Asparagine	6	6	8
Glutamine	3	4	3
Cysteine(half-cystine)	3	4	2
Methionine	1	0	1
Histidine	8	8	6
Lysine	10	11	10
Arginine	4	4	4
Tryptophan	0	1	0
Total	151	153	153

Djinovic-Carugo et al., 1993). In early 1970's, Fridovich and coworkers (Keele et al., 1970; Yost & Fridovich, 1973) isolated two other enzymes with SOD activity which contained either manganese or iron; they found that the amino acid sequences of FeSODs were extremely similar to those of MnSODs from all sources, and yet totally different from the sequences of Cu, Zn-SODs from different sources

Wild-type Cu, Zn-SOD can be used as an antioxidant agent in human therapy (Omar et al., 1992).

Amyotrophic Lateral Sclerosis (ALS), also called motor neuron disease, Charcot's disease, or Lou Gehrig's disease is a progressive paralytic disorder that is usually fatal within 5 years from the onset of symptoms (Deng et al., 1993). About 10% of ALS cases are familial (FALS) (Rosen et al., 1993; Borchelt et al., 1995; Rabizadeh et al., 1995). It has been hypothesized that the mutants of Cu, Zn-SOD 1 (Cu, Zn-SOD 1 is the gene encoding the cytosol antioxidant enzyme Cu, Zn-SOD) lead to FALS, which are responsible for decreased enzymatic activity of Cu, Zn-SOD (Deng et al., 1993).

## **1.2. Structure of Cu, Zn-SOD**

The x-ray studies of the oxidized bovine Cu, Zn-SOD showed that the protein consists of two identical subunits each of which binds one copper ion ( $\text{Cu}^{2+}$ ) and one zinc ion ( $\text{Zn}^{2+}$ ) in close proximity. Both subunits are held together by hydrophobic interactions. The major structural feature of each subunit consists of a flattened cylindrical barrel of  $\beta$ -sheet made up of 8 antiparallel chains from which three external loops of irregular structure

extend (Tainer et al., 1982).  $\text{Cu}^{2+}$  is coordinated to four imidazole nitrogen atoms, coming from His-44, 46, 61, and 118. In addition, a water molecule is coordinated to  $\text{Cu}^{2+}$ , giving a distorted square pyramidal geometry.  $\text{Zn}^{2+}$  is coordinated to imidazole nitrogens from His-61, 69, and 78 as well as the carboxylate group from Asp-81, in an approximately tetrahedral geometry. Finally, the deprotonated imidazole (imidazolate) ring of His-61 bridges  $\text{Cu}^{2+}$  and  $\text{Zn}^{2+}$ , holding them at a distance of 6.3 Å apart (Figure 1).  $\text{Zn}^{2+}$  is buried in the protein structure, while  $\text{Cu}^{2+}$  is solvent-accessible (Tainer et al., 1982).

X-ray studies of the oxidized form of bovine Cu, Zn-SOD also indicated that the positively charged side chains of Arg-141, Lys-120, and Lys-134 are located 5, 12, 13 Å, respectively, away from the  $\text{Cu}^{2+}$  (Figure 2). The negatively charged residues Glu-130 and Glu-131 are also located at the entrance to the active site of the enzyme, and have been proposed to play major and minor roles, respectively, in the electrostatic guidance of the substrate (Tainer et al., 1982; Getzoff et al., 1983). The distances between the positively- and negatively charged-residues which are located at the solvent channel are indicated in Table 2 (QUANTA96).

The active site is the  $\text{Cu}^{2+}$  ion, which undergoes alternate reduction and oxidation during the catalytic cycle.  $\text{Cu}^{2+}$  is located at the bottom of a deep and narrow solvent channel. Metal ligands form the narrow part of the channel (Tainer et al., 1983).  $\text{Cu}^{2+}$  is involved directly in the catalytic process, whereas  $\text{Zn}^{2+}$  plays a structural role in the protein (Forman & Fridovich, 1973).

Very recently, single crystals of the reduced form of the bovine Cu, Zn-SOD have been obtained and their x-ray structure refined to 1.9 Å resolution (Banci et al., 1994a;



**Figure 1.** Schematic drawing of the metal binding region of one subunit of bovine erythrocyte cuprozinc protein with amino acid residues indicated (adapted from Valentine & Mota de Freitas, 1985).

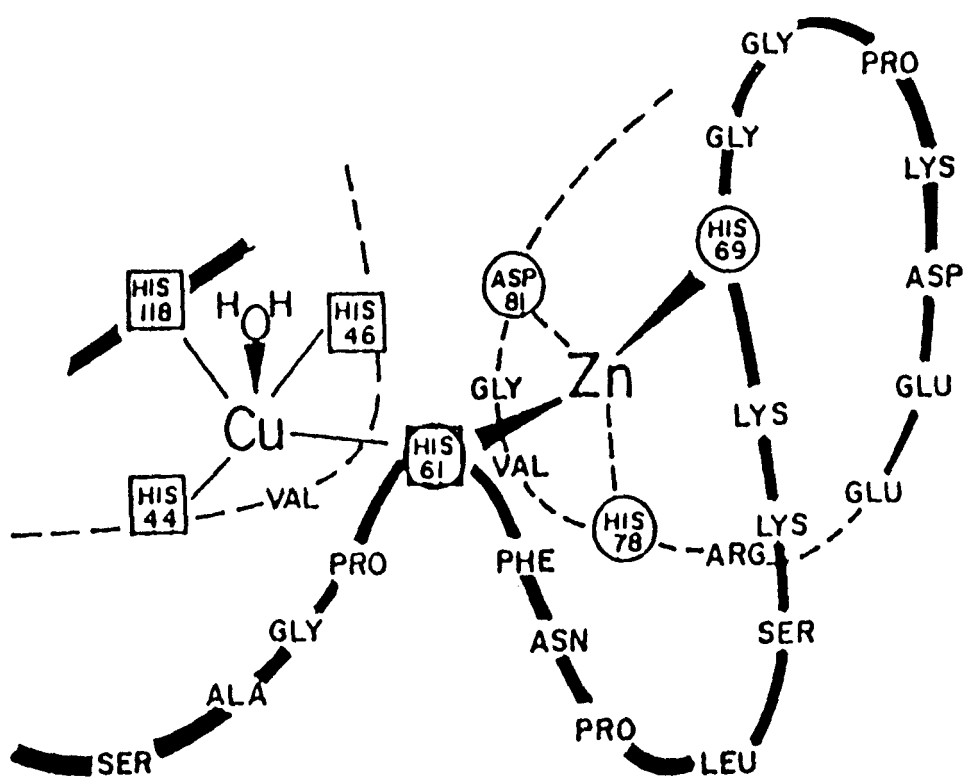


**Figure 2.** Molecular Graphics of the solvent channel of bovine Cu, Zn-SOD indicating the charged amino acid residues (QUANTA96).



**Table 2.** Distances (Å) from copper or Lys-134 (N) to positively- and negatively-charged amino acid residues at the active site of bovine Cu, Zn-SOD (QUANTA96).

Residue	Cu	Lys-134
Glu-130, O-1	16.11	8.24
O-2	17.80	9.318
Glu-131, O-1	9.48	5.43
O-2	10.61	3.801
Arg-141, N-1	7.563	10.03
N-2	5.588	8.999
Lys-120 (N)	12.85	15.86
Lys-134 (N)	10.35	-----

### 1.3. Function of Cu, Zn-SOD

The Cu, Zn-SOD enzyme has the important protective function of catalyzing disproportionation of the superoxide ion,  $O_2^-$  (McCord & Fridovich, 1969; Barrister et al., 1987; Fridovich, 1995). The substrate of the enzyme is the superoxide ion ( $O_2^-$ ), which is a

Rypniewski et al., 1995). The overall structure is superimposable on to that of the oxidized protein. The x-ray structural studies show that the imidazolate bridge is maintained in the reduced form. The x-ray structural studies of yeast Cu, Zn-SOD show, however, that the imidazolate bridge between  $\text{Cu}^{2+}$  and  $\text{Zn}^{2+}$  is broken, and unusual trigonal planar configuration characteristic of  $\text{Cu}^+$  rather than  $\text{Cu}^{2+}$  is revealed (Ogihara et al., 1996). Comparison studies of the three-dimensional structures showed that the structural and functional features of the Cu, Zn-SOD family are conserved (Bordo et al., 1994).

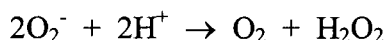
NMR and EXAFS measurements were available for the reduced Cu, Zn-SOD (McAdam et al., 1977a; Bertini et al., 1985a, 1991; Azab et al., 1992; Blackburn et al., 1984). In contrast to the x-ray structure, these methods show that in solution the bond between  $\text{Cu}^{2+}$  and N of the bridging imidazolate is broken.

UV/visible spectra of native, metal-substituted, and metal-free derivatives of Cu, Zn-SOD have given information about the nature of the metal binding region. Bovine Cu, Zn-SOD has unusually low absorbance at 280 nm because of the absence of tryptophan and the low amounts of tyrosine (Table 1) (Valentine & Pantoliano, 1981; Valentine & Mota de Freitas, 1985).

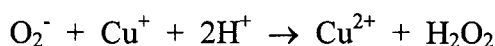
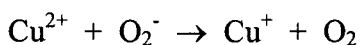
### **I.3. Function of Cu, Zn-SOD**

The Cu, Zn-SOD enzyme has the important protective function of catalyzing disproportionation of the superoxide ion,  $\text{O}_2^-$  (McCord & Fridovich, 1969; Bannister et al., 1987; Fridovich, 1995). The substrate of the enzyme is the superoxide ion ( $\text{O}_2^-$ ), which is a

negatively-charged (anionic), highly-reactive, toxic, free radical species, which is converted to dioxygen and peroxide in the enzyme-catalyzed reaction. The hydrogen peroxide thus formed is decomposed by the enzyme catalase, and these two enzymes protect cells from the byproducts of oxygen metabolism.



The catalytic process occurs through a two-step mechanism, in which copper with its variable oxidation state is responsible for the catalytic activity of the enzyme:



The rate of the reaction at the active site copper ion is nearly diffusion-limited and enhanced by electrostatic guidance (Rotilio et al., 1972a; McAdam, 1977b; Cudd & Fridovich, 1982; Argese et al., 1987; Sines et al., 1990). The diffusion of the superoxide anion toward the catalytic  $\text{Cu}^{2+}$  center has been proposed to be driven by the positive electrostatic force, generated by the metal ion and the basic residues surrounding the active site channel (Klapper et al., 1986); the observed catalytic rate constants for Cu, Zn-SOD are on the order of  $2\text{-}3 \times 10^9 \text{ M}^{-1} \text{ s}^{-1}$ .

The catalytic activity of bovine Cu, Zn-SOD enzyme is pH independent in the range  $5 \leq \text{pH} \leq 9.5$  (Klug et al., 1972; Ellerby et al., 1996). Above pH 12.2, native Cu, Zn-SOD loses its activity because it undergoes denaturation to an irreversible conformation (Boden et al., 1979). Human Cu, Zn-SOD also show pH independence in the same pH range, and a decrease in SOD activity at a higher pH value (Banci et al., 1990a). At high pH, the

decrease in the catalytic activity of the Cu, Zn-SOD enzymes was attributed to deprotonation of the water molecule which is coordinated to  $\text{Cu}^{2+}$  at the active site (Boden et al., 1979; Kowaleski et al., 1985; Banci et al., 1990a, 1991). Recent pH studies by Banci et al. (1993a) on human SOD mutants of Lys-136 (bovine 134) rule out the proposed explanation that the deprotonation of Lys-136 at high pH decrease the SOD activity (O'Neill et al., 1988).

At physiological pH, bovine Cu, Zn-SOD is negatively charged; its isoelectric point (pI) is 4.8 (Salin & Wilson, 1981; Marmocchi et al., 1983). One could expect that the electrostatic repulsion of the anionic substrate  $\text{O}_2^-$  by the net negative charge of the enzyme would diminish by increasing the ionic strength, resulting in an increase in the SOD activity of the enzyme. Instead, increasing the ionic strength decreases the SOD activity (Cudd & Fridovich, 1982; Getzoff et al., 1983). The decrease in the SOD activity is due to neutralization of the charged residues located at the active site of the enzyme such as Arg-Lys-120, 134 (Getzoff et al., 1983). The specific activity of native Cu, Zn-SOD, as assayed by the xanthine oxidase/cytochrome c assay, showed a decrease at higher phosphate concentrations, and was more sensitive to an increase in ionic strength at low phosphate concentrations (Mota de Freitas & Valentine, 1984).

#### **I.4. SOD Activity Assay Methods**

There are two classes of methods to measure the SOD activity (Bannister et al., 1987): a) direct methods, and b) indirect methods. The direct methods of assaying for SOD



activity depend on the physical properties of the substrate,  $O_2^-$ , and takes advantage of its paramagnetism and ultraviolet absorption (Ballou et al., 1969; Marklund, 1976). However, because of various technical difficulties, these methods have not been used as routine assays for the measurements of SOD activity. Pulse radiolysis is used as a direct method for the determination of SOD activity (Asmus, 1984). It has been useful in the investigation of the detailed mechanism of the enzyme-catalyzed reaction. This type of assay, however, requires sophisticated and expensive equipment (such as a linear electron accelerator) which is not available in most universities.

Indirect methods of assaying SOD activity are widely used; they are inexpensive and sensitive. In indirect assay methods, a unit of enzyme activity is generally defined as the amount of enzyme required to inhibit the reaction of  $O_2^-$  with the indicator by 50%. In the popular xanthine oxidase/cytochrome c assay method (McCord & Fridovich, 1969) xanthine and xanthine oxidase are used to generate  $O_2^-$ . The produced  $O_2^-$  reduces cytochrome c; the reduction of cytochrome c is monitored by an increase in the absorbance at 550 nm with time. One unit of SOD activity is defined as the amount of Cu, Zn-SOD required to give 50% inhibition of the rate of the reduction of cytochrome c.

### **I.5. Roles of Negatively and Positively Charged Residues in Cu, Zn-SOD**

Cu, Zn-SOD is one of the fastest enzymes known. Its activity is facilitated by local electrostatic potentials which result from positively-charged residues, such as Arg-141 in bovine SOD (Arg-143 in human SOD), Lys-120, Lys-134 in bovine SOD (Lys-122, Lys-

136 in human SOD), and the negatively-charged residues Glu-130 and Glu-131 in bovine (Glu-132 and Glu-133 in human SOD). The magnitude and distribution of such charged residues are conserved features in all Cu, Zn-SODs (Desideri et al, 1992).

Negatively-charged glutamate residues at position 132 and 133 in human Cu, Zn-SOD are located at the entrance to the active site cavity and affect the electrostatic interactions with the negative-charged substrate (Banci et al., 1993b; Getzoff et al., 1992). The channel structure is similar in both bovine and human Cu, Zn-SOD; Glu-132, Glu-133 in human SOD correspond to the Glu-130 and Glu-131 in the amino acid sequence of bovine SOD (Parge et al., 1992). Substitution of the Glu-133 and Glu-132 residues with both neutral and positively charged groups did not cause structural variations in the coordination sphere of  $\text{Cu}^{2+}$  (Banci et al., 1993b; Getzoff et al., 1992). The mutants (Glu→Gln) of Cu, Zn-SOD showed higher SOD activity and higher affinity toward a small anion, azide (Banci et al., 1993b; Getzoff et al., 1992).

The arrangement of electrostatic charge in Cu, Zn-SOD promotes productive enzyme-substrate interactions through substrate guidance. Charged sequence-conserved residues create an extensive electrostatic field that direct the negatively-charged  $\text{O}_2^-$  substrate to the highly positively-charged catalytic binding site at the bottom of the active-site channel (Getzoff et al., 1983). Dissection of the electrostatic potential gradient indicated the relative contributions of individual charged residues: Lys-120, 134 and Glu-131 seem to have important roles in directing the long-range approach of  $\text{O}_2^-$ , while Arg-141 has a local orienting effect (Getzoff et al., 1983). The residues Glu-130, Glu-131, Lys-134 and Thr-135 in the upper rim of the active site channel, together with Arg-141,

determine the shape and the strength of the electric field around the active site (Getzoff, 1983, Desideri et al., 1992, Bordo et al., 1994).

Chemical modification of positively-charged residues leads to a substantial loss of activity; modification of arginine or lysine residues at the active site of bovine Cu, Zn-SOD decrease the SOD activity to approximately 15% of that of the native protein (Malinowski & Fridovich, 1979a; Marmocchi et al., 1982; Cudd & Fridovich, 1982). Bovine Cu, Zn-SOD chemically modified at Arg-141 with phenylglyoxal has only one modified arginine residue per subunit (Malinowski & Fridovich, 1979a). Lysine residues were modified with succinic anhydride (Marmocchi et al., 1982); the actual number and location of the modified lysine residues is, however, not known.

Site-specific mutagenesis showed the importance of Arg-143 for catalysis. Mutation of Arg-143 in human SOD to Lys, Ile, Asp, or Glu showed a lower activity in the order of native Arg-143 > Lys-143 > Ile-143, Ala-143 > Asp-143, Glu-143 (Fisher et al., 1994). Computational and experimental results indicated that the Arg-143 is the single most important residue in Cu, Zn-SOD both electrostatically and mechanistically (Fisher et al., 1994).

Molecular dynamics (MD) studies on human Cu, Zn-SOD and its mutants at position 143 showed that when the native Arg-143 has been modified to Ile-143 or Glu-143, native Arg-143 is highly mobile, while the mutant Arg-143→Glu-143 show a large decrease in the mobility with respect to the Ile-143, and the enzymatic activity is in the order of Arg-143 > Ile-143 > Glu-143 (Banci et al., 1992).

Moreover, MD calculations on mutants at some positively and negatively charged residues, which are located in the electrostatic loop of the active site channel, have been conducted (Banci et al., 1994b). The MD calculations indicated that the mutation of Lys-136, Glu-132, and Glu-133 did not significantly alter the structural properties of the active site and of the electrostatic loop. However, the mutation of Thr-137 to Arg-137, i.e., the addition of a positive charge, showed a large effect on the structure of the electrostatic loop. The MD results showed that the electrostatic effects and the location of the charged residues as well as the structure of the electrostatic loop all contribute to the catalytic behavior (Banci et al., 1994b).

The electrostatic steering mechanism of bovine Cu, Zn-SOD was investigated by Brownian dynamics simulations (Sines et al., 1990), which indicated that the neutralization or reversal of the negative charge at Glu-131 of SOD increased the activity of Cu, Zn-SOD enzyme. Simulation calculations also showed that the maximum effects were observed upon alteration of the charge of the residues at Arg-141, Lys-134 and Glu-131. Mutagenesis of Glu-133 and Glu-132 on the human Cu, Zn-SOD enzyme confirmed the predictions made by Brownian dynamics simulations (Banci et al., 1993b; Getzoff et al., 1992).

The catalytic rate of *Xenopus Laevis* B (XSODB) in single and double mutants of conserved positively and negatively charged residues was determined by pulse radiolysis (Polticelli et al., 1995). The neutralization of Glu-131 increases the catalytic rate by 50% at physiological ionic strength, and by 80% at low ionic strength. By contrast, neutralization of the positively charged Lys-134 and Lys-120 in XSODB showed decreases in the catalytic

rate, while the Brownian simulation carried out on bovine SOD predicted a strong decrease for neutralization of Lys-134 but not for Lys-120 residues (Parge et al., 1992). The multiple charged mutation studies suggest an approach in which the catalytic rate of Cu, Zn-SOD will be independent of ionic strength (Polticelli et al., 1995).

## 1.6. Anion Binding to Cu, Zn-SOD

One of the characteristic properties of Cu, Zn-SODs is its high affinity for anions. Binding of small anions, such as  $\text{N}_3^-$ ,  $\text{CN}^-$ , to the oxidized form of bovine Cu, Zn-SOD has been widely studied, and established that the binding site is the  $\text{Cu}^{2+}$  ion for small anions. The stoichiometry of binding for the  $[\text{Cu}^{2+}]/[\text{anion}]$  ratio is 1:1 (Rotilio et al., 1972b; Bertini et al., 1981; Cudd & Fridovich, 1982; Bermingham-McDonogh et al., 1982; Mota de Freitas & Valentine, 1984; Valentine & Mota de Freitas, 1985).  $^{35}\text{Cl}$  and  $^1\text{H}$  NMR studies of anion binding to the reduced form of bovine Cu, Zn-SOD showed that the chloride anion ( $\text{Cl}^-$ ) binds weakly at or near the  $\text{Cu}^+$  ion; however, the positively-charged residues Arg-141, Lys-120, Lys-134 are the major anion binding sites (Mota de Freitas et al., 1990). These anions are monovalent negatively-charged ions, and act as inhibitors of SOD, presumably because they mimic the enzyme substrate interactions. Azide and cyanide bind in an equatorial position (Rotilio et al., 1972b; Morpurgo et al., 1973; Fee et al., 1981); this observation implies a displacement of a histidyl imidazole. Electron spin echo studies of the  $\text{CN}^-$  and  $\text{N}_3^-$  adducts, however, showed that the imidazole bridge remained intact (Fee et al., 1981).

These results taken together suggest that a histidyl imidazole other than the bridging histidine is displaced from an equatorial position of copper.

Anion binding interactions (with anions like  $\text{N}_3^-$ ,  $\text{CN}^-$ ,  $\text{NCO}^-$ ,  $\text{NCS}^-$ ) have been studied by NMR spectroscopy on the Cu, Co-SOD derivative, in which the native  $\text{Zn}^{2+}$  ion is substituted by  $\text{Co}^{2+}$  ion without changing the catalytic and structural properties of the enzyme (Ming et al., 1988; McAdam, 1977b; Djinovic et al., 1992b). The results were initially interpreted in terms of the removal of the His-44 residue from the  $\text{Cu}^{2+}$  coordination sphere upon binding of the anionic ligand (Bertini et al., 1985b; Banci et al., 1987). Such conclusion was supported by EXAFS studies on the azide-reacted SOD of the native Cu, Zn-SOD (Blackburn et al., 1987). More recent NMR studies on Cu, Co-SOD have proposed that the His-46 residue detached from the coordination sphere upon the binding of azide or cyanide to  $\text{Cu}^{2+}$  (Banci et al., 1989; Banci et al., 1990b).

Very recently, the crystal structure of the azide-inhibited bovine Cu, Zn-SOD has been studied which showed that the azide anion binds directly to  $\text{Cu}^{2+}$ , at the place of the metal-bound water molecule, and gives rise to a pyramidal configuration around  $\text{Cu}^{2+}$  (Djinovic et al., 1994). The coordination distance and geometry of the His-44 and His-61 residues are essentially maintained. His-46 and His-118 are the only two ligands in the  $\text{Cu}^{2+}$  coordination sphere that are affected by azide binding, whereas no rearrangement of the  $\text{Zn}^{2+}$  ligands was observed.

The anion affinity of the native and of Arg-143 mutants of the Cu, Co-SOD derivative of the human Cu, Zn-SOD have been investigated (Banci et al., 1988); Arg-143 (corresponding to the Arg-141 in bovine SOD) is immediately adjacent to the  $\text{Cu}^{2+}$  in the

active site of human SOD. These studies indicated that the substitution of Arg-143 by Lys-143, Ile-143, and Glu-143 showed a decrease in both the azide binding affinity and the SOD activity in the order of native Arg-143 > Lys-143 > Ile-143 > Glu-143 mutants (Banci et al., 1988). This indicates that the positive charge and its shape at the entrance of the active site determines the affinity of the anion. In contrast, the SOD activity and the azide binding affinity to the human Cu, Zn-SOD enzyme showed an increase in the trend of mutants Gln-133 and Gln-132 > native Glu-133 and Glu-132 (Banci et al., 1993b; Getzoff et al., 1992).

The UV/visible spectra of native and azide-bound bovine Cu, Zn-SOD showed broad d-d bands centered at 680 nm and at 643 nm, respectively (Fee & Gaber, 1972; Berminham-Mcdonogh et al., 1982; Cupane et al., 1994); addition of azide to the native bovine protein give a new band near 373 nm. This band has been assigned as an azide-to-copper charge transfer band (Morpurgo et al., 1973). Very recently, low-temperature studies of the UV/visible spectra of the native and the azide-reacted bovine Cu, Zn-SOD have been investigated in the range 300-10 K (Cupane et al., 1994). The broad d-d bands of the native and azide-reacted SOD are split at low temperature into two bands each, centered at 779 nm and 674 nm, and at 694 and 613 nm, respectively. These thermal studies indicated that a structural rearrangement occurred at about 170 K; in the native SOD the rearrangement involved all of the copper ligands except His-61, whereas in the azide-bound SOD it involved just the copper-bound anion. This different thermal behavior may help in elucidating the way the  $O_2^-$  substrate binds to the copper ion (Cupane et al., 1994).

The anion binding properties of Ni(II)-substituted derivatives of bovine SOD, in which  $Ni^{2+}$  is bound in the native copper site, have been investigated. The UV/visible

spectra of Ni, M-SOD (M = Zn, Co) upon addition of azide and cyanide indicated that the anions are directly bound to  $\text{Ni}^{2+}$  (Ming & Valentine, 1990a). Moreover, the NMR studies suggested that the geometric changes that occurred upon anion binding to  $\text{Ni}^{2+}$  are similar to those observed for the native protein (Ming & Valentine, 1990a).

Phosphate is also an inhibitor of Cu, Zn-SOD, but unlike other small anions, it does not bind directly to  $\text{Cu}^{2+}$  (Mota de Freitas & Valentine, 1984; Mota de Freitas et al., 1987). This conclusion was based on the observation that the visible and EPR spectra due to the  $\text{Cu}^{2+}$  ion in the protein were unchanged at high phosphate concentrations.  $^{31}\text{P}$  NMR relaxation studies on native and arginine-modified Cu, Zn-SOD showed that phosphate binds to the native protein via the guanidinium group of Arg-141 (Mota de Freitas et al., 1987, Valentine & Mota de Freitas, 1986).

$^{31}\text{P}$  and  $^1\text{H}$  NMR were used to probe the binding of low affinity anions, such as  $\text{Cl}^-$ ,  $\text{ClO}_4^-$ ,  $\text{CH}_3\text{COO}^-$ , and borate to bovine Cu, Zn-SOD (Desideri et al., 1988). The studies were carried out on Co(II)-substituted SOD, where  $\text{Co}^{2+}$  replaced the native  $\text{Zn}^{2+}$ ; because of the antiferromagnetic coupling between  $\text{Cu}^{2+}$  and  $\text{Co}^{2+}$  the  $^1\text{H}$  NMR resonances of the bound residues to  $\text{Cu}^{2+}$  were detected (Bertini et al., 1985b). The results showed that Arg-141 is the binding site for low affinity anions and that the  $^1\text{H}$  NMR line of His-46 is perturbed upon such interaction (Desideri et al., 1988).

Vanadate is a strong inhibitor of several phosphate dependent enzymes, including phosphatases, ATPase, and ribonucleases (VanEtten et al., 1974; Goodon et al., 1979; Linquist et al., 1973). The vanadate anion responsible for inhibition of phosphatases and ATPases is usually monomeric vanadate (VanEtten et al., 1974). Other reports have



provided evidence that vanadate oligomers including the dimer, tetramer, and decamer have biological activity and bind specifically to various proteins (Crans et al., 1989a; Crans & Schelble, 1990; Crans et al., 1990; Crans & Simone, 1991; Cremo et al., 1990; Wittenkerller et al., 1991). Interactions of vanadate with oxidized forms of native and chemically modified bovine Cu, Zn-SOD using  $^{51}\text{V}$  NMR spectroscopy showed that the vanadate tetramer binds with high affinity to the bovine Cu, Zn-SOD via the lysine residues (Wittenkeller et al., 1991). The vanadate tetramer is the first large anion found to show high affinity for native Cu, Zn-SOD. The absorbance spectra of native Cu, Zn-SOD upon vanadate binding showed, however, no changes ruling out direct binding of vanadate to the  $\text{Cu}^{2+}$  ion.

### **I.7. Cation Binding to Cu, Zn-SOD**

A lot of effort has been directed towards characterizing the anion binding properties of Cu, Zn-SOD (see section 1.6). Only one study has addressed the interactions between cations and Cu, Zn-SOD (Cocco et al., 1983). The relatively high density of positive charges at the active-site region makes binding of cations at that region unlikely. However, the rest of the protein has a net negative charge. The effects of cations such as  $\text{Ca}^{2+}$  and  $\text{Tb}^{3+}$  on bovine Cu, Zn-SOD were investigated (Cocco et al., 1983).  $\text{Ca}^{2+}$  binding had no effect on the enzyme activity. The low-temperature EPR spectra of the enzyme-bound copper were modified into a more axial line shape by addition of  $\text{Ca}^{2+}$  and  $\text{Tb}^{3+}$ . This effect was not observed by room-temperature EPR and was interpreted as being due to a long-

range conformation effect on the copper-binding site (Cocco et al., 1983).

### **I.8. Stability of Cu, Zn-SOD**

It is known that Cu, Zn-SOD is a dimeric enzyme of identical subunits held together by unusually strong noncovalent interactions, which are almost entirely hydrophobic in nature.

Native bovine Cu, Zn-SOD protein has a conformational melting temperature,  $T_m$ , of 83° C (Stellwagen & Wilgus, 1978; Roe et al., 1988), which is so far the highest value reported for any metalloprotein. It means that the bovine Cu, Zn-SOD protein has the highest degree of thermal stability.

Bovine dimer Cu, Zn-SOD does not dissociate into subunits even in 8 M urea for 72 h at 25° C (Malinowski & Fridovich, 1979b). It is however gradually denatured by guanidium chloride with EDTA present (Forman & Fridovich, 1973; Mach et al., 1991; Mei et al., 1992).

Recent studies of the effects of urea, temperature and SOD concentration on the inactivation and dissociation into subunits found that the activation energy of the inactivation of the bovine Cu, Zn-SOD decreased upon increasing the SOD concentration; Cu, Zn-SOD has a high resistance to inactivation by increasing the SOD concentration (Inouye et al., 1994). The dissociation of bovine Cu, Zn-SOD into subunits was carried out in 6 M urea at 45° C. The results showed that there are two monomer species (M1, M2) in addition to the dimer (D), the dimer has full enzymatic activity, whereas the monomers lost

their activity. At 25° C, the dissociation of Cu, Zn-SOD into subunits showed that the treatment with or without 6 M urea gave the monomer species M2, whereas the amount of monomer M1 was negligible. At temperatures below 45° C, the activity studies suggested that Cu, Zn-SOD mostly existed as monomer (M2) with full activity even after treatment in 6 M urea (Inouye et al., 1994).

### **I.9. Metal-Substituted Derivatives of Cu, Zn-SOD**

Several metal ions, such  $\text{Co}^{2+}$ ,  $\text{Hg}^{2+}$ ,  $\text{Cd}^{2+}$ , and  $\text{Ni}^{2+}$ , have been used to probe the zinc site (Calabrese et al., 1972; Fee, 1973b; Forman & Fridovich, 1973; Bertini et al., 1985b; Cass et al., 1978; Baily et al., 1980; Valentine & Pantoliano, 1981; Ming & Valentine, 1987).  $\text{Ag}^+$ ,  $\text{Ni}^{2+}$ ,  $\text{Co}^{2+}$ , and  $\text{Zn}^{2+}$  have been used successfully to substitute  $\text{Cu}^{2+}$  in the copper site (Beem et al., 1977; Roe et al., 1990; Ming & Valentine, 1990b; Fee, 1973a,b). The preparation of the Cu, Co-SOD derivative showed that the  $\text{Co}^{2+}$  ion selectivity replaced the  $\text{Zn}^{2+}$  ion (Calabrese et al., 1972). The most interesting feature of this derivative is that the cobalt and copper ions are antiferromagnetically coupled, as evidenced by the silence of the  $\text{Cu}^{2+}$  EPR signal (Rotilio et al., 1974; Morgenstern-Badaran et al., 1986). Such coupling gives, however, a chance to detect the NMR signals of the  $^1\text{H}$  NMR spectrum of the residues coordinated to copper and cobalt ions (Bertini et al., 1985b; Paci et al., 1988). Moreover, substitution of  $\text{Co}^{2+}$  in the native  $\text{Zn}^{2+}$  site of Cu, Zn-SOD leads to similar enzymatic catalytic properties as the native protein (McAdam, 1977b), and has a similar overall three-dimensional structure of the native site metal coordinating

residues because they are thoroughly conserved in both Cu, Co-SOD and native Cu, Zn-SOD (Djinovic et al., 1992b).

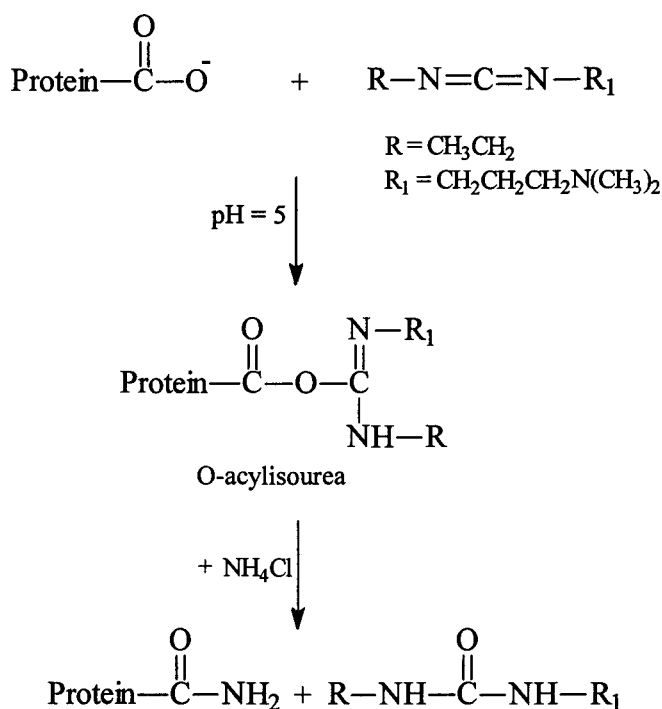
Substitution of metal ions in the native  $\text{Cu}^{2+}$  and  $\text{Zn}^{2+}$  binding sites of Cu, Zn-SOD are pH dependent (Pantoliano et al., 1982; Ming & Valentine, 1990b). At low pH, UV/visible and EPR results show that the metal ion bound in the native  $\text{Zn}^{2+}$  binding site in Cu, Zn-SOD, Cu, Cu-SOD, or Cu, Co-SOD is reversibly released in the pH range  $3 \leq \text{pH} \leq 4.5$  (Pantoliano et al., 1979; Pantoliano et al., 1982). At high pH, a metal migration from one binding site to another was observed; a solution of the zinc-free derivative, Cu, E-SOD (E = empty), at pH 9.3 undergoes  $\text{Cu}^{2+}$  ion migration from the copper sites to the zinc sites in order to make subunits containing  $\text{Cu}^{2+}$  in both the copper and zinc sites (Valentine et al., 1979).

#### **I.10. Modification of Carboxylate Groups in Proteins**

Chemical modifications of amino acid side chains result in alteration of enzyme function and are powerful tools in enzymology. Water-soluble carbodiimides, such as 1-ethyl-3-[3(dimethylamino)propyl]carbodiimide hydrochloride (EDC), are used to convert glutamic acid or aspartic acid residues into neutral glutamine or asparagine residues (Carraway & Koshland, 1972; Pho et al., 1977; Matsuo et al., 1980; Desvages et al., 1980; Flier et al., 1981). Water-soluble carbodiimides have been used successfully for the modification of carboxyl groups in proteins under mild conditions (Wang & Young, 1978; Yamada et al., 1981; Esch et al., 1981). The addition of the carboxyl group across one of

the double bonds of the carbodiimide gives an O-acylisourea. The coupled reaction with a suitable nucleophile, such as an amine, causes the displacement of the carbodiimide from its adduct with the carboxyl group and result in a modified protein (Scheme 1). Ammonia is preferred as the nucleophile over other amines because its size is nearly the same as the  $\text{OH}^-$  being replaced in glutamate and aspartate residues (Lewis & Shafer, 1973).

**Scheme 1:** The reaction of carbodiimide with protein carboxyl groups (adapted from Lundblad, 1991).



The use of carbodiimide-mediated modification of carboxylate groups in proteins is by far the most widely used method for the study of such functional groups (Lundblad, 1991). Water-soluble carbodiimides such as EDC are the most popular reagents for

effecting the modification of glutamate and aspartate in proteins with nucleophiles and operate under mild conditions and with good selectivity (Hoare & Koshland, 1966; Yamada et al., 1981; Esch et al., 1981).

### **I.11. Vanadium in Biological Systems**

Vanadium plays an important role in biological systems. The essentiality, the distribution and the toxicology of vanadium in organisms are all areas of ongoing research at the present time. In biological systems, vanadium can be found in the oxidation states +3, +4, and +5 (Saponja & Vogel, 1996). The oxovanadium(IV) or vanadyl ( $\text{VO}^{2+}$ ) ion in which vanadium in the oxidation state +4 is one of the most stable diatomic ions known. The free solvated vanadyl ion exist as the  $\text{VO}(\text{H}_2\text{O})_5^{2+}$  species at low pH; at neutral pH forms a polymeric  $\text{VO}(\text{OH})_2$  which is electron paramagnetic resonance (EPR) silent. In the pH range of 5 to 11, the EPR signal intensity is proportional to ligand- or macromolecular-bound  $\text{VO}^{2+}$  (Makinen & Mustafi, 1995). Vanadyl forms strong anionic, cationic, and neutral complexes with all types of ligands (Selbin, 1965). The spectroscopic and chemical properties of vanadyl ion make it particularly useful as a probe ion (Selbin, 1966). This versatility permits binding studies to be conducted with the variety of coordinating functional groups encountered in biological systems (Chasteen, 1981). The complexes of vanadyl(IV) typically have square pyramidal or bipyramidal structures in which the vanadyl-oxygen occupies an apical position; a few complexes have been reported that have five coordinate trigonal bipyramidal structures (Chasteen, 1981).

The paramagnetic properties of vanadyl complexes make them of value as EPR spectroscopic probes. The  $3d^1$  ground state of vanadyl is orbitally nondegenerate with no electronic excited state nearby in energy. These are requirements for observation of room temperature and frozen EPR spectra. Of all paramagnetic metal ion compounds, only those of  $VO^{2+}$  consistently give relative sharp EPR spectra in both frozen and room temperature solutions with the exception of binuclear vanadyl compounds. There are also several factors such as the high abundance (more than 99%) of  $^{51}V$  with a nuclear spin  $I$  of  $7/2$ ; the electronic spin relaxation rate is relatively slow, which gives rise to sharp EPR lines (Eaton & Eaton, 1990). EPR method is the most widely employed technique for studying vanadium(IV) (Chasteen, 1995). Recently,  $VO^{2+}$  electron nuclear double resonance (ENDOR) and electron spin echo envelope modulation (ESEEM) have been used to probe the ligand nuclei directly (Chasteen, 1993).

The EPR spectroscopy of  $VO^{2+}$  has been used to probe metal binding sites in several proteins, such as insulin, transferrin, carboxypeptidase A, carbonic anhydrase, and in nucleotides (Chasteen et al., 1973; Cannon & Chasteen, 1975; Dekoch et al., 1974; Fitzgerald & Chasteen, 1974; Baran, 1995).  $VO^{2+}$  EPR studies of transferrin indicated that there are two nonequivalent binding sites in human serum transferrin (Cannon & Chasteen, 1975).  $VO^{2+}$  was substituted for  $Zn^{2+}$  in the insulin hexamer at the two symmetry sites, and is bound to the three imidazole groups of the B10 His residues. In other investigations,  $VO^{2+}$  replaced the native  $Zn^{2+}$  in carboxypeptidase A and carbonic anhydrase B (Dekoch et al., 1974). Full activity of vanadyl derivative of carboxypeptidase A was achieved at 1:1 ratio of  $VO^{2+}$ :Protein. The vanadyl carbonic anhydrase B derivative was inactive.

Recently, Chasteen has reviewed some of the salient features of the most studies of vanadyl-protein complexes (Chasteen, 1995).

The chemistry of vanadium in aqueous solution is very complex. A large variety of species can form depending on the pH, ionic strength, and concentration (Saponja & Vogel, 1996). In many of its biological functions, vanadium acts in the +5 ( $d^0$ ) state, where it is diamagnetic and inaccessible to electron absorption spectroscopy in the visible region.  $^{51}\text{V}$  NMR provides an excellent diagnostic tool for investigations of vanadium(V) coordination environments due to a large magnetic moment, high natural abundance (99.7%), rapid quadrupolar relaxation in solution, and the chemical shifts being very sensitive to changes in the nature of the environments (Butler & Danzitz, 1987).  $^{51}\text{V}$  NMR have been used to investigate the vanadate interactions with several proteins such as vanadate binding to bovine serum albumin, human serum transferrin, alkaline phosphatase and ribonucleases (Rehder, 1990).  $^{51}\text{V}$  NMR has also been used to study the *in vivo* metabolism of vanadate in yeast cells (Rehder, 1990). The studies indicate that the vanadate species is responsible for cellular toxicity.

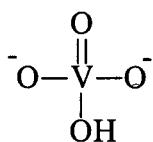
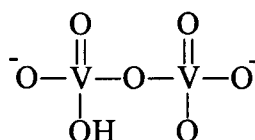
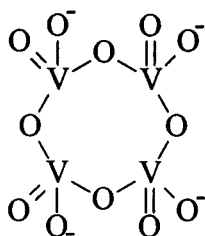
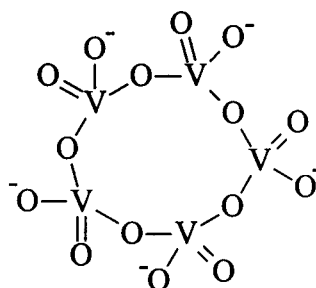
An aqueous solution of vanadate contains a series of oxovanadate(V) species whose relative abundances depend on concentration, pH, ionic strength (as mentioned previously), temperature, and the presence of other substances (Crans, 1995). Vanadate is a term used to describe these vanadium(V) species in aqueous solutions.

In the neutral pH range, an aqueous colorless solution of vanadate consists of a mixture of anionic species, named oxovanadate. The simplest oxovanadate is the monomeric vanadate,  $\text{V}_1$  in Scheme 2 (next page). The monomer is commonly



recognized as a phosphate analog and can exist as a mono-, di-, or trianion ( $\text{H}_2\text{VO}_4^-$ ,  $\text{HVO}_4^{2-}$ , and  $\text{VO}_4^{3-}$ ). There are other oxovanadates present in the physiological pH range including vanadate dimer ( $\text{V}_2$  in Scheme 2), vanadate tetramer ( $\text{V}_4$  in Scheme 2), and vanadate pentamer ( $\text{V}_5$  in Scheme 2). These species are conveniently distinguished by  $^{51}\text{V}$  NMR (Crans, 1995). There are a few other species in cationic forms of vanadium that may be present at physiological pH, these are  $\text{VO}^{3+}$ ,  $\text{VO}_2^+$ ,  $\text{V(IV)}$ , and  $\text{V(V)}$ , which can exist at pH values around 7 and only stabilized by complex formation (Rehder, 1992).

**Scheme 2:** Structural representations are shown for vanadate monomer ( $\text{V}_1$ ), vanadate dimer ( $\text{V}_2$ ), vanadate tetramer ( $\text{V}_4$ ), and vanadate pentamer ( $\text{V}_5$ ).

 $\text{V}_1$  $\text{V}_2$  $\text{V}_4$  $\text{V}_5$

In the absence of strongly complexing ligands,  $\text{VO}^{2+}$  undergoes a number of hydrolytic reactions. At physiological pH, vanadyl(IV) ion exists as  $\text{VO}(\text{OH})_{2(s)}$  (Chasteen, 1983). The limited solubility of  $\text{VO}(\text{OH})_2$ ,  $K_{sp} \sim 10^{-22}$ , can restrict the maximum value of the  $\text{VO}^{2+}$  concentration which can be used in biological studies (Chasteen, 1983). When  $\text{VO}^{2+}$  is slowly added to a HEPES buffer solution or to water maintained at pH  $\sim 7.5$ , no precipitate is observed (Chasteen, 1983). The species, however, is EPR silent and therefore contains more than one metal ion (Makinen & Mustafi, 1995).

Vanadium(IV) polymerizes under physiological conditions at concentrations above  $10^{-6}$  M, and oxidizes in the presence of oxygen. In contrast, vanadium(V) is more stable as free vanadate ( $\text{H}_2\text{VO}_4^-$ ,  $\text{HVO}_4^{2-}$ ) in the presence of oxygen but is readily reduced by various organic molecules and oligomerizes at concentrations above  $10^{-4}$  M (Crans et al., 1989b). Generally, at physiological conditions, the most common forms of vanadium are vanadate ( $\text{H}_2\text{VO}_4^-$ ) and vanadyl ( $\text{VO}^{2+}$ ). The standard potential for pair ( $\text{H}_2\text{VO}_4^-$ ) +  $4\text{H}^+ \leftrightarrow \text{VO}^{2+} + 3\text{H}_2\text{O}$  is 1.31 V (Rehder, 1992). Hence, vanadyl undergoes autooxidation to vanadate in the presence of oxygen, and vanadate in turn is reduced by a reductant such as glutathione, ascorbate and NADH. This change between V(V) and V(IV) is an especially interesting feature because : a) vanadium can act as a competitor to phosphate ( $\text{HPO}_4^{2-}$ ), and b) it can also act as a transition metal ion which competes with other metal ions in coordination to biogenic compounds (Rehder, 1992).

$\text{VO}^{2+}$  is also reported to bind albumin from different species (Sakurai et al., 1987) and calmodulin (Nieves et al., 1987). Vanadium(II) or vanadium(IV) is present in the

vanadium nitrogenases found in nitrogen fixing bacteria; the chemical environment of vanadium in this protein has been studied by x-ray absorption spectroscopy edge fine structure and vanadium was found to have a distorted octahedral coordination (Shah & Brill, 1977; George et al., 1988).

Vanadium(V) is present at the active center of vanadium haloperoxidases isolated from some brown and red algae, and was confirmed by using  $^{51}\text{V}$  NMR spectroscopy. Vanadium(V) is surrounded by oxygen ligands, presumably by bidentate carboxylate groups (Rehder et al., 1991). X-ray absorption near-edge structure spectroscopy was used to study the coordination charge on vanadium in the native and reduced enzyme (Kusthardt et al., 1993), and confirmed the charge obtained from the  $^{51}\text{V}$  NMR study. Reduced peroxidases have vanadium(IV) in the active center; they show axially symmetric vanadyl-type EPR spectra, and are similar irrespective of the source of the protein (Wever and Kustin, 1990).

Voltammetric techniques are also other methods that can be used in characterizing the redox properties of vanadium-containing compounds. The standard reduction potential ( $E^\circ$ ) of  $\text{VO}^{2+}/\text{V}^{3+}$  is +360 mV. Cyclic voltammetry of metalloproteins is limited by the formation of an adsorbed layer of denatured protein on the electrode surface itself. It is well known that proteins adsorb strongly and often denature at the electrode surface (Armstrong, 1990). Very recently, cyclic voltammetry studies of bovine Cu, Zn-SOD were reported at pH 4 and showed that the midpoint potential of the enzyme is +400 mV (Verhagen et al., 1995).

## CHAPTER II

### STATEMENT OF THE PROBLEMS

The purpose of this thesis is two-fold: 1. Preparation and characterization of a glutamate-modified Cu, Zn-SOD derivative which will lead to a better understanding of the electrostatic interactions in this enzyme and to the discovery of possible alternate functions; and 2. Preparation and characterization of a vanadyl-substituted derivative of bovine Cu, Zn-SOD which will tell us whether replacement of the copper(II) by vanadyl leads to an enzyme with similar biological function.

Native bovine Cu, Zn-SOD has a net negative charge at physiological pH. It would be of interest to clarify the role of the negatively charged glutamate residues in the electrostatic interaction with the substrate. A new protein derivative, Glu-modified bovine Cu, Zn-SOD, will be prepared and characterized. We anticipate that the affinity of Glu-modified enzyme toward anions will be enhanced because of its decrease in overall negative charge. Conversely, we anticipate that the Glu-modified enzyme will have reduced cation affinity relative to the native enzyme. Water-soluble carbodiimides such as 1-ethyl-3-[3-(dimethylamino)propyl]carbodiimide hydrochloride (EDC) have been used successfully for modification of glutamate residues in proteins (Lundblad, 1991). The Glu-modified Cu, Zn-SOD derivative will be prepared using (EDC) in the presence of ammonium chloride to

convert glutamate residues into neutral glutamine residues. A pure modified Cu, Zn-SOD will be obtained by using FPLC, and its purity will be verified by electrophoresis. The % yield of the modified Cu, Zn-SOD will be determined by densitometer measurements. Activity assays of the proteins will be measured by the xanthine oxidase/cytochrome c method to verify the role of the negatively charged residues on the dismutation mechanism (McCord & Fridovich, 1969). The number of modified glutamate residues in SOD will be estimated from gel electrophoresis of Cu, Zn-SOD, E, Zn-SOD (E = empty), E, E-SOD and Glu-modified Cu, Zn-SOD.

Glu-modified Cu, Zn-SOD will be characterized by studying its interactions with the anions azide, cyanide, phosphate, and vanadate, as well as with the cations  $Mg^{2+}$ ,  $Ca^{2+}$ ,  $Li^+$ , and  $Na^+$ . The results of the Glu-modified Cu, Zn-SOD will be compared to those obtained for the native SOD at similar experimental conditions. The interactions of such anions and cations will provide information on whether the negatively-charged glutamate residues in the native protein play a role in the enzyme mechanism of the superoxide dismutation.

Small anions like azide bind directly at the  $Cu^{2+}$  site (Djinovic-Carugo et al., 1994), whereas large anions like phosphate and vanadate bind at the positively-charged Arg and Lys residues respectively, which are located at the entrance of the active site of each subunit (Mota de Freitas et al., 1987; Wittenkeller et al., 1991). UV/visible spectroscopy will be used to determine the azide and cyanide affinities of the Glu-modified and native Cu, Zn-SOD.  $^{31}P$  NMR will be conducted to determine the interaction between Glu-modified Cu, Zn-SOD and phosphate. Phosphate binding constants to SOD will be obtained by James-

Noggle plots from  $^{31}\text{P}$   $T_1$  relaxation measurements (James & Noggle, 1969).  $^{51}\text{V}$  NMR spectroscopy will be applied to monitor the interaction of native and Glu-modified Cu, Zn-SOD with vanadate. The change in the intensity of the  $^{51}\text{V}$  NMR resonances and in the line widths will provide information about the modification of the Glu-130 and Glu-131 which are very close to the binding sites (Lys-120, 134) of vanadate in native Cu, Zn-SOD (Wittenkeller et al., 1991).

Fluorescence measurements will be conducted to determine the binding constants of  $\text{Mg}^{2+}$  and  $\text{Ca}^{2+}$  to native-SOD, Glu-modified-SOD, and Apo-SOD. Binding of  $\text{Li}^+$  and  $\text{Na}^+$  to Glu-modified and native Cu, Zn-SOD will be probed by  $^7\text{Li}$  and  $^{23}\text{Na}$  NMR spectroscopy.

EPR techniques provide extremely powerful probes of the electronic structure of materials with unpaired electrons and give information concerning the electronic and geometric structure of a paramagnetic species (Garner et al., 1995). Vanadium in  $\text{VO}^{2+}$  is present in the + 4 ( $d^1$ ) oxidation state, where EPR can be used for the characterization of the vanadyl ion environment. The standard reduction potential of  $\text{VO}^{2+}/\text{V}^{3+}$  (0.36 V) is similar to that of  $\text{Cu}^{2+}/\text{Cu}^+$  (0.34 V) (Butler, 1990). It would be of interest to prepare a vanadyl-substituted derivative of Cu, Zn-SOD in which  $\text{VO}^{2+}$  is bound to the native  $\text{Cu}^{2+}$  site. We hypothesize that the  $\text{VO}^{2+}$ -SOD derivative may also have SOD activity. EPR titration will be carried out by injecting increments of a  $\text{VO}^{2+}$  solution into Apo-SOD or E, Zn-SOD solutions under a nitrogen gas atmosphere. A typical procedure will be followed as described by Chasteen (Chasteen, 1981). X-band EPR spectroscopy will be applied to determine the suitable molar ratio of  $\text{VO}^{2+}$  to SOD that yield the largest amount of the

vanadyl-substituted SOD derivative. The EPR parameters ( $g_{\parallel}$  and  $A_{\parallel}$ ) of the  $\text{VO}^{2+}$ -SOD derivative will be compared to those in the literature to determine the number of nitrogen atoms bound to  $\text{VO}^{2+}$ . This comparison will enable us to determine the site to which  $\text{VO}^{2+}$  is bound. The activity of the new  $\text{VO}^{2+}$ -SOD derivative will be verified by the xanthine/cytochrome c assay. The cyclic voltammogram of the  $\text{VO}^{2+}$ -SOD derivative will be obtained and compared to that reported for native Cu, Zn-SOD (Verhagen et al., 1995).

## CHAPTER III

### EXPERIMENTAL APPROACH

#### III.1. Materials

##### III.1.1. Reagents

Xanthine, xanthine oxidase (grade I), horse heart cytochrome c (type III), [4-(2-hydroxyethyl)-1-piperazineethanesulfonic acid] (HEPES), and tris[hydroxymethyl]amino-methane hydrochloride (Tris-Cl) were purchased from Sigma. The protein assay dye reagent (Folin-Ciocalteu phenol) was also obtained from Sigma. 1-Ethyl-3-[3-(dimethyl-amino)propyl]carbodiimide hydrochloride (EDC), vanadyl sulfate ( $\text{VOSO}_4$ ) trihydrate, sodium chloride ( $\text{NaCl}$ ), lithium chloride ( $\text{LiCl}$ ), magnesium chloride ( $\text{MgCl}_2$ ) hexahydrate, calcium chloride ( $\text{CaCl}_2$ ) hydrate, diethanolamine (DEA), and sodium dithionite ( $\text{Na}_2\text{S}_2\text{O}_4$ ) were from Aldrich. Ammonium metavanadate ( $\text{NH}_4\text{VO}_3$ ) was purchased from Johnson Matthey. Sodium acetate (enzyme grade), sodium phosphate dibasic ( $\text{Na}_2\text{HPO}_4$ ) heptahydrate, sodium phosphate monobasic ( $\text{NaH}_2\text{PO}_4$ ) dihydrate, (Ethylenedinitrilo)-tetraacetic acid disodium salt (EDTA), sodium chloride standard (1 M), and the ionic strength adjuster (5 M  $\text{KNO}_3$ ) were purchased from Fisher. The potassium salt derivatives of the  $\text{Mg}^{2+}$  and  $\text{Ca}^{2+}$  fluorescence indicators furaptra and fura-2, respectively, were



purchased from Molecular Probes. All chemicals were used as received and without further purification.

### **III.1.2. Enzymes**

Bovine liver Cu, Zn-SOD was purchased as a lyophilized powder from OXIS International, Inc. (Mountain View, CA).

## **III.2. Sample Preparation**

### **III.2.1. Preparation of Apoprotein and Zinc-Only Derivative Forms of Bovine Cu, Zn-SOD**

The apoprotein (E, E-SOD) (E = Empty) form of bovine Cu, Zn-SOD was prepared by dialyzing the native enzyme against EDTA in 3 L of 0.05 M acetate buffer at pH 3.9 for 24 hours (the buffer was changed 3 times), followed by extensive dialysis against NaCl to remove the excess EDTA (McCord and Fridovich, 1969). The zinc-only derivative (E, Zn-SOD) was prepared by the addition of calculated amounts of zinc nitrate to an apo preparation at pH 5.5 followed by incubation in the cold for 12 to 24 hours (Valentine & Pantiliano, 1981).

The apo protein and the zinc-only derivative of Cu, Zn-SOD were characterized by the activity assay and by AA to determine the metal ion content. The apo enzyme had < 5% of  $\text{Cu}^{2+}$  or  $\text{Zn}^{2+}$  and an activity of < 4% of the native enzyme. The zinc-only derivative was

found to contain  $< 5\%$   $\text{Cu}^{2+}$  and  $> 98\%$   $\text{Zn}^{2+}$ , and the activity was determined to be  $< 5\%$  of the native enzyme.

### **III.2.2. Preparation and Purification of Glu-modified Cu, Zn-SOD**

Native bovine Cu, Zn-SOD was added to ammonium chloride at pH 5.0. EDC was then added to the solution with stirring at room temperature. The pH was maintained at 5.0 by addition of small aliquots of 0.5 M HCl during the reaction. After stirring for about 3 hours at room temperature, the solution was dialyzed exhaustively against 3.5 L of deionized water for 3 days in a cold room to remove excess EDC and ammonium chloride. A chloride electrode and  $^{35}\text{Cl}$  NMR were used to verify the removal of  $\text{Cl}^-$  ( $[\text{Cl}^-]$  was found to be less than 0.2 mM), and then the modified Cu, Zn-SOD was isolated by FPLC. The conditions used for the coupling reaction were either Cu, Zn-SOD (20mg, 0.50 mM), ammonium chloride (1.0, 2.0, 3.0, 4.0, and 5.5 M), and EDC (2 mM), or Cu, Zn-SOD (20 mg, 0.50 mM), ammonium chloride (5.5 M), and EDC (0.5, 1.0, 1.5, 2, and 5 mM). In both cases, the final volume was 1.28 mL.

The Glu-modified protein was purified with the FPLC system using a Mono Q 5/5 (0.5x5 cm) or a 10/10 (1x10 cm) column with a salt gradient of 0.0-0.15 M NaCl in 10 mM Tris-Cl buffer at pH 7.5. The desired fractions were concentrated by using an Amicon apparatus, and then a centricon microconcentrator with a molecular weight cutoff of 10000. The Glu-modified Cu, Zn-SOD sample was subjected to agarose gel electrophoresis to verify its purity, and to determine the extent of modification relative to native Cu, Zn-SOD.

Densitometer measurements were conducted to determine the % yield of the Glu-modified Cu, Zn-SOD.

### III.2.3. Preparation of Vanadyl-SOD Derivative

In a 4-mL conical flask, a 300-340  $\mu\text{L}$  solution containing Apo-SOD in 0.1 M HEPES buffer at pH 7.4 was flushed for a few minutes with nitrogen gas. Sodium dithionite was added in a 2:1 molar ratio of dithionite:vanadyl to avoid hydrolysis of  $\text{VO}^{2+}$  (Chasteen, 1981). The vanadyl stock solution, which was kept under a nitrogen atmosphere, was added slowly to the protein solution with a 10  $\mu\text{L}$  syringe. The final mixture was stirred rapidly with a micro-spin-bar, and kept under nitrogen gas for at least two minutes, and then transferred to the EPR tube via a needle with two tips (cannula technique). The sample was frozen by liquid nitrogen (77 K) to be ready for EPR measurements. The final EPR solution contained 0.6 mM SOD protein, 0.1 M HEPES, pH 7.4, dithionite, and appropriate amounts of vanadyl solution to give the desired  $[\text{VO}^{2+}]/[\text{protein}]$  ratio; concentration ratios of 0.25 to 20 were used.

E, Zn-SOD was also treated with vanadyl under similar experimental conditions to prepare a VO, Zn-SOD derivative.

### III.2.4. NMR Measurements of Sodium, Lithium, Phosphate, and Vanadate

#### Binding to Cu, Zn-SOD

$^7\text{Li}$  and  $^{23}\text{Na}$   $T_1$  measurements were conducted for 0.20, 0.50, 1.0, and 2.0 mM of native bovine Cu, Zn-SOD in the presence of 20%  $\text{D}_2\text{O}$ , 0.20 M HEPES, pH 7.4, and at 37 °C. The viscosity of the solutions were measured.

$^{31}\text{P}$   $T_1$  measurements were carried out using 0.15 mM protein and a phosphate concentration ranging from  $5 \times 10^{-3}$  to 0.3 M in 50 mM HEPES, pH 7.0, 0.1 mM EDTA, 20%  $\text{D}_2\text{O}$ , and at 23 °C.

In  $^{51}\text{V}$  NMR experiments, a stock solution of 10 mM ammonium vanadate was prepared and diluted to a final concentration of 2 mM. The native and modified protein samples were added to obtain the desired concentrations, the samples being buffered with 0.10 M HEPES, pH 7.4 and containing 15%  $\text{D}_2\text{O}$ . The vanadate chemical shifts were reported relative to an external reference of the V-DEA complex (Crans & Shin, 1988).

### III.2.5. EPR Measurements

EPR measurements were carried out for a frozen solution (77 K) containing 0.6 mM SOD derivatives, such as apo protein E, E-SOD, zinc-only derivative E, Zn-SOD, or native Cu, Zn-SOD, in 0.1 M HEPES, pH  $7.4 \pm 0.1$ , and a ratio of 2:4:1 of  $\text{VO}^{2+}$ :dithionite:SOD. The solution was kept under nitrogen atmosphere. Solutions were frozen by dipping the filled tubes in liquid  $\text{N}_2$  (77 K).

### III.2.6. Fluorescence Measurements

$\text{Ca}^{2+}$  fluorescence measurements were made in solutions containing 2  $\mu\text{M}$  fura-2, 0.10 mM to 0.30 mM protein, 0.03 mM EGTA, and buffered with 150 mM Tris-Cl, pH  $7.4 \pm 0.1$ .  $\text{Ca}^{2+}$  aliquots were added in the range of 5 nM to 70 nM. Fluorescence measurements for  $\text{Mg}^{2+}$  were carried out in solutions containing 2  $\mu\text{M}$  furaptra, 0.10 mM to 0.40 mM protein, and 150 mM Tris-Cl buffer, pH  $7.4 \pm 0.1$ .  $\text{Mg}^{2+}$  aliquots were added to give a desired concentration in the range of 0.25 mM up to 20 mM. The final volumes were either 0.5 mL or 2.5 mL depending on the size of the cuvette used. Fura-2 and furaptra were used as fluorophores indicators for  $\text{Ca}^{2+}$  and  $\text{Mg}^{2+}$ , respectively (Grynkiewicz et al., 1985; Raju et al., 1989).

### III.2.7. Alkaline Agarose Gel Electrophoresis

Alkaline agarose gel electrophoresis was carried out using a commercially available alkaline hemoglobin gel kit. The gel sheet was coated with 1% agarose and 0.64 M Tris buffer (pH 8.6) and non-reactive ingredients. The alkaline buffer which consists of 16.7 g sodium barbital and 2.5 g barbital was dissolved in 2 L of deionized water and stored in a refrigerator. The Amido Black B10 was dissolved in 1 L of 5% acetic acid and used as the staining solution. The destaining solution was 5% acetic acid.

Each chamber of the universal electrophoresis cell base was filled with 75 mL of alkaline buffer. Each well in the gel was loaded with 1-2  $\mu\text{L}$  of sample. The gel is inserted into the electrophoresis cell cover, agarose side up, matching the (+) and the (-) on the cover

with the gel. Electrophoresis was performed at 240 volts for 20 minutes. The gel was stained for 10 minutes and transferred to 5% acetic acid for 30 seconds. The gel was dried in an oven at about 55 °C and destained in 5% acetic acid several times till there was no more stain on the gel.

### **III.2.8. Activity Assay**

The activities of native Cu, Zn-SOD, Glu-modified Cu, Zn-SOD, E, E-SOD, and E, Zn-SOD were measured by the xanthine oxidase/cytochrome c assay (McCord & Fridovich, 1969). The ionic strength was adjusted by HEPES when necessary.

### **III.2.9. Protein Concentration Determination**

Protein concentration was determined by the method of Lowry et al. (Lowry et al., 1951; Bollag & Edelstein, 1991) at 750 nm. The dye reagent, Folin-ciocalteu phenol, was diluted two-fold in deionized water. Protein standards were prepared from bovine Cu, Zn-SOD. Protein concentration was also determined by measurement of the absorbance at 680 nm ( $\epsilon = 300 \text{ M}^{-1} \text{ cm}^{-1}$ ) for native Cu, Zn-SOD, and at 258 nm ( $\epsilon = 2920 \text{ M}^{-1} \text{ cm}^{-1}$ ) for apo protein (Valentine & Pantoliano, 1981). The two methods generated protein concentrations that agreed within 5%. Protein concentration based on a molecular weight of 31200 for native Cu, Zn-SOD was also determined by weighing the powder to be dissolved, and this method was in agreement within 5% with those using the Lowry assay and the  $\epsilon_{680}$  value.

### **III.3. Instrumentation**

#### **III.3.1. Fast Protein Liquid Chromatography (FPLC)**

The fast protein liquid chromatography (FPLC) system was purchased from Pharmacia Biotech Inc.; the major components included a Liquid Chromatography Controller (LCC-501), two P-500 pumps, a UV-1 monitor, a Fraction Collector (Frac-100), and Mono-Q 5/5 or 10/10 ion exchange columns. The Mono-Q 10/10 column was purchased from the Waters company, and the Mono-Q 5/5 was from Pharmacia.

#### **III.3.2. Electrophoresis**

The Universal electrophoresis cell which consists of a cell cover and a cell base combined to a power supply was purchased from Ciba Corning. The gel electrophoresis plate used was a hemoglobin alkaline kit from Ciba Corning.

#### **III.3.3. UV/Visible Spectrophotometer**

All studies were conducted on either an IBM UV/VIS model 9420 or on a JASCO model V-550 double-beam UV/VIS spectrophotometer.

#### **III.3.4. Nuclear Magnetic Resonance (NMR) Spectrometer**

$^7\text{Li}$ ,  $^{23}\text{Na}$ ,  $^{35}\text{Cl}$ ,  $^{31}\text{P}$ , and  $^{51}\text{V}$  were obtained at 116.5, 79.4, 29.4, 121.4, and 78.9 MHz, respectively, on a Varian VXR-300 NMR spectrometer. The instrument was

equipped with 10 mm multinuclear probes and a variable temperature unit. Spin-lattice relaxation time ( $T_1$ ) measurements were conducted by the inversion recovery method ( $180^\circ$ - $\tau$ - $90^\circ$ ) at a spinning rate of 16 Hz and at 23 °C. The delay time was five times the values of  $T_1$ . Table 3 shows the NMR parameters that were used.

### **III.3.5. Electron Paramagnetic Resonance (EPR) Spectrometers**

EPR experiments were done at the National Biomedical EPR Center at the Medical College of Wisconsin-Milwaukee. The X-band EPR spectra were recorded on a Varian E-109 operating at the frequency 9.5 GHz with 100 KHz field modulation.  $\text{VO}^{2+}$  bound to SOD in a frozen solution at 77 K begins to saturate at a power of 5 mW.

### **III.3.6. Fluorimeter**

Magnesium and calcium fluorescence measurements were made on a Photon Technology International spectrofluorometer, model Quanta Master QM-1, using a Felix software program. The excitation scan mode was used, with the emission wavelength set at 510 nm.

### **III.3.7. Cyclic Voltammetry Equipment**

The cyclic voltammetry measurements were performed on a potentiostat/galvanostat, model 273 from EG&G Princeton Applied Research. The recorder was an x-y



**Table 3.** NMR Parameters of Nuclei Investigated at 7.0 T.

	<sup>7</sup> Li	<sup>23</sup> Na	<sup>31</sup> P	<sup>35</sup> Cl	<sup>51</sup> V
Frequency/MHz	116.5	79.4	121.4	29.4	78.9
SW/KHz	4.5	15	10	8	73
AT/s	1.5	1.5	0.75	0.5	0.15
PW 90/ $\mu$ s	27 <sup>a</sup> , 32 <sup>b</sup>	28	13	78	78
Flip angle/ degree	45	45/90	45/90	90	90

<sup>a</sup>90° pulse in low ionic strength solutions (1-20 mM) in 10 mm probe

<sup>b</sup>90° pulse in high ionic strength solutions (500 mM) in 10 mm probe.

omnigraphic recorder (Houston instrument), model 2000. The measurements were carried out with a glassy carbon working electrode, platinum wire as counter electrode, and  $\text{Ag}^+$  Sat'd/  $\text{AgCl}$  as a reference electrode.

### **III.3.8. Atomic Absorption Spectrophotometer**

A Perkin Elmer 5000 spectrometer equipped with a flame source and a graphite furnace was used for AA studies. Cu and Zn were measured at wavelengths of 324 nm and 213 nm, respectively. The slit width was set at 0.7 nm. Acetylene and compressed air were used as a fuel and oxidant, respectively. The flow rate for fuel and oxidant were 35 and 50, respectively.

### **III.3.9. Centrifuge and Amicon Equipment**

A Savant refrigerated centrifuge, model 10000, using a Centricon microconcentrator with a molecular cutoff of 10000, was used for concentration of proteins. Amicon equipment of 50-mL and 10-mL cells with a molecular weight cutoff of 10000 was also used to concentrate protein samples further.

### **III.3.10. Chloride Electrode**

An Orion combination chloride electrode, model 96-17B, connected to a pH meter set in the mV mode was used to measure the chloride ion concentration.

### **III.3.11. Densitometer**

An ISCO scanner, model 1312, operating with an ISCO computer program was used to determine the percentage of each band on the gel electrophoresis.

### **III.3.12. Viscometer**

The viscosities of some protein solutions were measured with a Brookfield Cone Plate Viscometer, equipped with a 8° CP-40 cone, at 12 rpm.

## **III.4. Data Analysis**

### **III.4.1. Determination of Azide and Cyanide Binding Constants to Cu, Zn-SOD Derivatives**

The binding of the azide anion to the native and modified Cu, Zn-SOD were followed by the change in the absorbance of the azide-protein adducts as measured by UV/visible spectroscopy. The experiments were performed at pH 5.5, in the presence of 0.20 mM protein, and 0.01 M HEPES. The binding constant ( $K_b$ ), according to equation 1, was obtained from plots of the differences between the absorbance of azide-protein adducts and of protein only divided by the azide concentration added versus the differences in the absorbance (i.e  $\Delta A/[NaN_3]$  vs.  $\Delta A$ ); the slope is equal to  $-K_b$  (Connors, 1987).

$$\Delta A/b[NaN_3] = -K_b\Delta A/b + C \quad (1)$$

where  $b$  is the light path length and is equal to 1 cm, and  $C$  is a constant related to the protein concentration,  $K_b$ , and absorptivity.

The binding constants of cyanide to native and Glu-modified Cu, Zn-SOD were calculated from the absorbance of the bands at 680 and 530 nm by the method described in Rotilio et al. (1972b). The measurements were performed with solutions containing 0.2-0.5 mM of protein in the presence of 100 mM HEPES, pH  $7.4 \pm 0.1$ , 0.10 mM EDTA, and sufficient NaF to adjust the ionic strength to 0.30 M (Mota de Freitas & Valentine, 1984).

### III.4.2. Determination of Phosphate Binding Constants to Cu, Zn-SOD

#### Derivatives

The binding of phosphate to native and Glu-modified Cu, Zn-SOD was followed by  $^{31}\text{P}$  NMR relaxation measurements, using a protein concentration of 0.15 mM and phosphate concentrations ranging from  $5 \times 10^{-3}$  to 0.3 M in 50 mM HEPES, pH 7, 0.1 mM EDTA, 20%  $\text{D}_2\text{O}$ , and at 23 °C. The binding constants of phosphate to the protein derivatives were calculated using James-Noggle plots (James & Noggle, 1969). The equations used are as follows:

$$1/\Delta R = 1/(K_b C_e \Delta R') + C_p/(C_e \Delta R') \quad (2)$$

$$\Delta R = 1/T_{1\text{obs}} - 1/T_{1\text{free}}$$

$$\Delta R' = 1/T_{1\text{bound}} - 1/T_{1\text{free}}$$

where  $T_{1\text{obs}}$ ,  $T_{1\text{free}}$ , and  $T_{1\text{bound}}$  are the spin-lattice relaxation time values for observed, free, and bound phosphate,  $R$  is the reciprocal of  $T_1$ ,  $K_b$  is the binding constant,  $C_e$  and  $C_p$  are the

concentration of enzyme and of phosphate. The binding constant,  $K_b$ , was obtained from the expression (Slope / Intercept) of the plot of  $1/\Delta R$  versus  $C_p$ .

### III.4.3. Determination of Binding Constant of $VO^{2+}$ to Apo-SOD

The binding constant of  $VO^{2+}$  to apo-SOD ( $K_b$ ) was calculated from the equilibrium expression (equation 3).

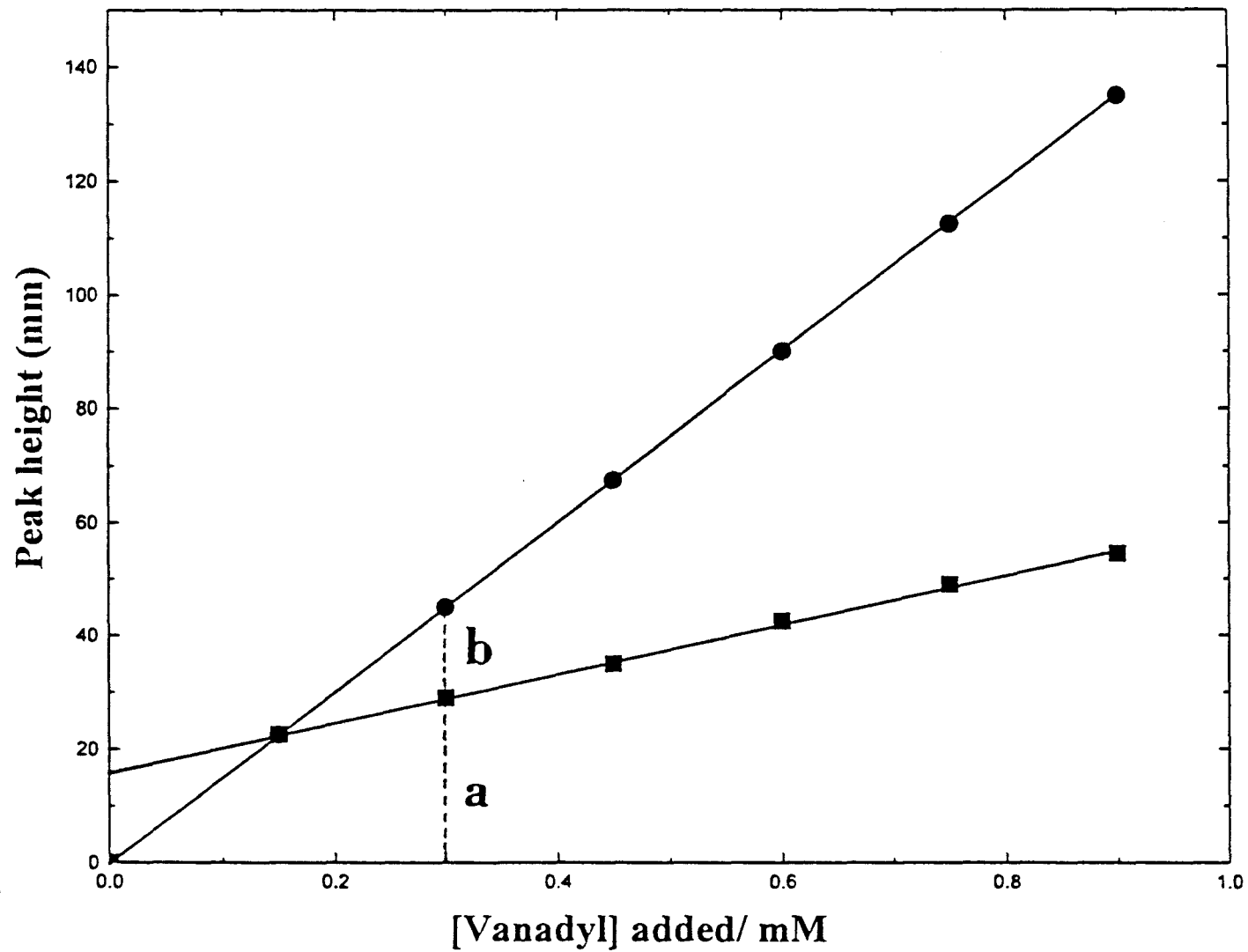
$$K_b = [VO^{2+}\text{-SOD}] / [VO^{2+}]_{\text{free}}[Apo\text{-SOD}] \quad (3)$$

where  $[Apo\text{-SOD}]$  is the concentration of apo protein at equilibrium, and  $[VO^{2+}\text{-SOD}]$  is equal to the  $[VO^{2+}]_{\text{bound}}$  at the ratio 2:1 of  $[VO^{2+}]:[Apo\text{-SOD}]$ . To calculate  $[VO^{2+}]_{\text{bound}}$ , we first normalized the experimentally-measured EPR peak intensities for bound signal by assuming that at the lower concentration of  $VO^{2+}$  added, i.e., 0.15 mM, all  $VO^{2+}$  was bound to the protein, and forcing the curve to go through the origin of the Cartesian axes (see Figure 3). For any other concentration,  $[VO^{2+}]_{\text{bound}} = (a/a+b) \times [VO^{2+}]_{\text{added}}$ .  $[VO^{2+}]_{\text{free}}$  was obtained by subtraction of  $[VO^{2+}]_{\text{bound}}$  from  $[VO^{2+}]_{\text{added}}$ .

### III.4.4. Determination of Dissociation Constants of $Ca^{2+}$ and $Mg^{2+}$ from Apo-SOD

$Ca^{2+}$  dissociation constants ( $K_d$ ) from native Cu, Zn-SOD and E, E-SOD were obtained by measuring the excitation fluorescence spectra of solutions containing 0.1 or 0.3 mM protein, 2  $\mu$ M Fura-2 (Scheme 3), 0.15 M Tris-Cl, pH 7.4. The  $K_d$  values were obtained from the slope of linear Klotz plots of  $([SOD]_t/[Ca^{2+}]_b)$  versus  $1/[Ca^{2+}]_f$  as indicated

**Figure 3.** Peak height of experimentally-measured EPR (■) and of theoretical 100% bound  $\text{VO}^{2+}$  (●) versus  $[\text{VO}^{2+}]_{\text{added}}$ .

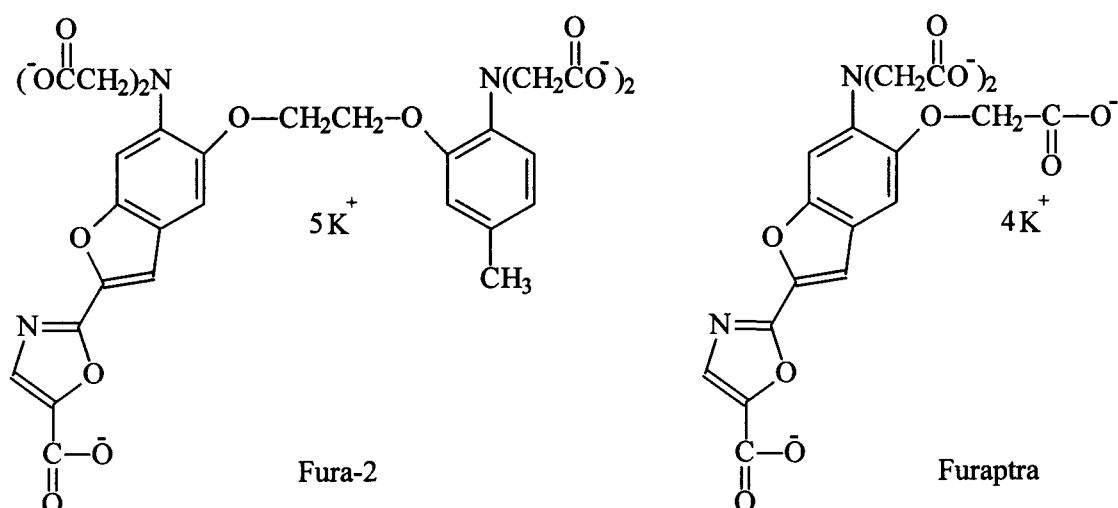


in equation 4 (Segel, 1993).

$$[\text{SOD}]_t/[\text{Ca}^{2+}]_b = (K_d/n)(1/[\text{Ca}^{2+}]_f) + 1/n \quad (4)$$

where  $[\text{SOD}]_t$  is the total enzyme concentration,  $[\text{Ca}^{2+}]_b$  is the concentration of bound  $\text{Ca}^{2+}$ ,  $[\text{Ca}^{2+}]_f$  is the concentration of free  $\text{Ca}^{2+}$ , and  $n$  is the number of binding sites. The y-axis intercept gives  $1/n$ , whereas the slope is  $K_d/n$ .

**Scheme 3:** Structural representations are shown for fura-2 and furaptra.



The concentrations of free  $\text{Ca}^{2+}$  were calculated from equation 5 (Grynkiewicz et al., 1985):

$$[\text{Ca}^{2+}]_{\text{free}} = K_d' [\log(R_{\text{min}} - R/R_{\text{max}} - R)] [S_{\text{min}}/S_{\text{max}}] \quad (5)$$

where  $K_d'$  is the dissociation constant of the fura-2 (Scheme 3) complex of  $\text{Ca}^{2+}$ ,  $R$  is the ratio of the intensities at the wavelengths 340 and 380 nm in the fluorescence excitation spectrum;  $R_{\text{min}}$ ,  $R_{\text{max}}$  are the fluorescence intensity ratios in the absence and presence of



saturating amounts of  $\text{Ca}^{2+}$ ;  $S_{\min}$  and  $S_{\max}$  are the fluorescence intensity at 380 nm in the absence and presence of saturating  $\text{Ca}^{2+}$ .

Similar calculations were conducted to obtain the dissociation constants of  $\text{Mg}^{2+}$  to Cu, Zn-SOD derivatives using furaptra (Scheme 3) as the fluorophore (Raju et al., 1989).

#### **III.4.5. Chloride Concentration Determination**

A chloride electrode and  $^{35}\text{Cl}$  NMR measurements were used to verify the concentration of  $\text{Cl}^-$  in the modified SOD.

The chloride electrode calibration curve of potential (mV) versus  $[\text{Cl}^-]$  ( $r^2 = 0.95$ ) was constructed by using standard NaCl solutions in the range of  $1.0 \times 10^{-5}$  to  $1.0 \times 10^{-4}$  M. For  $^{35}\text{Cl}$  NMR, the calibration curve of the area versus  $[\text{Cl}^-]$  ( $r^2 = 0.98$ ) was constructed by using standard NaCl solutions in the range of 2 to 12 mM.

## CHAPTER IV

### RESULTS

#### IV.1. Preparation and Characterization of Glu-modified Cu, Zn-SOD

##### IV.1.1. Preparation of Glu-modified Cu, Zn-SOD

To optimize the conditions that lead to a maximal yield of glutamate-modified Cu, Zn-SOD, we studied the coupling of EDC to protein at different ratios (see III.2.2). The Glu-modified Cu, Zn-SOD reaction mixture was dialyzed for 3 days to remove excess EDC and ammonium chloride. A chloride electrode and  $^{35}\text{Cl}$  NMR were used to verify the removal of chloride. In  $^{35}\text{Cl}$  NMR, the calibration curve of area versus  $[\text{Cl}^-]$  was constructed using standard NaCl solutions in the range of 2 to 12 mM; the estimated amount of chloride in the Glu-modified Cu, Zn-SOD was 0.11 mM ( $r^2 = 0.98$ ,  $n = 1$ ) (Table 4). The chloride electrode results (Table 5) showed that  $[\text{Cl}^-]$  in the Glu-modified Cu, Zn-SOD sample was 0.084 mM ( $r^2 = 0.95$ ,  $n = 2$ ).

Agarose gel electrophoresis of native and modified protein mixtures was carried out for 0.21 mM protein in 50 mM HEPES at pH  $7.4 \pm 0.1$ . Native Cu, Zn-SOD showed one very intense band by gel electrophoresis (Figure 4, Lane A), whereas unpurified modified protein mixtures of SOD showed two or more bands (Figure 4, Lanes B-F).

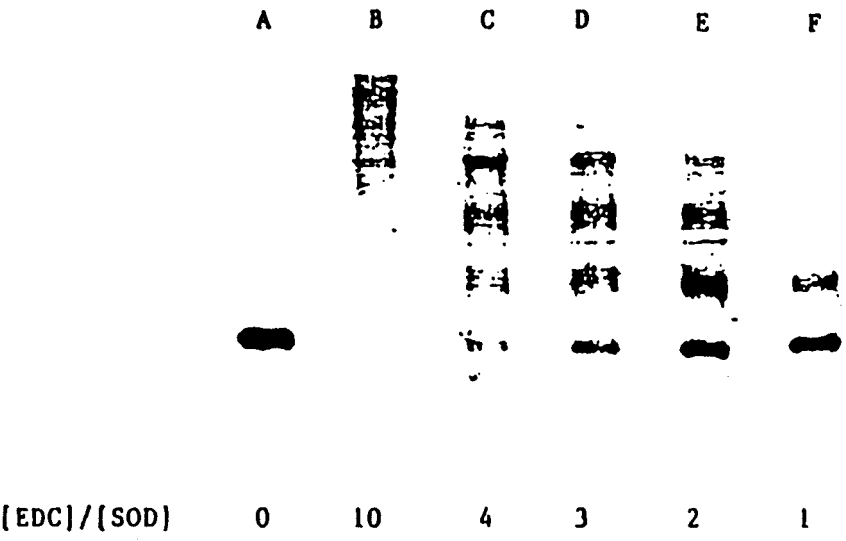
**Table 4.**  $^{35}\text{Cl}$  NMR measurements of dialyzed Glu-modified Cu, Zn-SOD solutions.

[Cl <sup>-</sup> ]/ mM	Area
2	0.858
4	1.936
6	3.285
9	4.453
12	5.758

**Table 5.** Chloride electrode measurements of dialyzed Glu-modified Cu, Zn-SOD solutions.

[Cl <sup>-</sup> ]/ mM	mV
0.01	185.2 ± 0.42
0.02	175.1 ± 0.47
0.04	161.8 ± 0.50
0.06	152.7 ± 0.45
0.10	140.4 ± 0.52

**Figure 4.** Agarose gel electrophoresis of native bovine Cu, Zn-SOD, lane A; and of modified Cu, Zn-SOD prepared in 5.5 M  $\text{NH}_4\text{Cl}$  in the ratios of EDC:Protein of 10, 4, 3, 2, 1 (lanes B, C, D, E, F, respectively). All samples contained 0.21 mM protein in 50 mM HEPES buffer at  $\text{pH } 7.4 \pm 0.1$ . The gel was stained with universal dye. The bottom of the figure corresponds to the anode.



The top bands resulted from modified Cu, Zn-SOD because the loaded protein moved from the positive electrode toward the negative electrode; by decreasing the negative charge in the modified protein as a result of the modification of the negatively charged carboxylate residues the mobility toward the anode decreased. Therefore the distances moved by the modified Cu, Zn-SOD components are less than that of native Cu, Zn-SOD. The bottom bands (Figure 4, Lanes B-F) moved the same distance as the native Cu, Zn-SOD band indicating that the modified protein reaction mixture contains some native protein.

The effect of the concentration of ammonium chloride on the coupling reaction showed that the intensity of the band of the modified protein increased as the concentration of ammonium chloride increased and reached a plateau for a concentration of 5.5 M  $\text{NH}_4\text{Cl}$  (data not shown). The yield of the modified protein was investigated by preparing the modified protein in 5.5 M  $\text{NH}_4\text{Cl}$  and different ratios of EDC: protein (1, 2, 3, 4, 10). Agarose gel electrophoresis of modified protein shows that the intensity of the modified protein band reached a maximum at the ratio 2:1 of EDC: Protein (Figure 4, Lane E). Densitometer data confirm these results (Table 6).

#### **IV.1.2. Purification of Glu-modified Cu, Zn-SOD**

The purification of modified Cu, Zn-SOD was accomplished by an FPLC system which showed that modified Cu, Zn-SOD (Figure 5, peak #2) could be separated from native Cu, Zn-SOD (Figure 5, peak #3). The purification by FPLC was verified by agarose electrophoresis (Figure 6, Lanes B & G).

**Table 6.** Densitometer results of gel electrophoresis.

EDC: Protein	% Yield	%Yield
Ratio	Modified SOD	Native SOD
1	29.7 <sup>a</sup>	70.3
2	39.6 <sup>a</sup>	46.9
3	32.3 <sup>a</sup>	25.4
4	23.0 <sup>a</sup>	8.5
10	0.0 <sup>b</sup>	0.0

<sup>a</sup>Obtained by adding all bands in the modified Cu, Zn-SOD mixture to 100%

<sup>b</sup>Quantitation not attempted because the band was not clearly defined.



**Figure 5.** Purification of modified Cu, Zn-SOD with an FPLC system using a Mono-Q 5/5 column. The eluting solution was a salt gradient of 0.0-0.15 M NaCl in 10 mM Tris-Cl buffer at pH  $7.5 \pm 0.1$ . The flow rate was 0.5 mL/min.

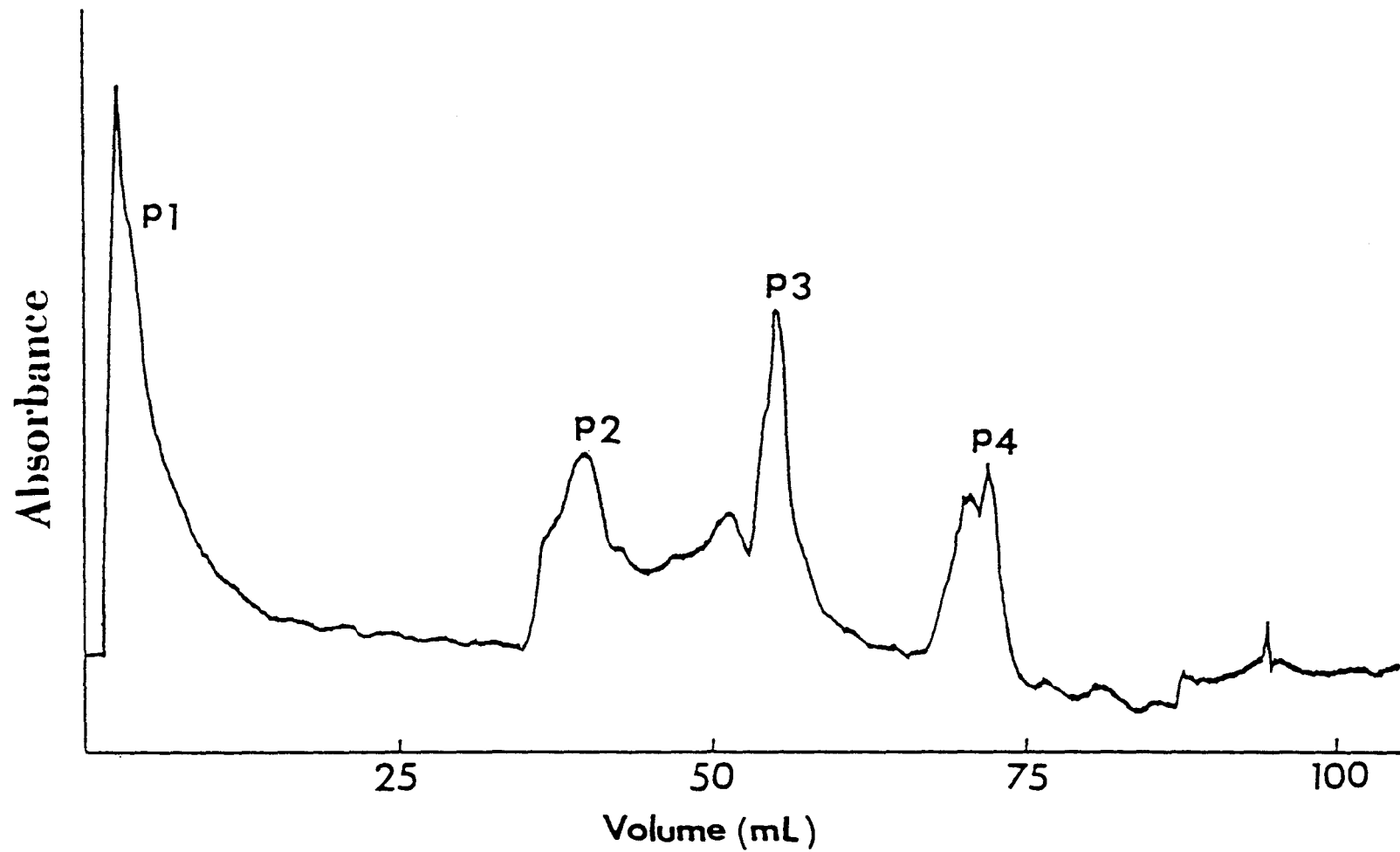


**Figure 6.** Agarose gel electrophoresis of native Cu, Zn-SOD (H), of the modified Cu, Zn-SOD reaction mixture (E), and of the effluents from FPLC peaks #1 (A), 2 (B&G), 3 (C&F), and 4 (D), respectively. All samples are in 50 mM Tris-Cl at pH 7.6. The protein concentration was 0.10-0.30 mM. The gel was stained with universal dye. The bottom of the figure corresponds to the anode.

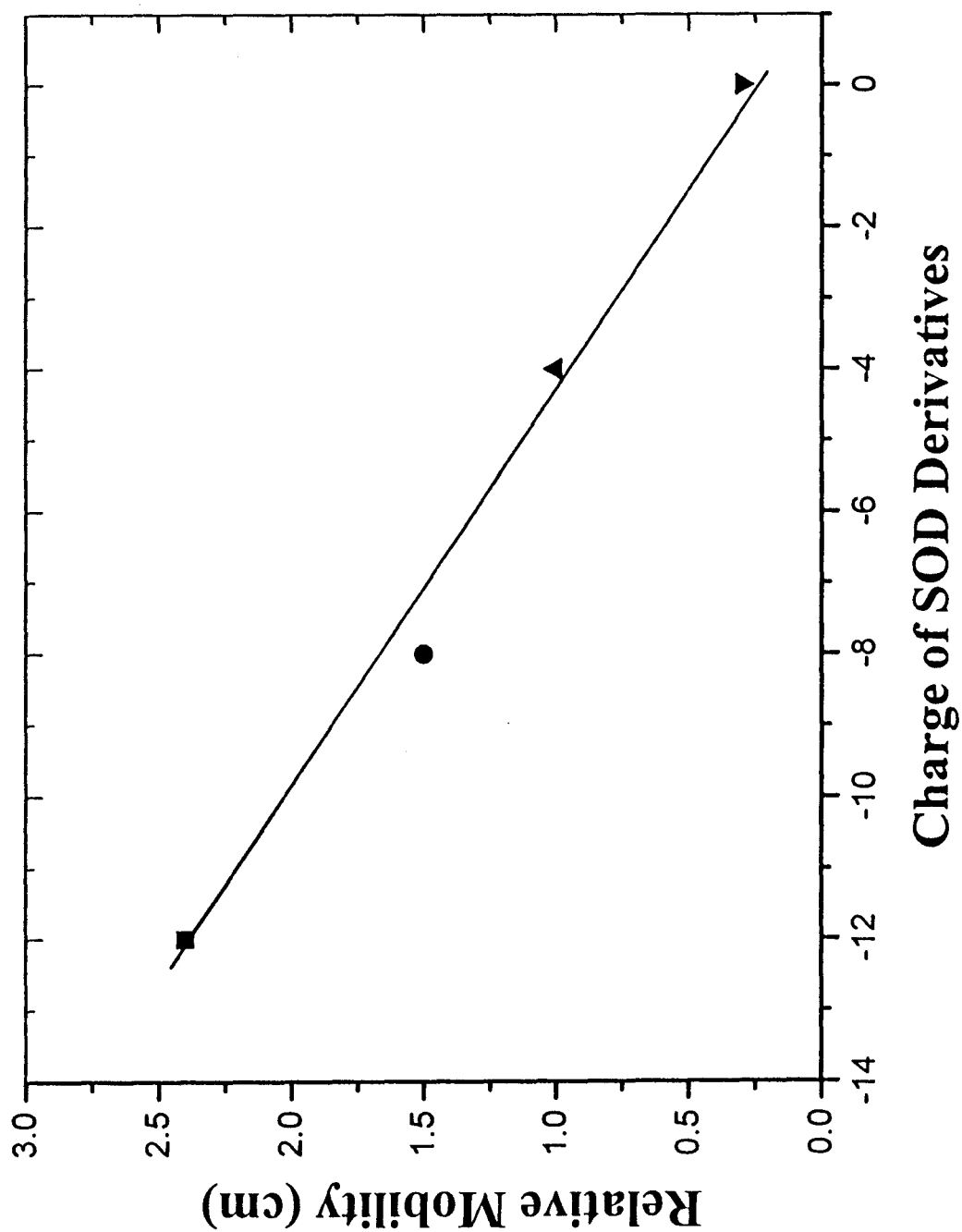


The assignment of peak #3 to native Cu, Zn-SOD was confirmed by two methods: (1) by addition of pure native Cu, Zn-SOD as a solid to the modified reaction mixture just before injection of the sample; the FPLC profile showed enlargement of peak #3; and (2) by injection of pure native Cu, Zn-SOD solution using the same gradient used for the modified solution; the FPLC profile showed one peak at the same position as peak #3. Moreover, gel electrophoresis of the peak #3 moved the same distance as native protein (Figure 6, Lanes C, F, and H), and has the same activity as native Cu, Zn-SOD. Peak #4, which is more negative than native Cu, Zn-SOD, is probably an impurity which is difficult to remove from native Cu, Zn-SOD or because of an artifact. Gel electrophoresis also showed a faint band which moved toward the anode more than the native (Figure 6, Lane D). Peak #1 might have resulted from modification of many carboxyl groups because it is very positive and moved toward the cathode (Figure 6, Lane A). Figure 6, Lane E is for the reaction mixture before loading the protein on the FPLC system indicating the presence of modified and unreacted native Cu, Zn-SOD.

#### **IV.1.3. Determination of the Charge of Glu-modified Cu, Zn-SOD**

Agarose gel electrophoresis of Cu, Zn-SOD, E, Zn-SOD, E, E-SOD and Glu-modified Cu, Zn-SOD in 50 mM HEPES at pH 7.4 was used to estimate the number of modified glutamate residues. Figure 7 shows that a plot of the charges of these derivatives versus the relative mobility provides an estimate of the net charge of Glu-modified Cu, Zn-SOD. The net charge per dimer of modified Cu, Zn-SOD at pH 7.4 was

**Figure 7.** Plot of the overall net charges of E, E-SOD (■), E, Zn-SOD (●), Cu, Zn-SOD (▲), and Glu-modified Cu, Zn-SOD (▼) versus the relative mobility values in agarose electrophoresis at pH 7.4,  $r^2 = 0.97$ .



calculated to be zero. Based on the overall charge estimate of the Glu-modified Cu, Zn-SOD derivative, we conclude that two Glu residues per subunit were modified.

#### **IV.1.4. UV/visible Studies of the Interactions of Azide and Cyanide with Glu-modified and Native Cu, Zn-SOD**

The binding of the azide anion to native and Glu-modified Cu, Zn-SOD were followed by the changes in the absorbance of the azide-protein adducts as measured by UV/visible spectrophotometry. Figure 8 shows the addition of azide to both Glu-modified (A) or native (B) Cu, Zn-SOD gave a new charge transfer band at  $373 \pm 2$  nm ( $n = 3$ ). The increase in the absorbance of the azide-Glu-modified adducts was significantly higher than that of the azide-native adducts for the addition of the same azide equivalents. This observation indicates that Glu-modified Cu, Zn-SOD has higher affinity toward the azide anion than to native Cu, Zn-SOD. The azide binding constants of native and Glu-modified Cu, Zn-SOD were  $206 \pm 16$  M<sup>-1</sup> ( $n = 3$ ) and  $370 \pm 17$  M<sup>-1</sup> ( $n = 3$ ), respectively (Table 7).

Cyanide binding to native and Glu-modified Cu, Zn-SOD was studied in the presence of 0.2 - 0.5 mM of the protein, 100 mM HEPES, pH  $7.4 \pm 0.10$ , 0.10 mM EDTA, and NaF to adjust the ionic strength to 0.30 M. Addition of CN<sup>-</sup> caused the  $\lambda_{\max}$  for the d-d band to shift from  $680 \pm 4$  nm ( $n = 3$ ) and  $684 \pm 11$  nm ( $n = 3$ ) to  $547 \pm 8$  nm ( $n = 3$ ) and  $552 \pm 16$  nm ( $n = 3$ ) for native Cu, Zn-SOD (Figure 9, B) and Glu-modified Cu, Zn-SOD (Figure 9, A), respectively. The cyanide binding constants of native Cu, Zn-



**Figure 8.** UV/visible titration of Glu-modified (A) and of native Cu, Zn-SOD (B) with  $\text{NaN}_3$ . The titrations were carried out by using 1.3 mL of a 0.20 mM protein. Spectrum (a) is of protein alone. Spectra (b)-(f) correspond to the addition of 1, 2, 4, 10, and 100 equivalents of  $\text{NaN}_3$ .

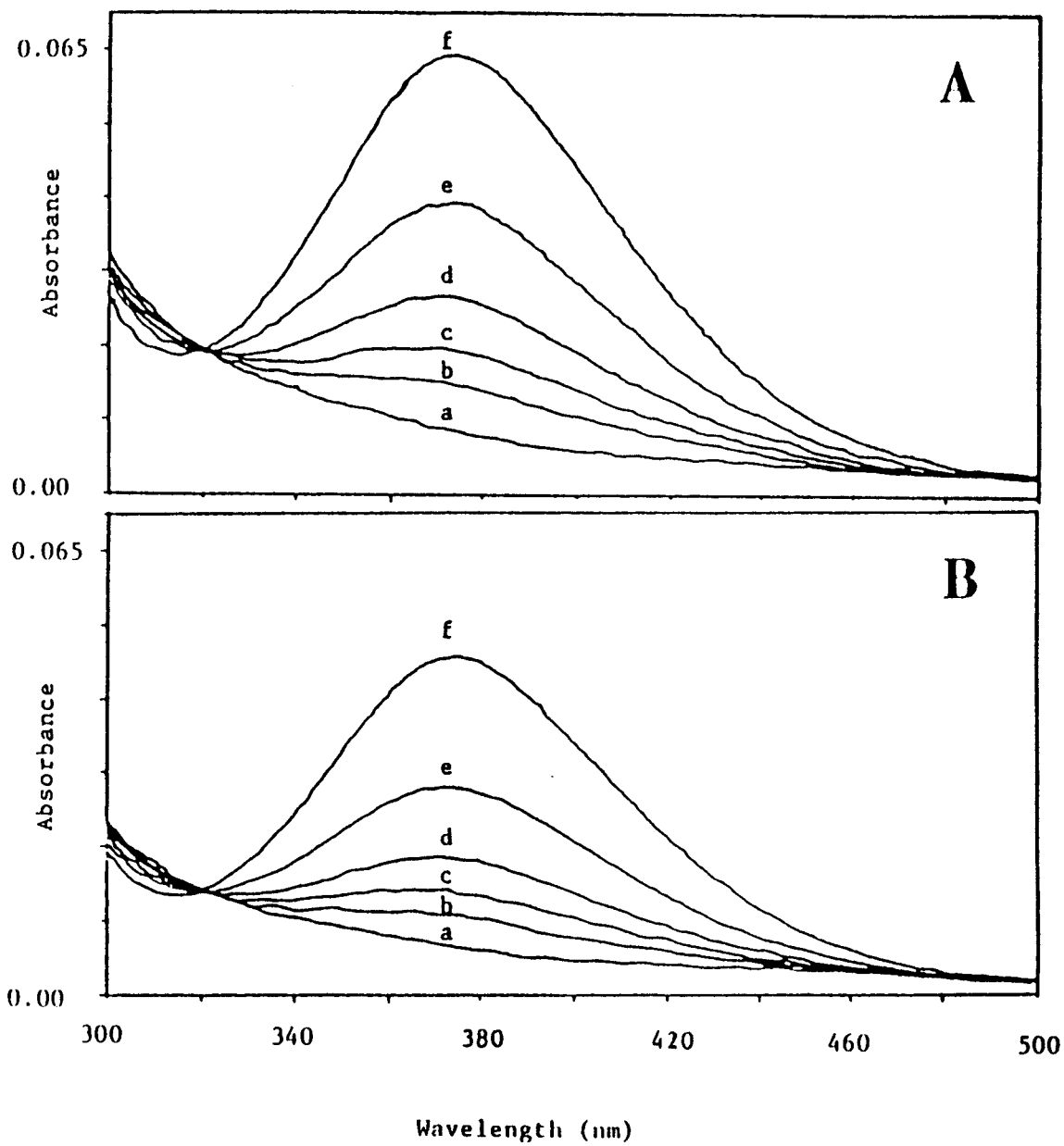
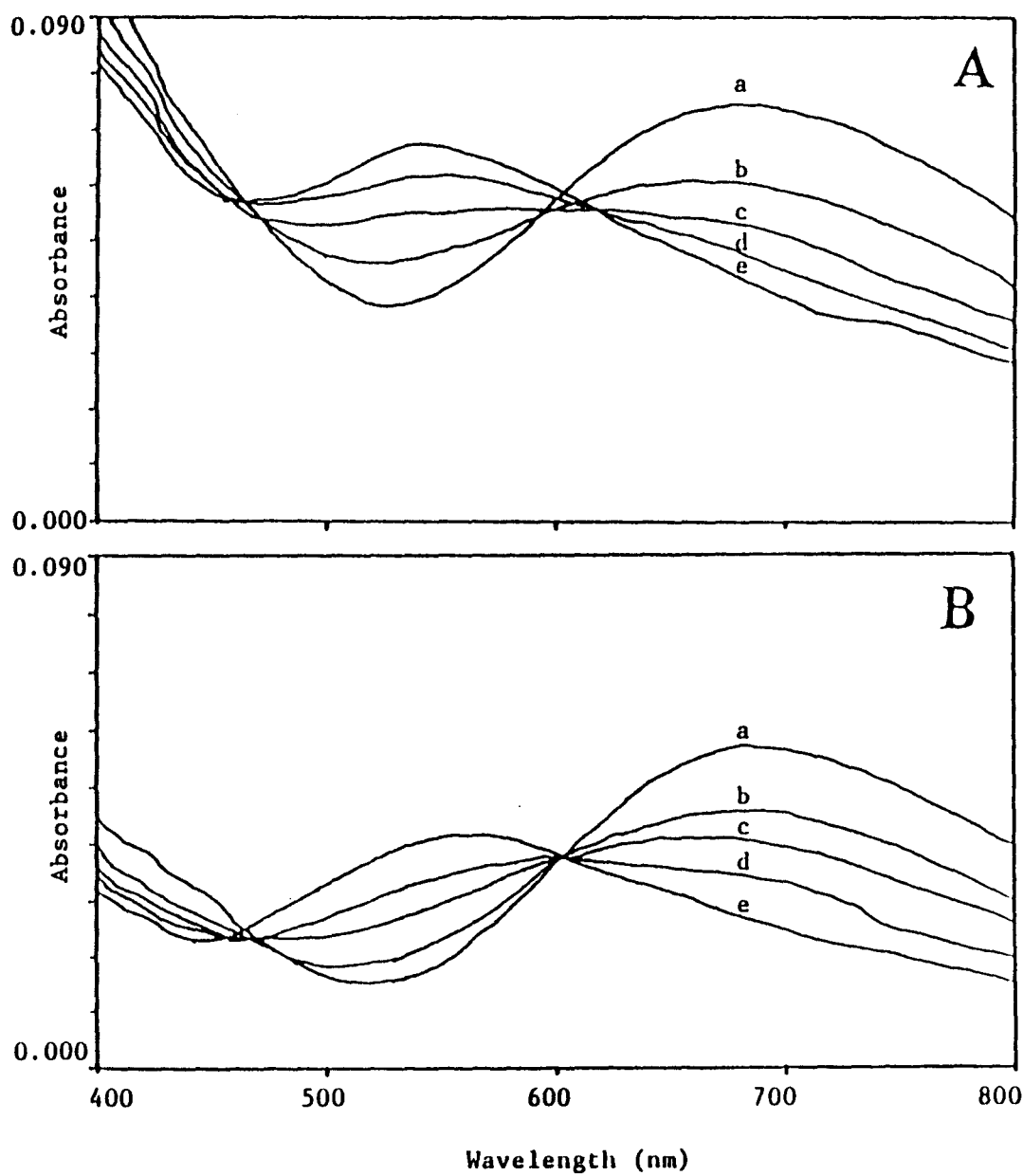


**Table 7.** Binding constant values of anions to Native and Modified Cu, Zn-SOD.<sup>a-d</sup>

Ligand	$K_b / M^{-1}$		
	Native SOD (n)	Modified SOD (n)	P
$N_3^-$	$206 \pm 16$ (3)	$370 \pm 17$ (3)	0.001
$CN^-$	$(1.43 \pm 0.08) \times 10^5$ (3)	$(2.20 \pm 0.24) \times 10^5$ (3)	0.006
$HPO_4^{2-}/H_2PO_4^-$	$28 \pm 2.0$ (3)	$173 \pm 20$ (3)	0.000

<sup>a</sup> The calculations of  $K_b$  for all ligands are described in III.4.1 and III.4.2. <sup>b</sup> The azide binding constant was calculated from the absorbance at 373 nm. <sup>c</sup>The cyanide binding constant was calculated by the method described in Rotilio et al. (1972b). <sup>d</sup>The phosphate binding constant was calculated from a James-Noggle plot (1969).  $P \leq 0.05$  is considered significantly different.

**Figure 9.** UV/visible titration of Glu-modified Cu, Zn-SOD (A) and of native Cu, Zn-SOD (B) with KCN. The titration was carried out using 1.3 mL of 0.25 mM protein in 100 mM HEPES, pH  $7.4 \pm 0.1$ , 0.10 mM EDTA, and NaF to adjust the ionic strength to 0.3 M. Spectrum (a) is of protein alone. Spectra (b) to (e) correspond to the addition of 0.5, 1.0, 2.0, and 4.0 equivalents of KCN. The KCN solutions were prepared in 100 mM HEPES buffer just prior to titration.



SOD and Glu-modified Cu, Zn-SOD were  $(1.43 \pm 0.08) \times 10^5$  ( $n = 3$ ) and  $(2.20 \pm 0.24) \times 10^5$  ( $n = 3$ ), respectively (Table 7). The results indicate that the cyanide binding constant of Glu-modified Cu, Zn-SOD was larger than that of native Cu, Zn-SOD. The cyanide binding constant reported here for native Cu, Zn-SOD is in agreement with that reported previously (Mota de Freitas & Valentine, 1984).

#### **IV.1.5. $^{31}\text{P}$ NMR Studies of the Interaction of Phosphate with Glu-modified and Native Cu, Zn-SOD**

Figure 10 shows that the spin-lattice relaxation time ( $T_1$ ) values of phosphate with Glu-modified Cu, Zn-SOD were lower than those with native Cu, Zn-SOD suggesting that the interaction of phosphate with Glu-modified Cu, Zn-SOD was greater than with native Cu, Zn-SOD. The phosphate binding constants at pH 7.0 of native and modified Cu, Zn-SOD were  $28 \pm 2.0 \text{ M}^{-1}$  ( $n = 3$ ) and  $173 \pm 20 \text{ M}^{-1}$  ( $n = 3$ ), respectively, as calculated from James-Noggle plots (Table 7). The reported  $K_b$  value for the native Cu, Zn-SOD with phosphate is  $34 \pm 3 \text{ M}^{-1}$  at pH 7.0 (Mota de Freitas et al., 1987).

#### **IV.1.6. $^{51}\text{V}$ NMR Studies of the Interaction of Vanadate with Glu-modified and Native Cu, Zn-SOD**

Figure 11 showed that addition of either native or Glu-modified Cu, Zn-SOD to vanadate caused significant decreases in the intensities of the dimeric ( $V_2$ ) and tetrameric

**Figure 10.**  $^{31}\text{P}$  NMR  $T_1$  relaxation values for native (upper trace) and Glu-modified (lower trace) Cu, Zn-SOD. All solutions contained 0.15 mM protein, 0.1 mM EDTA, 20%  $\text{D}_2\text{O}$ , and 50 mM HEPES, pH 7.0.

# $^{31}\text{P}$ $T_1$ Values

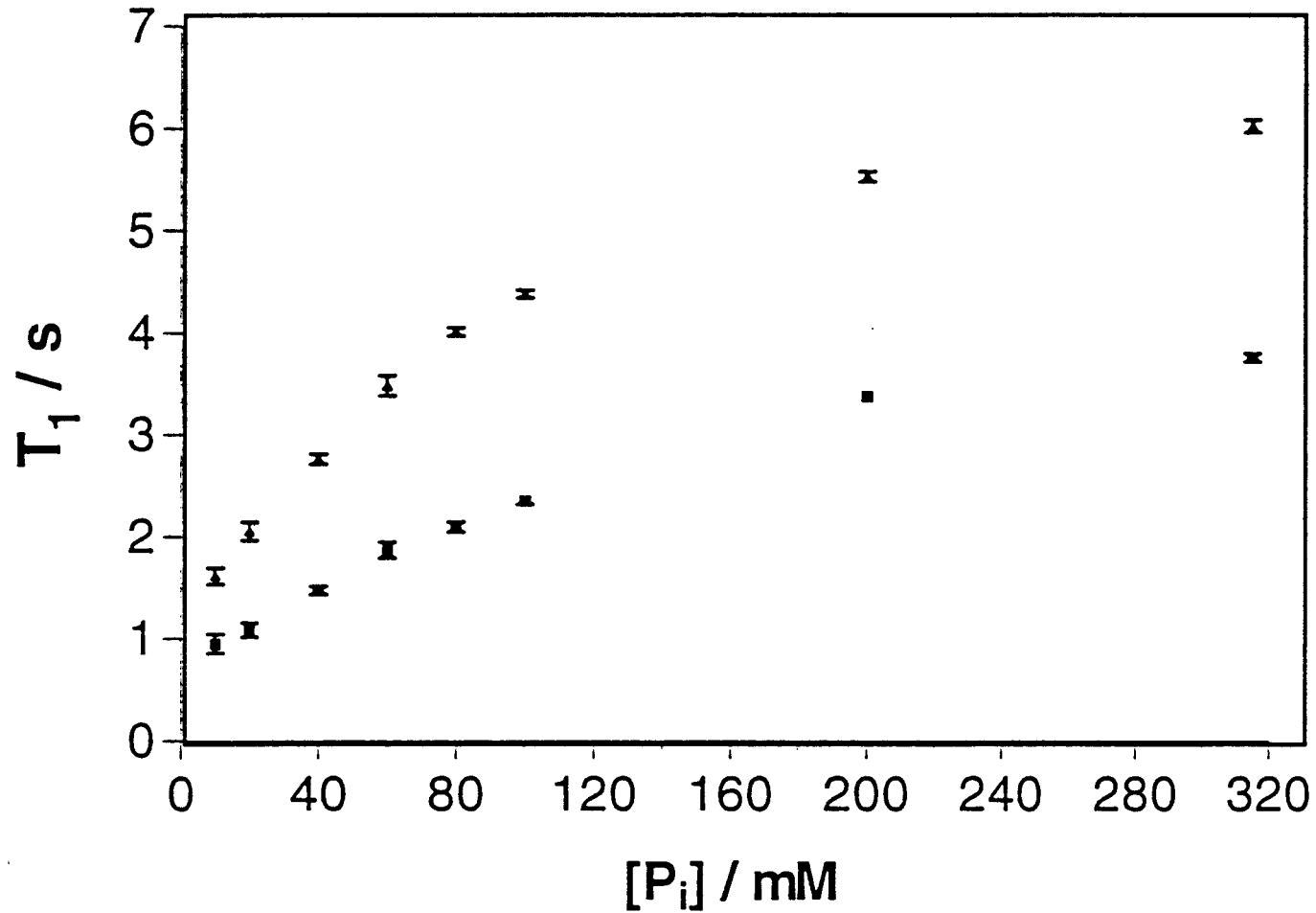
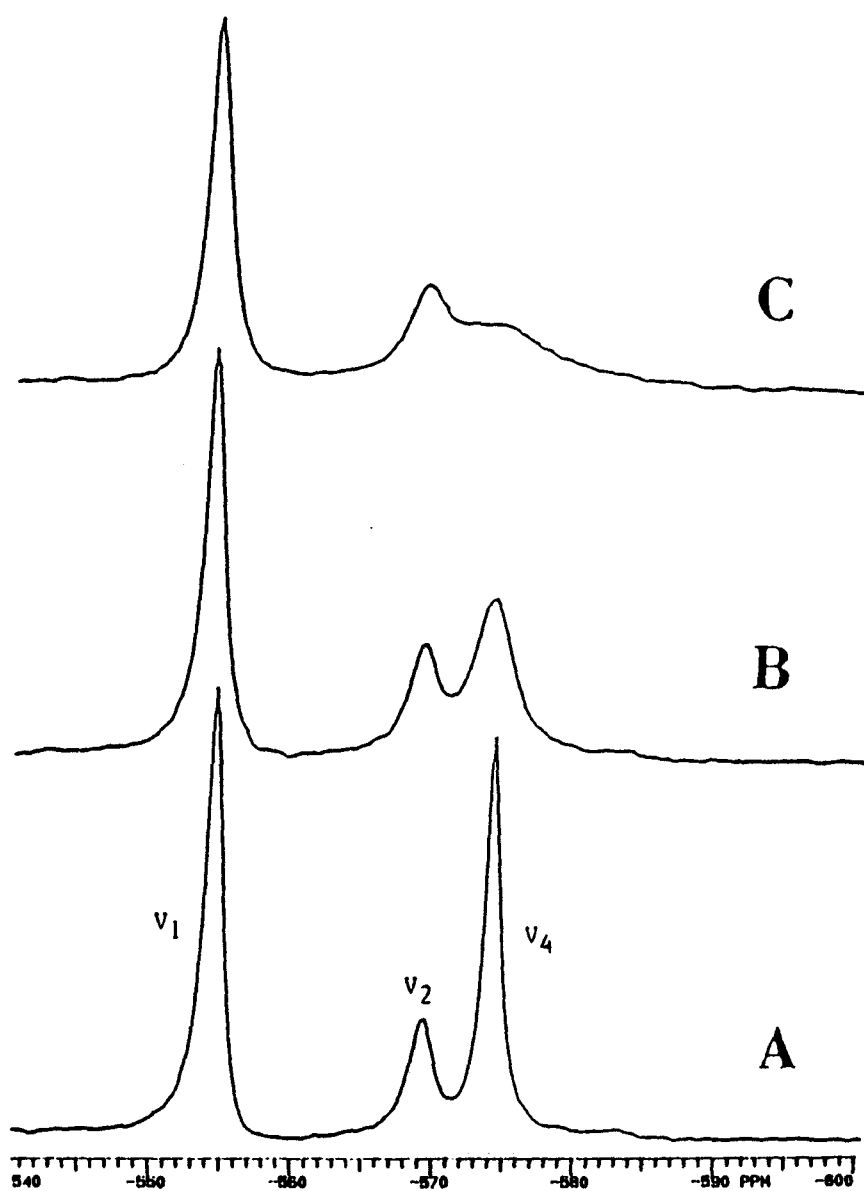




**Figure 11.**  $^{51}\text{V}$  NMR spectra of 2.0 mM vanadate in 0.10 M HEPES, pH 7.4, at 23° C in the absence (A), and in the presence of 0.05 mM native Cu, Zn-SOD (B) or 0.05 mM Glu-modified Cu, Zn-SOD (C).



(V<sub>4</sub>) vanadate <sup>51</sup>V NMR resonance. At the same concentration (0.05 mM) of both native and Glu-modified Cu, Zn-SOD, the decrease in the intensities of the <sup>51</sup>V resonance of vanadate anions in the presence of Glu-modified Cu, Zn-SOD (Figure 11, C) were significantly larger than those observed in the presence of native Cu, Zn-SOD (Figure 11, B) indicating that Glu-modified Cu, Zn-SOD interacts most strongly with vanadate than native Cu, Zn-SOD.

<sup>51</sup>V NMR chemical shift and line width values of the different forms of vanadate (namely monomer (V<sub>1</sub>), dimer (V<sub>2</sub>) and tetramer (V<sub>4</sub>)) present in a 2.0 mM vanadate solution in the absence and in the presence of 0.003 - 0.015 mM Glu-modified Cu, Zn-SOD are provided in Table 8. Figure 12 shows <sup>51</sup>V NMR spectra of 2.0 mM vanadate with increasing concentrations of Glu-modified Cu, Zn-SOD. There were no significant changes in the chemical shifts values of the vanadate monomer, dimer and tetramer with increasing concentrations of modified Cu, Zn-SOD. Addition of the modified Cu, Zn-SOD (0.003 - 0.015 mM) to the vanadate solution led, however, to an increase in the line widths of the vanadate tetramer (from 98.5 - 707.2 Hz). Much smaller changes in the line widths of the vanadate monomer (96.2 - 117.6 Hz) and dimer (151.4 - 242.8 Hz) were observed. The intensity of the vanadate tetramer decreased to a greater extent than those of the monomer and dimer. Concentrations of vanadate monomer, dimer and tetramer in the presence of increasing concentrations of Glu-modified Cu, Zn-SOD are provided in Table 9. The concentration of the tetramer decreased from 0.211 mM to 0.148 mM, while the monomer showed an increase from 0.881 mM to 0.987 mM, and that of the dimer increased from 0.137 to 0.196 mM.

**Table 8.**  $^{51}\text{V}$  Chemical shift and line width values of monomeric ( $V_1$ ), dimeric ( $V_2$ ), and tetrameric ( $V_4$ ) species in 2.0 mM vanadate in the absence and presence of Glu-modified Cu, Zn-SOD in 0.10 M HEPES, pH 7.4, at 23° C.<sup>a</sup>

	$V_1$	$V_2$	$V_4$
No Glu-modified Cu, Zn-SOD			
$\delta/\text{ppm}$	$-554.8 \pm 0.0$	$-569.6 \pm 0.2$	$-574.5 \pm 0.2$
$\Delta_{v1/2}/\text{Hz}$	$96.2 \pm 12$	$151.4 \pm 1.8$	$98.5 \pm 7.1$
0.003 mM Glu-modified Cu, Zn-SOD			
$\delta/\text{ppm}$	$-554.5 \pm 0.1$	$-569.6 \pm 0.1$	$-574.5 \pm 0.1$
$\Delta_{v1/2}/\text{Hz}$	$95.6 \pm 9.9$	$150.4 \pm 33.8$	$131.3 \pm 19.9$
0.005 mM Glu-modified Cu, Zn-SOD			
$\delta/\text{ppm}$	$-554.3 \pm 0.4$	$-569.6 \pm 0.1$	$-574.6 \pm 0.2$
$\Delta_{v1/2}/\text{Hz}$	$101.2 \pm 4.3$	$176.4 \pm 7.8$	$184.3 \pm 19$
0.010 mM Glu-modified Cu, Zn-SOD			
$\delta/\text{ppm}$	$-554.9 \pm 0.1$	$-569.5 \pm 0.1$	$-574.4 \pm 0.2$
$\Delta_{v1/2}/\text{Hz}$	$116.3 \pm 18.2$	$174.1 \pm 4.0$	$287.6 \pm 70$
0.012 mM Glu-modified Cu, Zn-SOD			
$\delta/\text{ppm}$	-554.8	-569.7	-574.5
$\Delta_{v1/2}/\text{Hz}$	103.1	209.5	294
0.015 mM Glu-modified Cu, Zn-SOD			
$\delta/\text{ppm}$	$-554.8 \pm 0.0$	$-569.6 \pm 0.1$	$-574.4 \pm 0.0$
$\Delta_{v1/2}/\text{Hz}$	$117.6 \pm 12$	$242.8 \pm 0.0$	$707.2 \pm 43$

<sup>a</sup>Chemical shifts and line widths are expressed as mean  $\pm$  range of 2 separate trials except at the concentration of 0.012 mM of Glu-modified Cu, Zn-SOD where only one sample was studied.

**Figure 12.**  $^{51}\text{V}$  NMR spectra of 2.0 mM vanadate in HEPES, pH 7.4, at 23° C in the absence (a) and in the presence of 0.003 mM (b), 0.005 mM (c), and 0.010 (d) Glu-modified Cu, Zn-SOD.

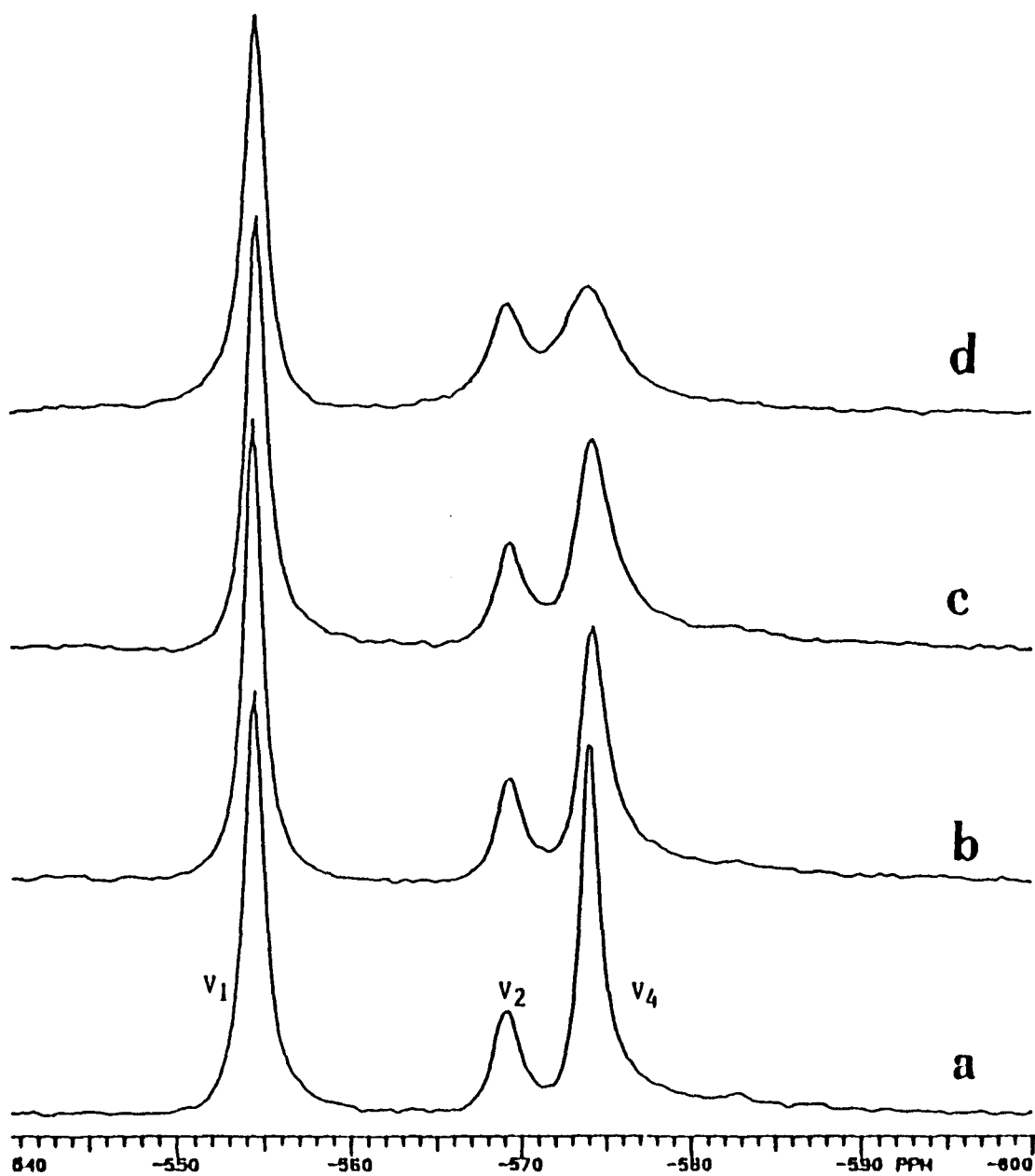


**Table 9.** Concentrations (mM) of vanadate species in the presence of increasing concentrations of Glu-modified Cu, Zn-SOD at pH 7.4 at 23° C in the 0.10 M HEPES containing 2 mM total vanadate.<sup>a</sup>

[SOD]	[V <sub>1</sub> ]	[V <sub>2</sub> ]	[V <sub>4</sub> ]	[V <sub>x</sub> .SOD] <sup>b</sup>
0.000	0.881	0.137	0.211	0.001
0.003	0.918	0.137	0.201	0.004
0.005	0.914	0.152	0.193	0.010
0.010	0.955	0.167	0.177	0.003
0.012	0.966	0.185	0.165	0.007
0.015	0.987	0.196	0.148	0.029
0.050	1.010	0.220	0.130	0.030

<sup>a</sup>The concentration of the vanadate species were calculated by the method described by Wittenkeller et al. (1991). <sup>b</sup>[V<sub>x</sub>SOD] represents the concentration of protein-bound vanadate calculated by the equation  $[V_xSOD] = [V]_{total} - [V_1]_{observed} - 2[V_2]_{calculated} - 4[V_4]_{calculated}$ .

#### **IV.1.7. Activity Assay for Glu-modified and Native Cu, Zn-SOD**

The enzyme activities, as determined by the indirect xanthine oxidase/cytochrome c assay method of native and Glu-modified Cu, Zn-SOD were investigated in phosphate and HEPES buffers (Table 10). Increasing phosphate concentrations resulted in decreases in the activities of both native and modified Cu, Zn-SOD. The enzyme activities of both native and modified Cu, Zn-SOD measured in 0.15 M HEPES, pH 7.8 were approximately 62% larger than those measured in 0.05 M phosphate pH 7.8 at the same ionic strength. Although the SOD activities of the Glu-modified derivative appear to be larger than those of native protein under all buffer conditions studied, these differences are not statistically significant (Student's unpaired t-test;  $P > 0.05$ ).

### **IV.2. Preparation and Characterization of the Vanadyl-SOD derivative**

#### **IV.2.1. Preparation and EPR Spectra and Parameters of the Vanadyl-SOD derivative**

When  $\text{VO}^{2+}$  was added to an oxygen-free solution of Apo-SOD (E, E-SOD) containing 0.10 M HEPES at pH 7.4 no color change was observed, but a frozen EPR spectrum was produced (Figure 13) indicating binding of the vanadyl ion to the protein. The appearance of a single set of lines indicated by the low field resonances (labeled by a & b) (Figure 13) suggest that one vanadyl bound environment is contributing to the spectrum.

Figure 14 shows the results of EPR titrations at pH 7.4. The peak-to-peak intensity of the X-band spectra was plotted as a function of  $\text{VO}^{2+}$  added to apo protein.



**Table 10.** SOD activity of native and Glu-modified bovine Cu, Zn-SOD as determined by the xanthine oxidase/cytochrome c assay (McCord & Fridovich, 1969).<sup>a</sup>

Buffer	[buffer]/ mM	Native SOD (n)	Modified SOD (n)	P
Phosphate	50.0	$(4.11 \pm 0.06) \times 10^3$ (7)	$(4.26 \pm 0.17) \times 10^3$ (5)	0.153
Phosphate	30.0	$(4.76 \pm 0.04) \times 10^3$ (3)	$(4.95 \pm 0.26) \times 10^3$ (3)	0.318
Phosphate	20.0	$(5.36 \pm 0.11) \times 10^3$ (3)	$(5.69 \pm 0.21) \times 10^3$ (3)	0.120
HEPES	150	$(6.69 \pm 0.44) \times 10^3$ (3)	$(6.67 \pm 0.37) \times 10^3$ (3)	0.952

<sup>a</sup>All buffers contained 0.1 mM EDTA and were adjusted to an ionic strength of 0.15 by adding appropriate amount of HEPES, at pH 7.8. The letter n in parenthesis indicates the number of separately prepared samples measured.  $P \leq 0.05$  is considered significantly different.

**Figure 13.** X-band EPR spectrum of  $\text{VO}^{2+}$  in a frozen solution (77 K) of apo protein (E, E-SOD) in the presence of 0.1 M HEPES, pH 7.4, and dithionite. The vanadyl:protein:dithionite ratio was 2:1:4. Spectrometer conditions: microwave frequency, 9.1 GHz; microwave power, 5 mW; modulation frequency, 100 kHz, modulation amplitude, 5 G, receiver gain,  $1.0 \times 10^3$ .

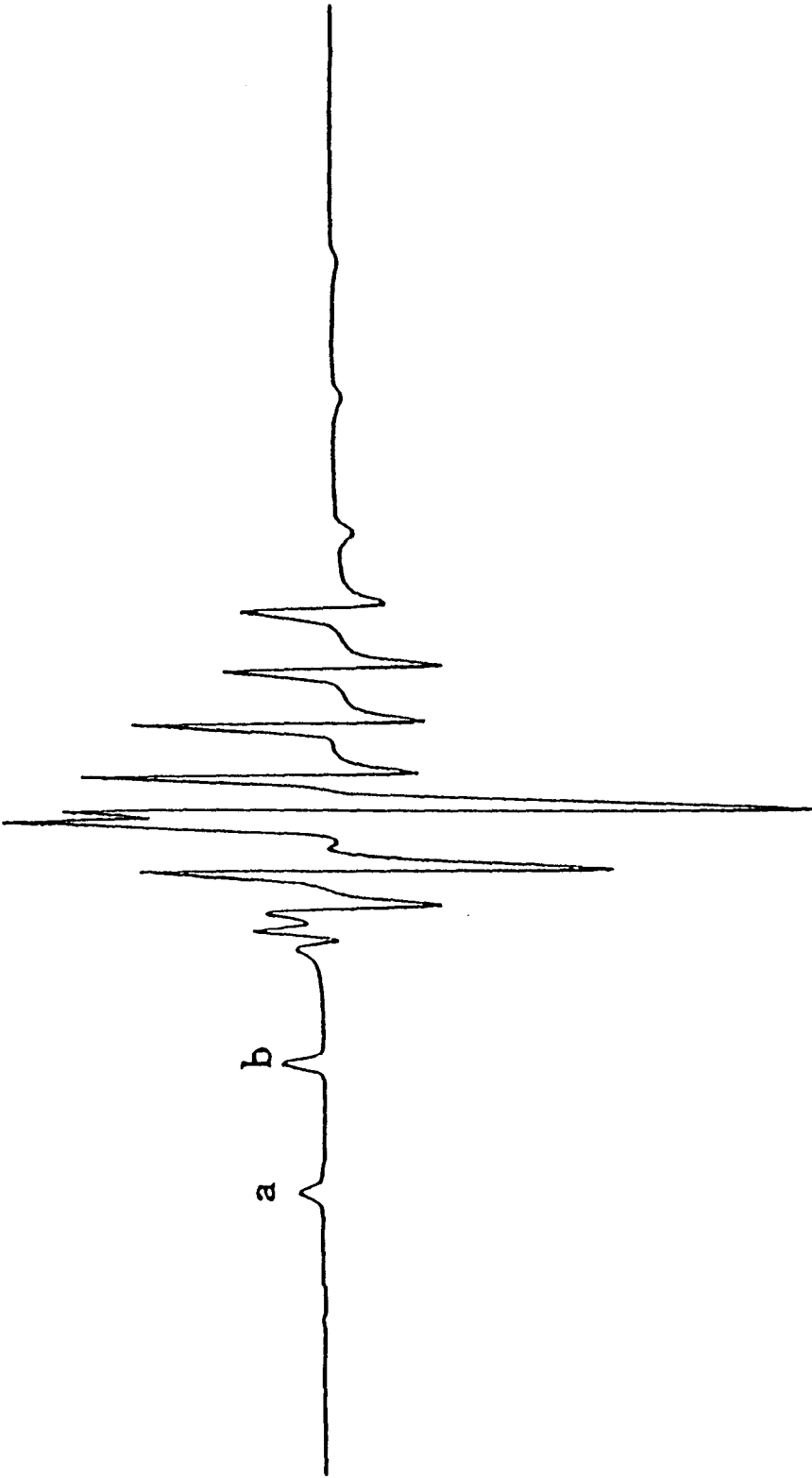
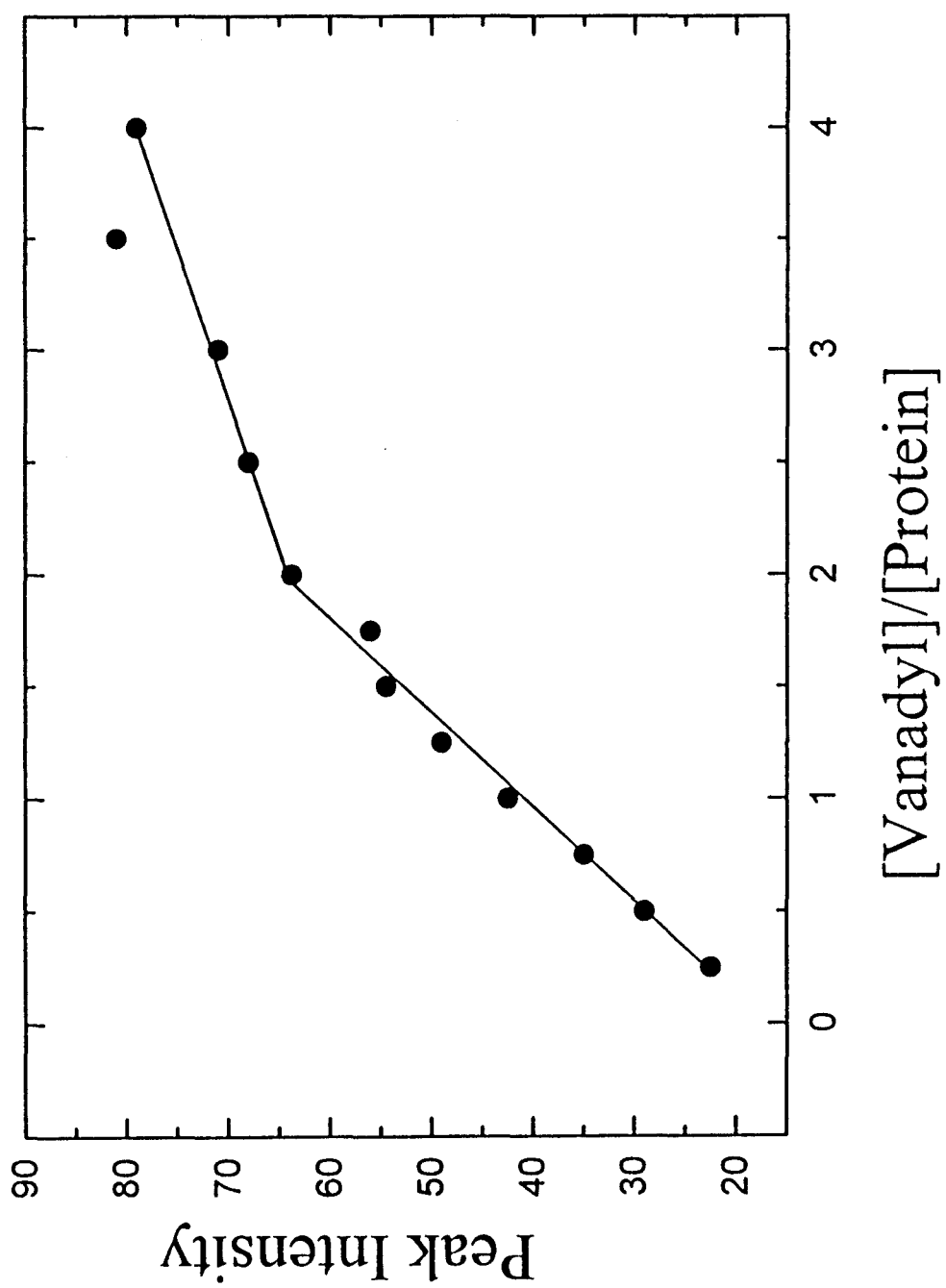


**Figure 14.** EPR titration of 0.6 mM apo protein (E, E-SOD) in 0.1 M HEPES, pH 7.4 with  $\text{VO}^{2+}$ . Intensity is based on the intensity of Peak (a) of the spectrum presented on Figure 13.



strong binding of vanadyl ion to the protein was observed when up to 2.0 equivalents of  $\text{VO}^{2+}$  ions were added per dimer of apo protein; at higher ratios (more than 2:1 of  $\text{VO}^{2+}$ :apo protein) the binding was, however, weak. The binding constant of the vanadyl-SOD derivative, calculated from the equilibrium expression (see III.4.3), was  $6.8 \times 10^4 \text{ M}^{-1}$  and the number of binding sites (n) per SOD dimer was 2.0.

Table 11 shows the EPR parameters of the vanadyl-SOD derivative, which were obtained from Figure 13. EPR parameters for  $\text{VO}^{2+}$  derivatives of other metalloproteins and of model compounds are also listed in Table 11. The values of  $g_{\parallel}$ ,  $g_{\perp}$ ,  $A_{\parallel}$ , and  $A_{\perp}$  observed for the vanadyl-SOD derivative suggested that there were 4 nitrogen atoms coordinated to the  $\text{VO}^{2+}$  ion.

The spectrum on Figure 15 was obtained for the zinc-only derivative (E, Zn-SOD) with  $\text{VO}^{2+}$  in 0.10 M HEPES at pH 7.4, and under a nitrogen atmosphere to elucidate the binding site of vanadyl ion with the protein. A titration of the zinc-only derivative with  $\text{VO}^{2+}$  does not lead to increases in the intensity of the peaks (a) and (b) indicating that the occupation of the native zinc site prevents the binding of  $\text{VO}^{2+}$  to the native copper site.

At similar experimental conditions,  $\text{VO}^{2+}$  was added to native Cu, Zn-SOD to investigate whether the  $\text{VO}^{2+}$  ion bound to the vacant sites of  $\text{Cu}^{2+}$  and  $\text{Zn}^{2+}$  in the apo protein or to the negatively charged residues of the protein. A typical  $\text{Cu}^{2+}$  EPR spectrum was produced (Figure 16) indicating that the vanadyl ion bound to either the native copper or zinc sites in apo protein. The absence of EPR lines of free  $\text{VO}^{2+}$  was due to the formation of  $\text{VO}^{2+}$  polymer in basic medium, pH 7.4 (Chasteen et al., 1981, Makinen &

**Table 11.** EPR parameters of the vanadyl-SOD derivative and model compounds.<sup>a</sup>

Protein	Probable Ligands	$g_{\parallel}$	$g_{\perp}$	$A_{\parallel}^b$	$A_{\perp}^b$	$K_b/M^{-1}$	Reference
Vanadyl-SOD	4 histidines	1.955	2.007	163.4	65.4	$6.8 \times 10^4$	This work
$VO^{2+}-(\text{imidazole})_4$	4 imidazole	1.952	1.981	162.2	57.4	Not reported <sup>c</sup>	Bogumil et al., 1991 <sup>d</sup>
Carbonic Anhydrase	3 histidines	1.943	1.977	167.7	62.1	$1.0 \times 10^{10}$	Fitzgerald & Chasteen, 1974.
Carboxypeptidase A	2 histidines	1.944	1.978	165.9	61.1	Not reported	DeKoch et al., 1974
Albumin (Strong)	1 histidine	1.939	1.979	172.8	64.0	$2.3 \times 10^6$	Chasteen & Francavilla, 1976
(Weak)	1 histidine	1.938	1.979	177.1	65.0	$2.5 \times 10^4$	Chasteen & Francavilla, 1976
$VO(H_2O)_5^{2+}$	5 waters	1.932	1.980	182.8	71.3	----- <sup>c</sup>	Makinen & Mustafi, 1995 <sup>e</sup>

<sup>a</sup>All parameters were obtained from aqueous frozen solutions. <sup>b</sup>Units of  $10^{-4} \text{ cm}^{-1}$ . <sup>c</sup>Not a protein derivative. <sup>d</sup>See also Mulks et al., 1982.

<sup>e</sup>See also Chasteen et al., 1973.

**Figure 15.** X-band EPR spectrum of a frozen solution (77 K) of the zinc-only derivative (E, Zn-SOD) at 0.60 mM containing 2 equivalents of  $\text{VO}^{2+}$ , 0.1 M HEPES, pH 7.4, and dithionite. The dithionite:protein ratio was 4:1. Spectrometer conditions: microwave frequency, 9.1 GHz; microwave power, 5 mW; modulation frequency, 100 kHz, modulation amplitude, 5 G, receiver gain,  $2.0 \times 10^4$ .



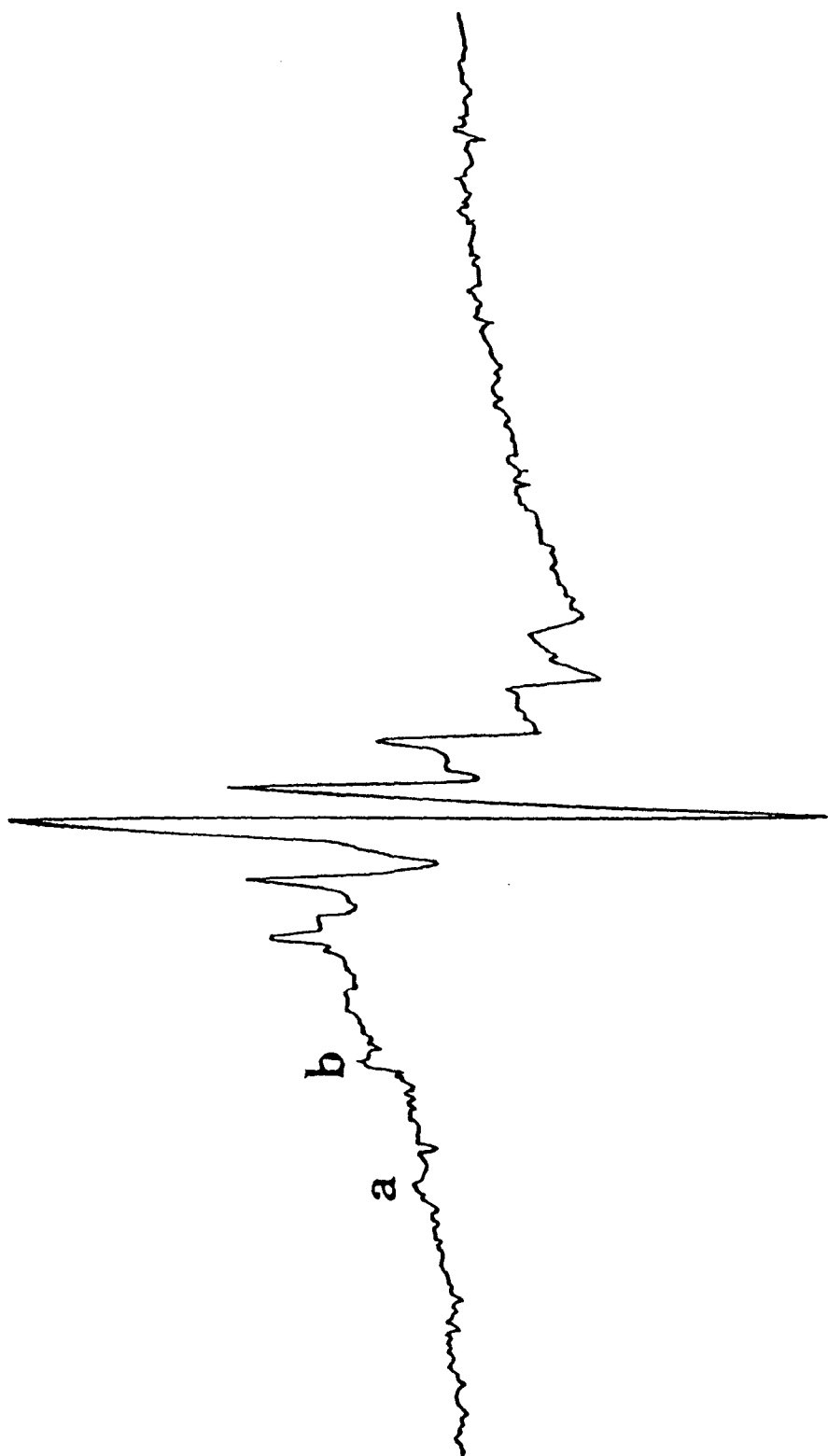
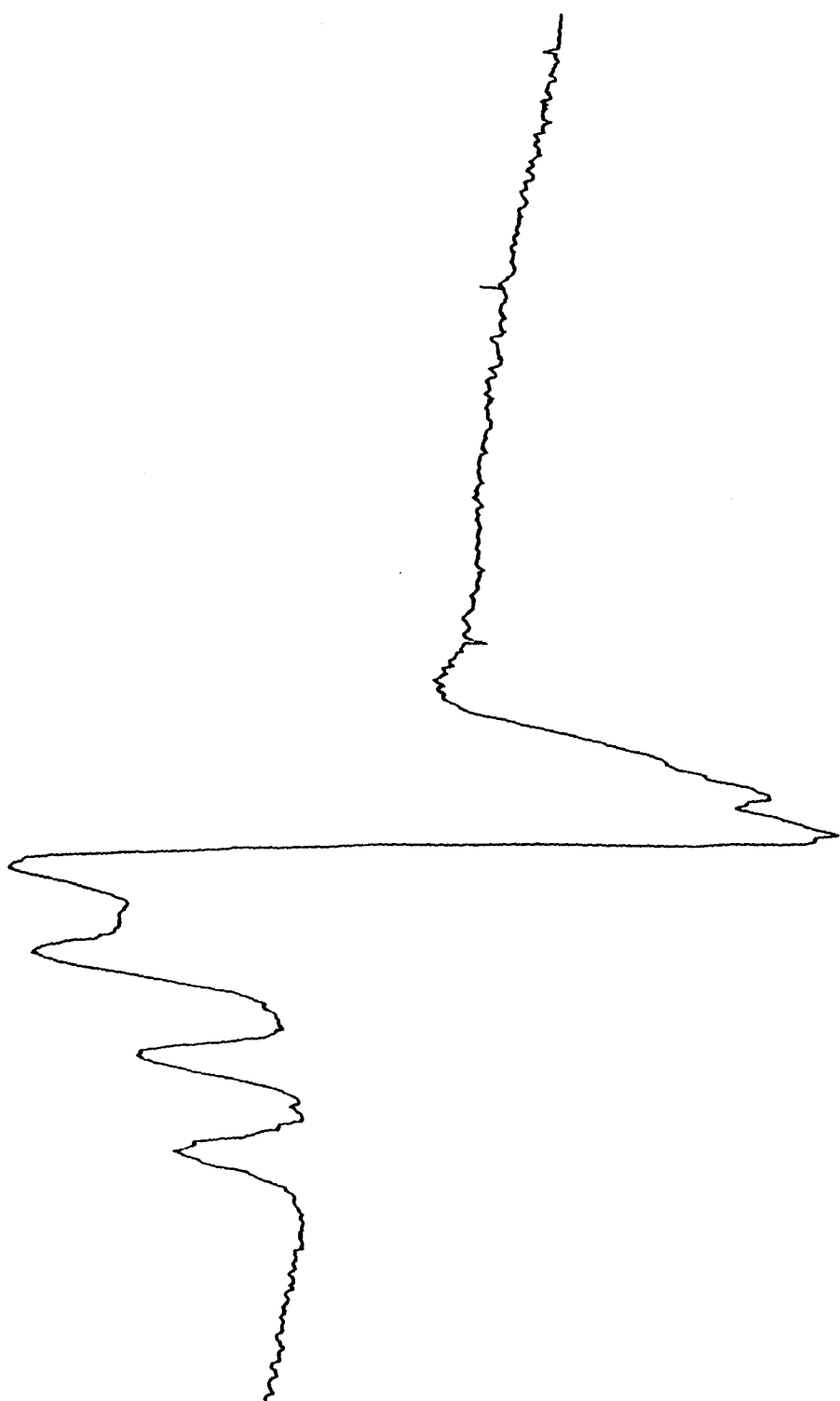


**Figure 16.** X-band EPR spectrum of a frozen solution of native Cu, Zn-SOD (0.60 mM) in the presence of  $\text{VO}^{2+}$  (1.2 mM), 0.1 M HEPES, pH 7.4, and dithionite at a 4:1 dithionite:protein ratio. Spectrometer conditions: microwave frequency, 9.1 GHz; microwave power, 5 mW; modulation frequency, 100 kHz, modulation amplitude, 5 G, receiver gain,  $1.0 \times 10^4$ .



Mustafi, 1995).

Figure 17 shows the changes in the EPR intensity of peaks (a) and (b) (see Figure 13) upon exposure of the  $\text{VO}^{2+}$ -SOD derivative to air after 40 and 90 minutes. The decreases in the intensities of the peaks (a) and (b) in Figure 13 indicate that a slow oxidation of the vanadyl ion occurred. There was no significant change in the overall EPR spectrum indicating that  $\text{VO}^{2+}$ -SOD is reasonably stable.

#### **IV.2.2. Activity Assay of the Vanadyl-SOD derivative**

The activity of  $\text{VO}^{2+}$ -SOD, apo E, E-SOD, and native Cu, Zn-SOD were measured as described by McCord and Fridovich (1969). The SOD activity of the vanadyl-SOD derivative was measured in the presence and absence (to prevent oxidation to vanadate) of  $\text{O}_2$ . The assay results of this derivative are given on Table 12. The SOD activity of the  $\text{VO}^{2+}$ -SOD derivative was < 5% of that of native Cu, Zn-SOD. The EPR spectrum of  $\text{VO}^{2+}$ -SOD under the conditions of the activity assay (data not shown) indicated that there were no significant changes in either the intensities or in the line shapes of the EPR resonances.

#### **IV.2.3. Cyclic Voltammetry of Native and Vanadyl-SOD derivatives**

Cyclic voltammetry experiments were performed on native Cu, Zn-SOD and on the vanadyl-SOD derivative as described by Verhagen et al. (1995) (Figure 18).

**Figure 17.** Air stability of the  $\text{VO}^{2+}$ -SOD derivative on the features of the 77 K EPR spectrum (similar experimental conditions as in Figure 13). The region shown corresponds to the inset of Figure 13: (a) immediately, (b) 40 minutes; and (c), 90 minutes after exposure to air.

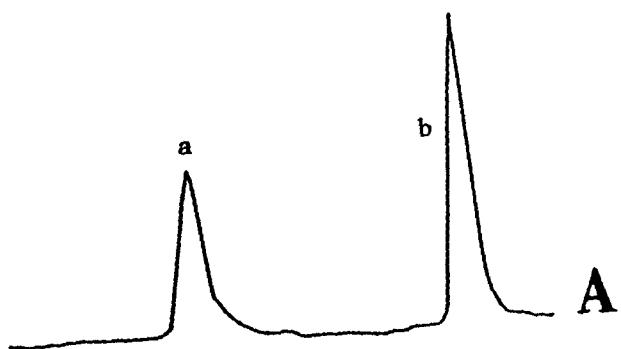
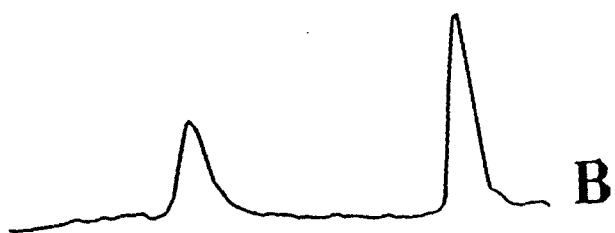


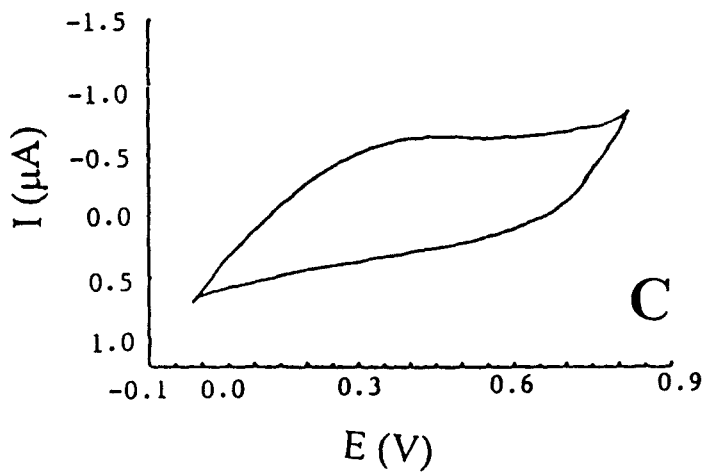
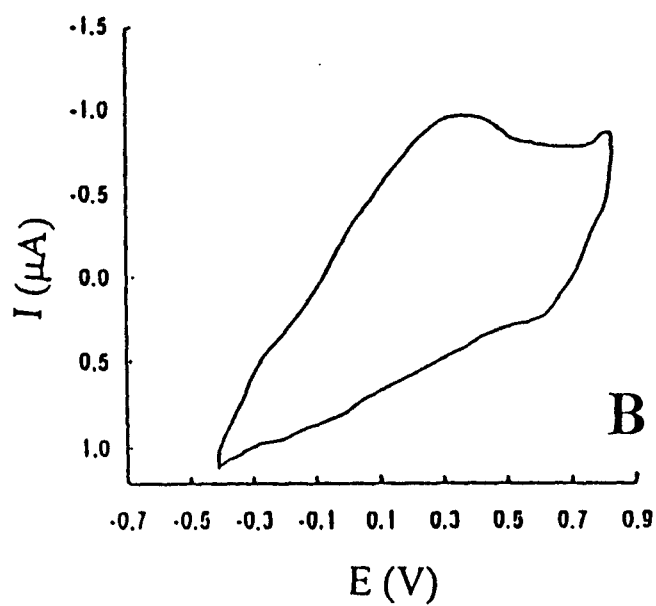
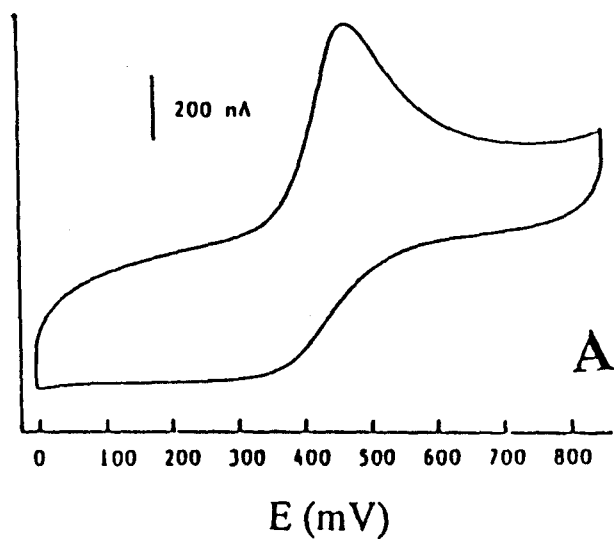
**Table 12.** SOD activity of the vanadyl-SOD derivative as determined by the xanthine oxidase/cytochrome c assay.<sup>a</sup>

Protein	Unit/mg
Vanadyl-SOD Derivative	$153 \pm 13$ (2) <sup>b</sup>
Vanadyl-SOD Derivative	$109 \pm 3.0$ (3)
Native Cu, Zn-SOD	$(4.11 \pm 0.06) \times 10^3$ (7)
Apo E, E-SOD	$86.3 \pm 17$ (3)

<sup>a</sup>All samples are in 50 mM phosphate, pH 7.8, 0.1 mM EDTA. <sup>b</sup>The activity assay was done under nitrogen atmosphere.

**Figure 18.** (A) Cyclic voltammogram of 2 mg/mL native Cu, Zn-SOD in 50 mM sodium acetate buffer (pH 4.0) containing 50 mM  $\text{Sc}^{3+}$  (adapted from Verhagen et al., 1995). Cyclic voltammograms of 3 mg/mL of native Cu, Zn-SOD (B) or of  $\text{VO}^{2+}$ -SOD (C) in 50 mM sodium acetate buffer (pH 4.0) containing 70 mM  $\text{Sc}^{3+}$ . Voltammograms were recorded at a scan rate of 10 mV/s.





Usually, an estimate of midpoint was made by taking the average of the anodic and cathodic peak potentials. We report the peak potential of the protein because it was difficult to obtain the midpoint (see Chapter V). This resulted in a value of +300 mV and +425 mV for native Cu, Zn-SOD (Figure 18, B) and the vanadyl-SOD derivative (Figure 18, C) at pH 4.0, respectively. The reported peak potential of the native Cu, Zn-SOD at pH 4.0 is +470 mV (Verhagen et al., 1995) (Figure 18, A).

The reported cyclic voltammogram of native Cu, Zn-SOD derivative by Verhagen et al. (1995) was asymmetric and had a sharp anodic peak (Figure 18, A). We were unable to reproduce the sharp anodic peak; this sharp anodic peak is unusual for the cyclic voltammogram of a metalloprotein in which the active site is not located close to the protein surface.

### **IV.3. Cationic Interactions with SOD Derivatives**

#### **IV.3.1. Fluorescence Studies of the Interactions of $\text{Ca}^{2+}$ and $\text{Mg}^{2+}$ with Native Cu, Zn-SOD and Apo-SOD**

Addition of  $\text{Ca}^{2+}$  to 2  $\mu\text{M}$  fura-2 in 150 mM Tris-Cl, pH  $7.4 \pm 0.1$ , and 0.03 mM EGTA caused a blue shift in the fluorescence excitation spectrum (Figure 19, A), as previously reported (Gynkiewicz et al., 1985). We found that the fura-2 parameters were  $R_{\min} = 0.58 \pm 0.03$ ,  $R_{\max} = 12.98 \pm 0.8$ ,  $S_{\min}/S_{\max} = 5.80 \pm 0.29$ , and  $K_d = 38.48 \pm 1.59$  mM ( $r^2 > 0.85$ ,  $n = 8$ ).

**Figure 19** Fluorescence excitation spectra of 2  $\mu\text{M}$  Fura-2 alone (A), and in the presence of 0.10 mM native Cu, Zn-SOD (B) or 0.10 mM apo-SOD (C) in solutions containing 0.03 mM EGTA, 150 mM Tris-Cl, at pH  $7.4 \pm 0.1$ . Spectra (a) to (e) correspond to the addition of 0.0, 30, 35, 43, and 60 nM  $\text{Ca}^{2+}$ .

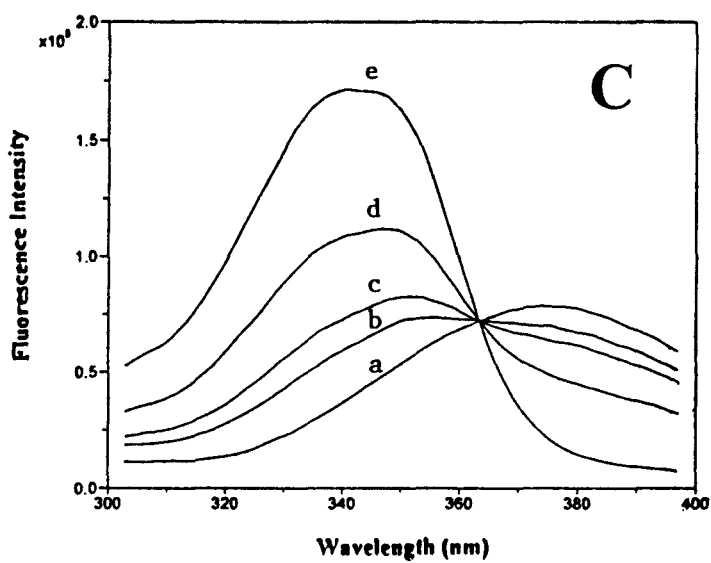
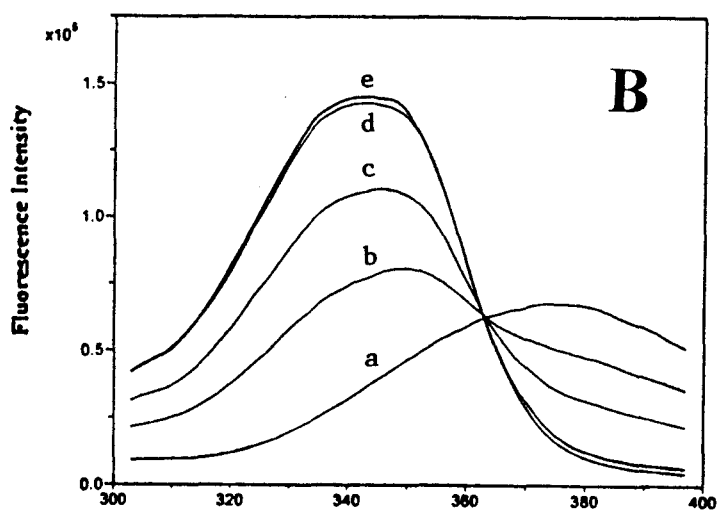
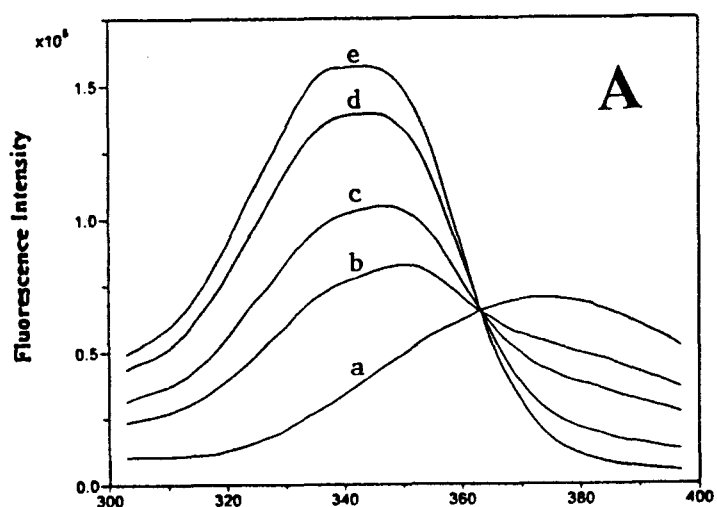
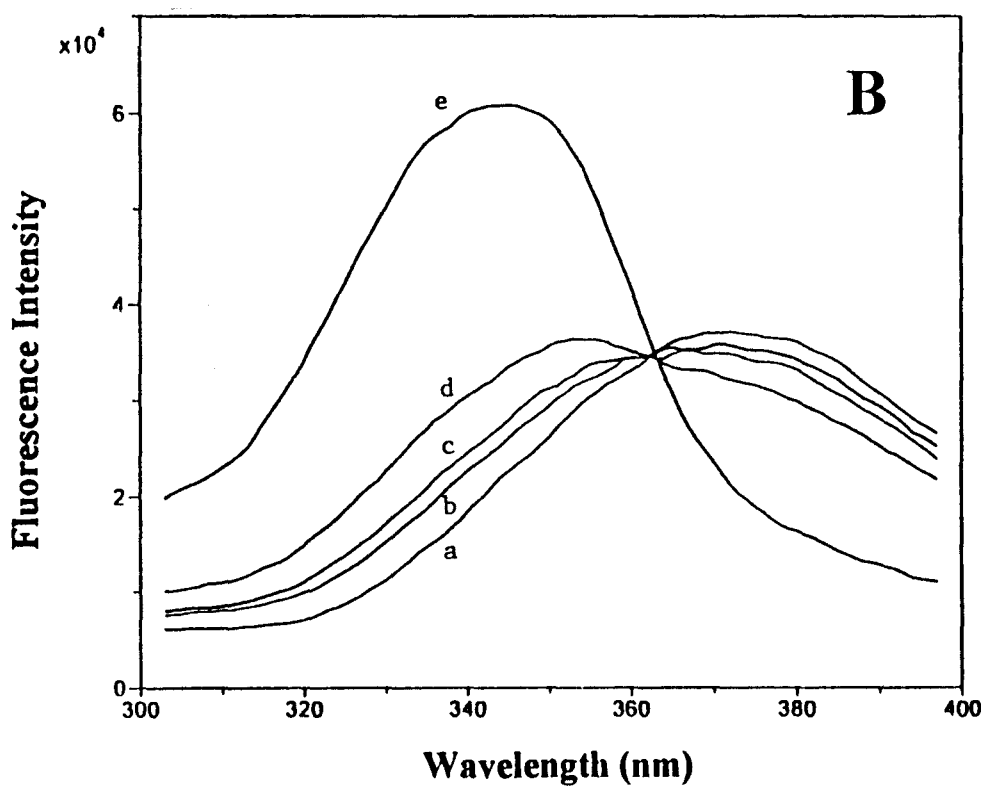
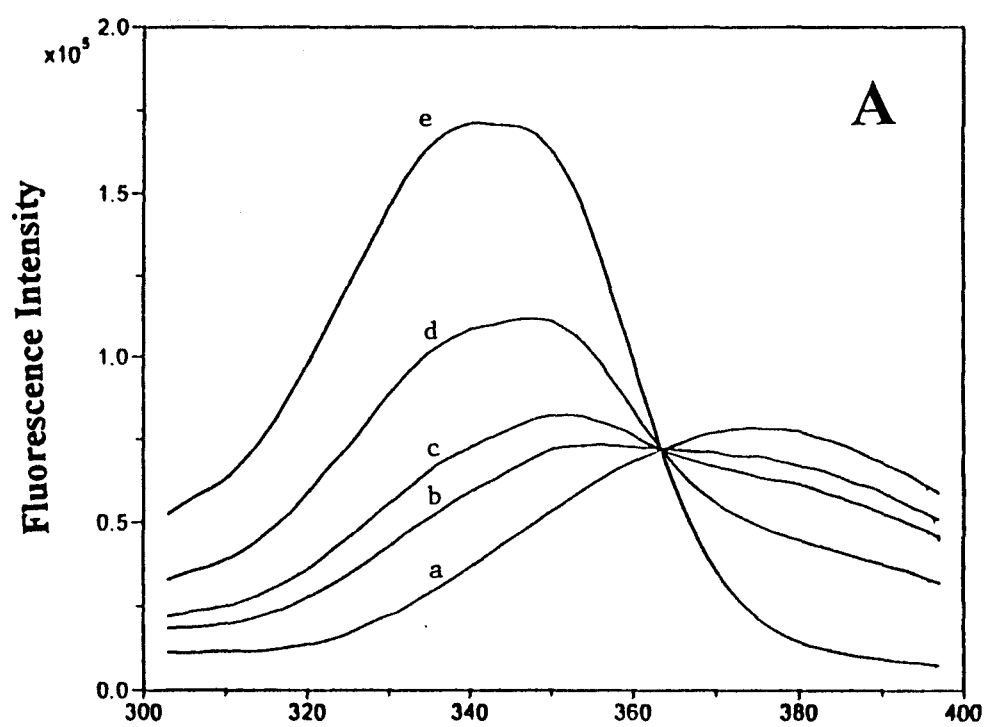


Figure 19 shows the excitation spectra corresponding to  $\text{Ca}^{2+}$  titrations of fura-2 only (Figure 19, A), fura-2 in the presence of 0.10 mM native Cu, Zn-SOD (Figure 19, B), and fura-2 in the presence of 0.10 mM apo-SOD (Figure 19, C) titrated with  $\text{Ca}^{2+}$ , respectively. In the absence of  $\text{Ca}^{2+}$ , the excitation spectra of free dye did not change appreciably in the presence of either native Cu, Zn-SOD or apo protein (spectra a in Figure 19, A, B & C) indicating that there were no specific interactions between the dye and the protein. The similarity of the spectra with fura-2 alone (Figure 19, A) and in the presence of native Cu, Zn-SOD (Figure 19, B) indicated that there was no significant interactions of  $\text{Ca}^{2+}$  with native Cu, Zn-SOD. If specific  $\text{Ca}^{2+}$ -protein interactions were present, we anticipated that the dye only should be more blue shifted than that in the presence of protein at the same  $\text{Ca}^{2+}$  concentration. In the presence of 0.10 mM apo-SOD (Figure 19, C) the excitation spectra are slightly less blue shifted than for fura-2 only (Figure 19, A) indicating some weak interactions between  $\text{Ca}^{2+}$  and apo-SOD. Figure 20 shows that by increasing the concentration of apo-SOD the interactions with  $\text{Ca}^{2+}$  increase. In the presence of 0.30 mM apo-SOD (Figure 20, B) the blue shift is less than in the presence of 0.10 mM apo-SOD for the same  $\text{Ca}^{2+}$  concentrations (Figure 20, A). Moreover, the value of R (Table 13) indicated that there is no interactions of  $\text{Ca}^{2+}$  with native Cu, Zn-SOD, and that the interactions with apo-SOD increase upon increasing the concentration of protein. The lower R value indicated less blue shifting of the dye spectrum and less free  $\text{Ca}^{2+}$ , and therefore more  $\text{Ca}^{2+}$ -protein interactions.

**Figure 20** Fluorescence Excitation Spectra of 2  $\mu\text{M}$  Fura-2 in the presence of 0.10 mM (A) or 0.30 mM apo-SOD (B), in a solution containing 0.03 mM EGTA, 150 mM Tris-Cl, pH  $7.4 \pm 0.1$ . Spectra (a) to (e) correspond to the addition of 0.0, 30, 35, 43, and 60 nM  $\text{Ca}^{2+}$ .



**Table 13.** Fluorescence excitation ratios (R) at 340/380 of fura-2 in the absence and presence of Cu, Zn-SOD, and E, E-SOD as a function of  $\text{Ca}^{2+}$ .<sup>a</sup>

$[\text{Ca}^{2+}]/\text{nM}$	Fura-2 only	Cu, Zn-SOD <sup>b</sup>	E, E-SOD <sup>c</sup>	E, E-SOD <sup>d</sup>
0.00	0.493	0.502	0.467	0.509
15.0	0.714	0.698	0.659	0.547
30.0	1.536	1.418	1.096	0.661
35.0	2.649	2.514	1.417	0.738
43.0	6.537	9.886	2.337	1.017
46.0	10.01	11.358	3.076	1.292
60.0	13.81	13.598	11.223	3.663

<sup>a</sup>All solutions contained 0.03 mM EGTA, 150 mM Tris-Cl, pH  $7.4 \pm 0.1$ , and 2  $\mu\text{M}$  fura-

2. <sup>b</sup>The concentration of Cu, Zn-SOD is 0.10 mM. <sup>c,d</sup>The concentrations of E, E-SOD are 0.10 mM and 0.30 mM, respectively.



We have studied in detail the interactions of  $\text{Ca}^{2+}$  with apo-SOD. The results of a series of studies of apo-SOD are given in Table 14. The values of  $K_d$  and of the number of binding sites ( $n$ ) of apo-SOD are  $2.46 \pm 0.71 \mu\text{M}$  and  $0.18 \pm 0.07$ , respectively. The value of  $0.18 \pm 0.07$  might indicate that there was no specific  $\text{Ca}^{2+}$  binding site in the apo protein.

Similar experiments were conducted with native Cu, Zn-SOD and apo-SOD in the presence of  $\text{Mg}^{2+}$  using furaptra as the fluorophore indicator (Raju et al., 1989). There were no observable interactions with  $\text{Mg}^{2+}$  in the presence of either native Cu, Zn-SOD (0.10-0.36 mM) or apo-SOD (0.10 mM). Figure 21 shows the excitation spectra of furaptra in the absence (Figure 21, A) and in the presence of 0.30 mM apo-SOD (Figure 21, B) in 150 mM Tris-Cl, pH  $7.4 \pm 0.1$ . In the presence of 0.30 mM apo-SOD and for the same  $\text{Mg}^{2+}$  concentrations there was less of a blue shift relative to that in the absence of protein indicating very weak interactions of  $\text{Mg}^{2+}$  with apo-SOD. Attempts to quantify  $\text{Mg}^{2+}$ -SOD interactions were unsuccessful.

#### **IV.3.2. $^7\text{Li}$ and $^{23}\text{Na}$ NMR Studies of $\text{Li}^+$ and $\text{Na}^+$ Interactions with Native Cu, Zn-SOD**

Lithium ions are in fast exchange in the NMR time scale and hence the observed lithium signal is a weighted average of free and bound  $\text{Li}^+$ . As the  $\text{Li}^+$  nucleus has a narrow chemical shift range the chemical shifts do not change upon  $\text{Li}^+$  binding to substrates. However, the lithium spin-lattice relaxation time ( $T_1$ ) values are sensitive to

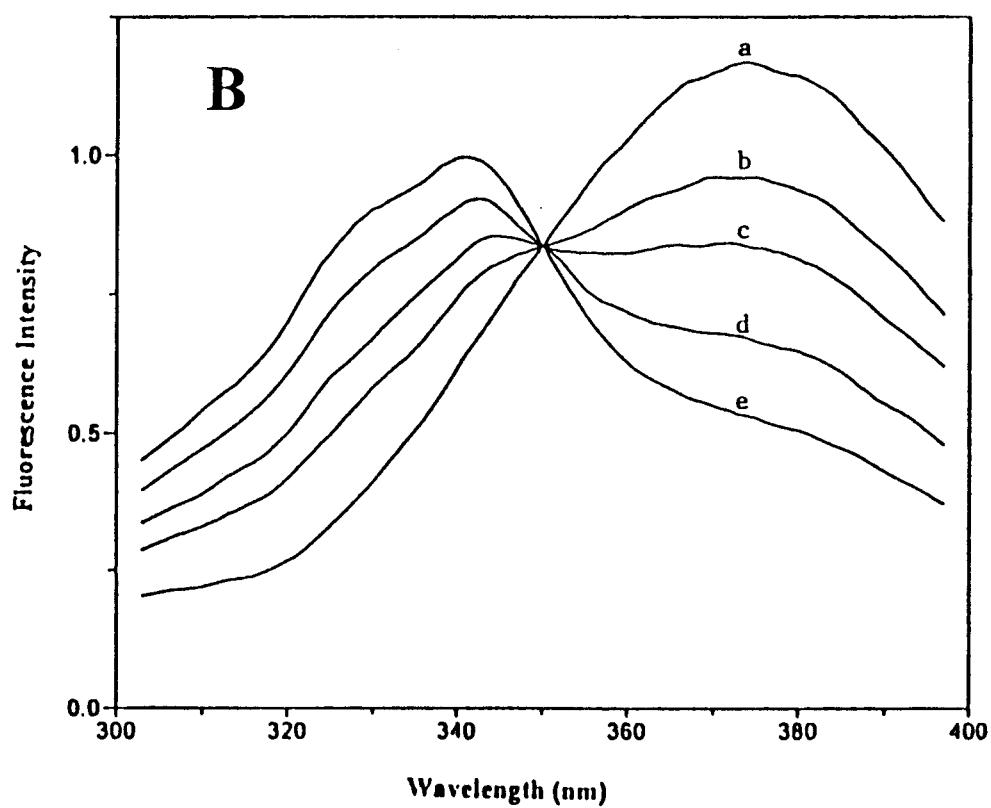
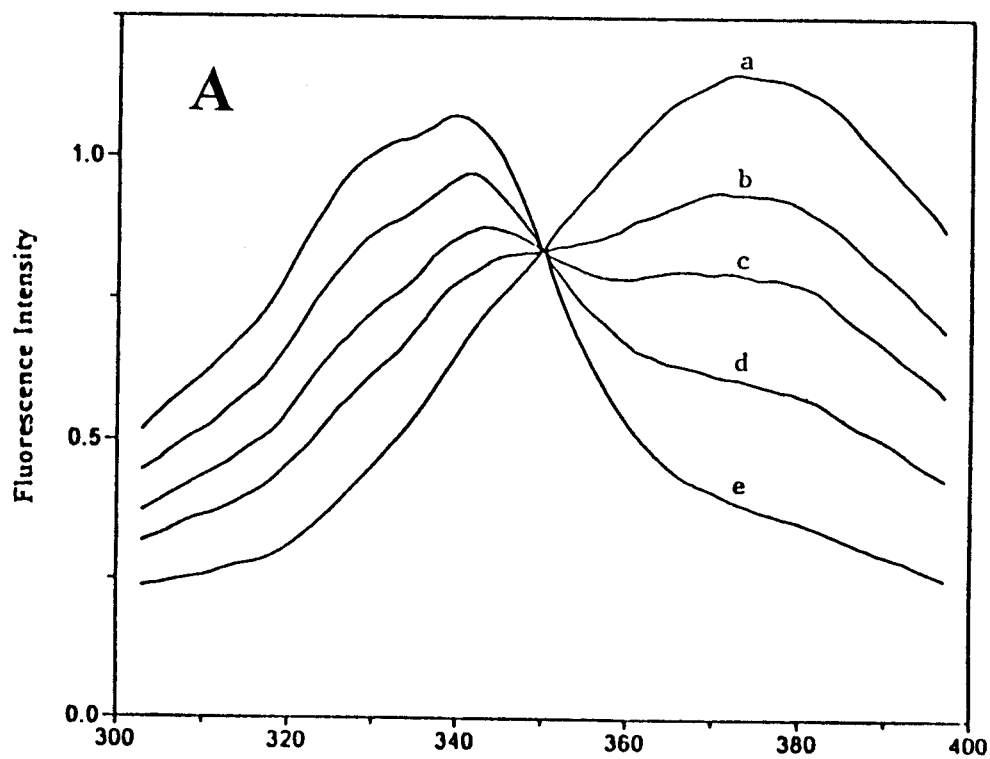
**Table 14.** Fluorescence-determined  $\text{Ca}^{2+}$  dissociation constants ( $K_d$ ), and the number of  $\text{Ca}^{2+}$  binding sites ( $n$ ) for apo protein (E, E-SOD).<sup>a</sup>

[protein]/ mM	$K_d$ / $\mu\text{M}$	$n$	$R^2$
0.10	2.39	0.30	0.98
0.18	2.19	0.15	0.91
0.18	2.56	0.24	0.99
0.18	3.29	0.18	0.99
0.30	1.07	0.12	0.99
0.30	2.77	0.15	0.99
0.30	2.98	0.10	0.98
AVG $\pm$ SD <sup>b</sup>	$2.46 \pm 0.71$	$0.18 \pm 0.070$	$0.97 \pm 0.03$

<sup>a</sup>All solutions contained 0.03 mM EGTA, 150 mM Tris-Cl, pH  $7.4 \pm 0.1$ , and 2  $\mu\text{M}$  fura-

2. <sup>b</sup>The average  $\pm$  standard deviation for 7 separate experiments.

**Figure 21** Fluorescence excitation spectra of 2  $\mu\text{M}$  furaptra only (A) and in the presence of 0.30 mM apo-SOD (B) in a solution containing 150 mM Tris-Cl, pH  $7.4 \pm 0.1$ . Spectra (a) to (e) correspond to the addition of 0.0, 1.0, 5.0, 10, and 20 mM  $\text{Mg}^{2+}$ .



motion with free nuclei having longer  $T_1$  values than tightly bound nuclei (Rong et al., 1993), and hence  $^7\text{Li}$   $T_1$  measurements provide good tools to monitor the interaction of  $\text{Li}^+$  with bio-molecules. Similarly,  $^{23}\text{Na}$   $T_1$  measurements were used to monitor the binding of  $\text{Na}^+$  to biomolecules.

The interactions of  $\text{Li}^+$  and  $\text{Na}^+$  with bovine Cu, Zn-SOD in its oxidized, native form were followed by the changes in the  $^7\text{Li}$  and  $^{23}\text{Na}$  NMR  $T_1$  values. The  $^7\text{Li}$  and  $^{23}\text{Na}$   $T_1$  relaxation times of  $\text{Li}^+$  and  $\text{Na}^+$  were obtained in the presence of 0.20 mM - 2.0 mM native Cu, Zn- SOD (Tables 15-18). There were slight changes in  $T_1$  values which were not significant even by increasing the concentration of native Cu, Zn-SOD (Table 17), or by increasing the  $\text{Li}^+$  concentration up to 278.5 mM (Table 15) or of  $\text{Na}^+$  up to 360 mM (Table 16) in 2.0 mM solutions of native Cu, Zn-SOD. The viscosity measurements indicate that there was no significant viscosity effect on the  $^7\text{Li}$   $T_1$  values even for high protein concentrations (Table 18). These observations indicate that there were no significant interactions of both  $\text{Li}^+$  and  $\text{Na}^+$  with native Cu, Zn-SOD.  $^7\text{Li}$  and  $^{23}\text{Na}$  NMR measurements for Glu-modified Cu, Zn-SOD were not attempted because we anticipated that the interactions of  $\text{Na}^+$  and  $\text{Li}^+$  with Glu-modified Cu, Zn-SOD would be even weaker than those with the native Cu, Zn-SOD, and NMR measurements would not be good tools to investigate such weak interactions.

**Table 15.**  $^7\text{Li}$   $T_1$  Relaxation Values for  $\text{Li}^+$ -containing solutions of Native Cu, Zn-SOD.<sup>a</sup>

$[\text{Li}^+]/\text{mM}$	$T_1/\text{s}$
2.0	$12.90 \pm 0.71$
4.0	$12.44 \pm 0.31$
6.0	$12.62 \pm 0.15$
8.0	$12.43 \pm 0.06$
20	$13.06 \pm 0.12$
40	$12.84 \pm 0.17$
60	$13.40 \pm 0.12$
100	$12.53 \pm 0.29$
150	$12.79 \pm 0.07$
200	$13.63 \pm 0.19$
287.5	$12.44 \pm 0.11$

<sup>a</sup>All samples contained 2.0 mM native SOD, in 20%  $\text{D}_2\text{O}$ ,  
0.2 M HEPES, pH 7.4, 0.1 mM EDTA, at 37 °C.

**Table 16.**  $^{23}\text{Na}$   $T_1$  Relaxation Values for  $\text{Na}^+$ -containing solutions of Native SOD.<sup>a</sup>

$[\text{Li}^+]/\text{mM}$	$T_1/\text{ms}$
2.0	$61.6 \pm 0.96$
4.0	$62.9 \pm 0.46$
6.0	$63.4 \pm 0.23$
8.0	$62.8 \pm 0.81$
12	$63.3 \pm 0.69$
16	$62.6 \pm 0.34$
20	$64.3 \pm 0.62$
24	$62.9 \pm 0.27$
40	$63.3 \pm 0.12$
80	$63.0 \pm 0.13$
160	$62.1 \pm 0.08$
360	$62.1 \pm 0.08$

<sup>a</sup>All samples contained 0.2 mM native SOD, in 20%  $\text{D}_2\text{O}$ ,

0.2 M HEPES, pH 7.4, at 37 °C.

**Table 17.**  $^7\text{Li}$   $T_1$  Relaxation Values for Native SOD with various enzyme concentrations.<sup>a</sup>

$[\text{Li}^+]/\text{mM}$	$T_1/\text{s}^b$	$T_1/\text{s}^c$
2.0	$18.41 \pm 0.82$	$16.55 \pm 0.82$
4.0	$19.36 \pm 0.29$	$16.87 \pm 0.45$
6.0	$19.40 \pm 0.35$	$16.26 \pm 0.18$
8.0	$18.49 \pm 0.08$	$16.87 \pm 0.26$

<sup>a</sup>All samples contained 20%  $\text{D}_2\text{O}$ , 0.2 M HEPES, pH 7.4, at 37 °C.

<sup>b</sup> $[\text{Native SOD}] = 0.50 \text{ mM}$ . <sup>c</sup> $[\text{Native SOD}] = 1.0 \text{ mM}$ .



**Table 18.**  $^7\text{Li}$   $T_1$  relaxation and viscosity values for  $\text{Li}^+$ -containing solutions- of native Cu, Zn-SOD.<sup>a</sup>

[SOD]/mM	$[\text{Li}^+]/\text{mM}$	$T_1/\text{s}$	Viscosity/cP
0.00	9.0	$22.8 \pm 0.10$	0.79
0.50	9.0	$18.80 \pm 0.07$	0.85
1.01	9.0	$16.94 \pm 0.23$	----- <sup>b</sup>
2.0	278.5	$12.44 \pm 0.11$	1.0

<sup>a</sup>All samples contained 20%  $\text{D}_2\text{O}$ , 0.20 M HEPES, pH 7.4, at 37 °C. <sup>b</sup>The viscosity was not measured for this solution.

## **CHAPTER V**

### **DISCUSSION**

#### **V.1. Preparation and Characterization of Glu-Modified Cu, Zn-SOD**

##### **V.1.1. Preparation and Determination of the Number of Glu-Modified**

##### **Residues in Glu-Modified Cu, Zn-SOD**

Glutamate-modified Cu, Zn-SOD was prepared by the reaction of bovine Cu, Zn-SOD with EDC in the presence of  $\text{NH}_4\text{Cl}$ . EDC is the most widely used reagent for the modification of carboxylate groups in proteins (Lundblad, 1991). A ratio of 2:1 of EDC: protein gave a maximum percentage yield of modified Cu, Zn-SOD (Figure 4, Table 4). The modified Cu, Zn-SOD was purified by FPLC (Figure 5, peak 2), and its purity was confirmed by agarose gel electrophoresis (Figure 6, lanes B & G). The number of modified glutamate residues in bovine Cu, Zn-SOD was estimated from agarose gel electrophoresis of Cu, Zn-SOD, E, Zn-SOD (E = Empty), and E, E-SOD. We plotted the charge (Getzoff et al., 1983; Sines et al., 1990) of Cu, Zn-SOD derivatives versus the distance moved; -4, -8, -12 were used as the estimated charges per dimer of Cu, Zn-SOD, E, Zn-SOD, and E, E-SOD at pH 7.4, respectively (Figure 7). The net charge per dimer of modified SOD at pH 7.4 was calculated to be zero indicating that two glutamate residues per monomer are modified.

Amino acid sequencing was attempted twice but failed to identify the Glu residues that were modified; this is probably due to the limitation of the stepwise Edman degradation which resulted from the blockage of the N-terminal of Gln (Glu→Gln) by reaction with aldehydes or isocyanate (Wittmann-Liebold, 1982).

### **V.1.2. Anionic Interactions with Glu-Modified Cu, Zn-SOD and Native Cu, Zn-SOD**

A small change in the UV/visible spectrum of bovine Cu, Zn-SOD was observed upon modification with EDC. The maximum of the d-d band of native Cu, Zn-SOD is located at  $680 \pm 4$  nm (Valentine & Mota de Freitas, 1985). Glu-modified Cu, Zn-SOD has a  $\lambda_{\max}$  value for the d-d transition at  $684 \pm 11$  nm. The small increase of  $\lambda_{\max}$  upon chemical modification indicated a small distortion around the  $\text{Cu}^{2+}$  occurred.

Addition of azide to modified Cu, Zn-SOD gave a new band at  $373 \pm 2$  nm (Figure 8). Similar results were obtained for binding of azide to native Cu, Zn-SOD (Bermingham-McDonogh et al., 1982). There is no change in the  $\lambda_{\max}$  value at  $373 \pm 2$  nm upon modification with EDC. The present results showed an increase in the binding between modified Cu, Zn-SOD and azide relative to that of native protein (Table 7). Therefore, the negatively charged groups at the entrance of the protein solvent channel play a key role in the binding of anions presumably by decreasing the localized negative charge at the entrance of the active site and thus increasing the electrostatic affinity for anions. Recently, Banci et al. (1993b) reported the essential role for the conserved Glu-133 (Glu-131 bovine)

residue in the anion ( $\text{N}_3^-$ ) interactions with human Cu, Zn-SOD. Our results with bovine Cu, Zn-SOD under similar experimental conditions are therefore consistent with those published for mutants of human Cu, Zn-SOD (Banci et al., 1993b; Getzoff et al., 1992).

Moreover, the binding constant of cyanide with Glu-modified Cu, Zn-SOD is higher than that of native Cu, Zn-SOD (Table 7). The increased electrostatic interactions of cyanide with modified Cu, Zn-SOD are consistent with the modification of Glu-130 and Glu-131 which are located at the rim of the active site entrance (Tainer et al., 1983; Getzoff et al., 1983).

Phosphate is known to bind to native Cu, Zn-SOD primarily via the guanidium group of arginine-141. The binding constant of phosphate with native SOD was  $28 \pm 2.0 \text{ M}^{-1}$ , at pH 7.0, in agreement with previously published data (Mota de Freitas et al., 1987). The binding constant of phosphate to Glu-modified protein was  $173 \pm 20 \text{ M}^{-1}$  (Table 7). The  $^{31}\text{P}$   $T_1$  relaxation time values of phosphate-containing solutions of Glu-modified Cu, Zn-SOD were smaller than those of phosphate-containing solutions of native Cu, Zn-SOD (Figure 10) also indicating a stronger interaction of phosphate with Glu-modified Cu, Zn-SOD relative to that with native Cu, Zn-SOD. The increase in phosphate affinity is in the same direction as that found with azide and cyanide.

The interactions of Glu-modified Cu, Zn-SOD with vanadate were characterized by  $^{51}\text{V}$  NMR spectroscopy.  $^{51}\text{V}$  NMR spectroscopy has been used to determine vanadate concentration in aqueous solutions, and allows for simultaneous detection and quantification of the different vanadate species in the solution (Crans & Simone, 1991; Wittenkeller et al., 1991).

Addition of either native or Glu-modified Cu, Zn-SOD to vanadate caused significant decreases in the intensities of the dimeric ( $V_2$ ) and tetrameric ( $V_4$ ) vanadate  $^{51}\text{V}$  NMR resonances (Figure 11, B&C). Much smaller changes were observed for the monomeric ( $V_1$ ) resonance. Similar results were reported for native Cu, Zn-SOD (Wittenkeller et al., 1991). At the same concentration (0.05 mM) of both native and modified SOD, the decreases in the intensities of the  $^{51}\text{V}$  NMR resonances of vanadate anions in the presence of Glu-modified Cu, Zn-SOD (Figures 11, C) were significantly larger than those observed in the presence of native Cu, Zn-SOD (Figure 11, B) indicating that the Glu-modified SOD derivative interacts most strongly with vanadate than native Cu, Zn-SOD. The concentration of vanadate bound to 0.05 mM Glu-modified Cu, Zn-SOD (0.03 mM) (Table 9) was also higher than that calculated (0.02 mM) for native Cu, Zn-SOD at the same protein concentration. Wittenkeller et al. (1991) reported that for bovine Cu, Zn-SOD the Lys-120, 134 residues are the major binding sites of vanadate. Our observations with the Glu-modified Cu, Zn-SOD are consistent with the modification of the Glu-130, 131 residues which are located at the entrance of the active site of the protein and are close to the Lys-120, 134 residues (Tainer et al., 1982 & 1983; Getzoff et al., 1983). Not surprisingly, a decrease in the negative charge of the protein resulted in an increase in its electrostatic interaction with vanadate.

On addition of increasing concentrations of Glu-modified Cu, Zn-SOD to a vanadate solution, the chemical shifts values of the vanadate species, namely  $V_1$ ,  $V_2$  and  $V_4$  did not show any significant changes (Table 8). Line width changes of the different vanadate species ( $V_1$ ,  $V_2$  and  $V_4$ ) in the presence of Glu-modified Cu, Zn-SOD (Table 8 and

Figure 12) indicate that the tetramer interacts most strongly with the enzyme derivative. In the presence of 0.003 mM - 0.015 mM Glu-modified Cu, Zn-SOD, the vanadate tetramer shows the largest line broadening (from 98.5 Hz to 707.2 Hz), while the monomer and dimer shows much smaller changes (96.2 Hz- 117.6 Hz for the monomer and 151.4 Hz - 242.8 Hz for the dimer). These trends are similar to those obtained for native Cu, Zn-SOD (Wittenkeller et al., 1991) but the extent to which the Glu-modified Cu, Zn-SOD interacts with vanadate is stronger, based on the observed effects on line widths of  $V_4$ . The intensities of the vanadate species decreased with increasing protein concentrations, the decrease being larger in the case of  $V_4$  (Figure 12). These changes were reflected in the concentrations of the vanadate species (Table 9). This observation along with the change in line width of  $V_4$  indicate that  $V_4$  interacts more strongly with the Glu-modified Cu, Zn-SOD. The interactions of vanadate with Glu-modified Cu, Zn-SOD are also in the same direction as azide, cyanide and phosphate.

The specific activity of Glu-modified Cu, Zn-SOD was similar to that of native SOD (Table 10). We anticipated that the specific activity of Glu-modified Cu, Zn-SOD would be slightly higher than that of native protein. Small increases in the activities of Glu-modified mutants of human Cu, Zn-SOD relative to that of the wild-type human Cu, Zn-SOD were reported (Banci et al., 1993b; Getzoff et al., 1992). The activity measurements for human SOD were, however, conducted by using a direct assay method (pulse radiolysis) whereas our activity measurements were made by using a less sensitive and indirect assay method. Because the rate of superoxide dismutation induced by bovine Cu, Zn-SOD is almost diffusion controlled, small variations in enzyme activity are difficult to measure.

The specific activities of both Glu-modified and native Cu, Zn-SOD increased by decreasing the concentration of phosphate indicating that phosphate is an inhibitor of bovine Cu, Zn-SOD. Moreover, the activity in the absence of phosphate, i.e, in HEPES buffer, pH 7.8 increased by 62 % relative to that measured with the regular activity assay (in 50 mM phosphate) (Table 10).

Electrostatic interactions play an important role in the catalytic mechanism of superoxide dismutase by Cu, Zn-SOD by attracting  $O_2^-$  to the cavity. The x-ray structure of bovine Cu, Zn-SOD showed that the Glu-130 and Glu-131 residues are located at the rim of the solvent channel and that they are water accessible (Getzoff et al., 1983). Studies of the charge residues near the active-site channel indicated that the largest angular changes in the electrostatic field are for Arg-141, Lys-134, and Glu-131 (Tainer et al., 1983). Glu-130 and Glu-131 have important roles in directing the long-range approach of  $O_2^-$  (Getzoff et al., 1983). Based on the crystal structure, Glu-130 and Glu-131 are expected to be the most reactive carboxylate residues in Cu, Zn-SOD toward the EDC reagent. Because Asp-122 is solvent inaccessible and Asp-81 is bound to  $Zn^{2+}$  ion and completely buried the modification of these two Asp residues at the active site is not likely. Therefore the Asp-122 and Asp-81 are inactive residues toward EDC. Moreover, the overall structure of bovine Cu, Zn-SOD is stabilized by an interlocked network of H-bonds, which decrease the reactivity of the remaining carboxylate groups from glutamate and aspartate residues present in Cu, Zn-SOD (Getzoff et al., 1983). The strong influence of electrostatic interactions upon modification of Glu-130 and Glu-131 was supported by the increase in the binding constant of azide the Glu-modified Cu, Zn-SOD. Azide binding, in particular, is considered

to be a reasonable model adduct for the characterization of Cu, Zn-SOD with the real substrate, superoxide (Banci et al., 1993b; Getzoff et al., 1992).

The change in the charge at the active-site solvent channel upon modification of Glu-130 and Glu-131 resulted in an increase in the anion affinity for azide, cyanide, phosphate, and vanadate, and in a small and yet insignificant increase in the SOD activity. Brownian calculations showed that the alternation of a single charge substantially affects the calculated reaction rates in the case of Arg-141, Lys-134, and Glu-131. Our experimental observations are also consistent with the reported Brownian calculations (Sines et al., 1990). Therefore modification of Glu-131 and Glu-130 has the most influence in the electrostatic interactions.

We conclude that the Glu-modified Cu, Zn-SOD was prepared with high degree of purity. The anion interaction studies showed that the binding of azide, cyanide, phosphate, and vanadate to Glu-modified Cu, Zn-SOD was larger than that for native Cu, Zn-SOD. These observations suggested that Glu-130 and Glu-131 are modified. The high reactivity of Glu-130 and Glu-131 was related to the location of the carboxyl side chain residues that are most exposed at the entrance of the solvent channel of the enzyme, and in the native protein structure are tied up in salt bridges with essential lysine residues. The critical location of these residues direct anions toward their binding sites located along the solvent channel of Cu, Zn-SOD.



## **V.2. Preparation and Characterization of the Vanadyl-SOD Derivative**

### **V.2.1. Preparation and EPR Spectra of the Vanadyl-SOD Derivative**

Vanadyl-SOD was prepared under a nitrogen atmosphere in 0.10 M HEPES at pH 7.4.  $\text{VO}^{2+}$  tends to be air oxidized as the pH is increased above 3.5. However, chelation tends to stabilize the +4 oxidation state, and slowing the oxidation process (Chasteen, 1983). The pH 7.4 was chosen to ensure that the N-atoms of the histidine residues at the vacant sites of native copper or zinc sites are unprotonated and are available for chelation with  $\text{VO}^{2+}$ . The HEPES buffer was chosen over other buffers, such as Tris-Cl or citrate, because of two reasons: a) addition of  $\text{VO}^{2+}$  to protein in HEPES buffer will not lead to the formation of a precipitate of  $\text{VO}(\text{OH})_2$  (Chasteen, 1983), b) HEPES has an appropriate buffering range, lack of affinity for metal ions, and steric bulk (Mota de Freitas & Valentine, 1984). Sodium dithionite was added in a ratio of 2:1 of  $\text{VO}^{2+}$ :apo-SOD to prevent rapid oxidation under alkaline conditions (Chasteen, 1981).

The very anisotropic frozen spectrum (Figure 13) is indicative of strong binding of the  $\text{VO}^{2+}$  ion to the protein moiety (Cannon & Chasteen, 1975); pentaquo vanadyl(IV) ion showed an isotropic X-band EPR spectrum (Chasteen, 1981). Based on the published spectrum of vanadyl-human serum transferrin by Cannon and Chasteen (1975), the undoubling of the resonance lines, specifically peaks (a) and (b) in Figure 13, is due to the magnetic equivalence of the  $\text{VO}^{2+}$  ion environments. This undoubling of the resonance lines rules out the possibility that  $\text{VO}^{2+}$  bound to both copper site and zinc site of the

same subunit. Usually, the doubling in the EPR lines indicates that more than one vanadyl environment exist (Cannon & Chasteen, 1975).

EPR spectroscopy titrations of apo-SOD with  $\text{VO}^{2+}$  have shown that two  $\text{VO}^{2+}$  ion bind strongly to apo-SOD. In Figure 14, plots of EPR signal height at the same instrument gain settings versus equivalents of  $\text{VO}^{2+}$  added show breaks at 2 equivalents per dimer of SOD, thus establishing a 1:1 complex per subunit. This means that apo-SOD exhibits a binding capacity of two  $\text{VO}^{2+}$  ions per protein dimer which is consistent with the occupation of  $\text{VO}^{2+}$  on one site per monomer.

Under similar experimental conditions, the titration of the zinc-only derivative with  $\text{VO}^{2+}$  ion does not lead to an increase in the intensities of peaks (a) and (b) in Figure 15. This observation indicated that the occupation of the zinc site prevents the binding of  $\text{VO}^{2+}$  to the copper site. This is not surprising, because occupation of the zinc site hinders metal ion binding at the copper site, especially in the mid-pH range (Valentine & Pantiliano, 1981).

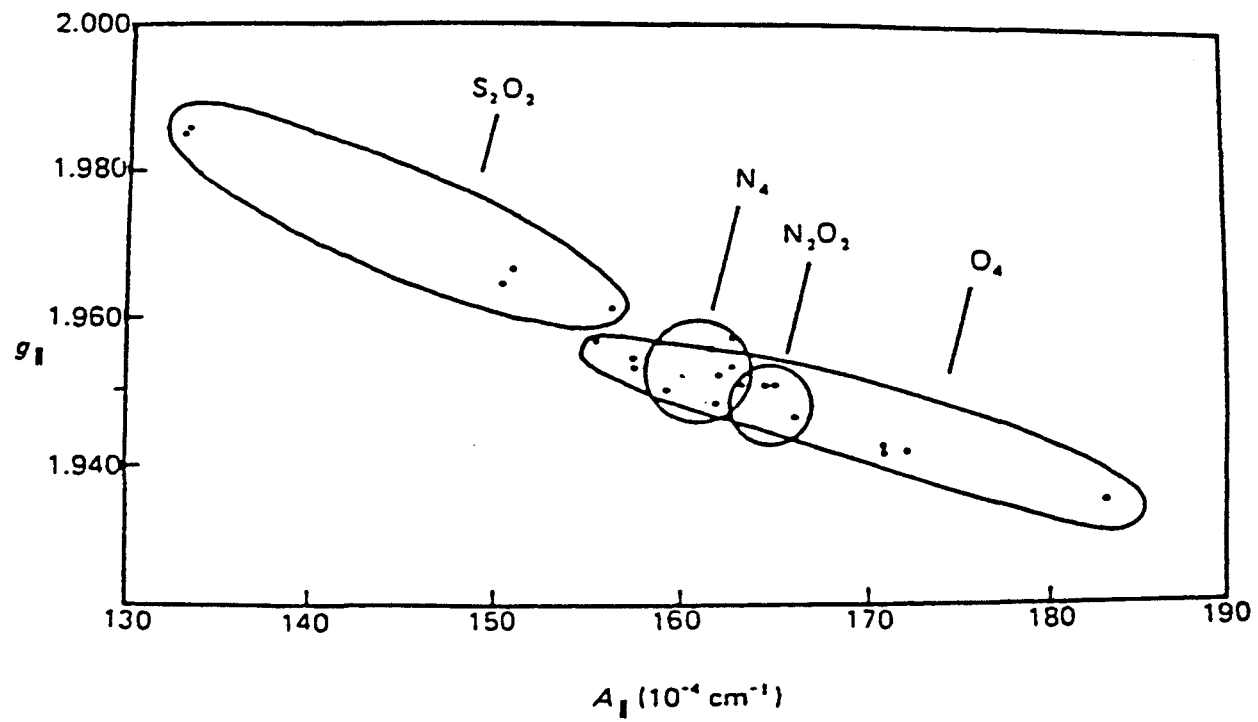
Furthermore, when  $\text{VO}^{2+}$  is added to a solution of native Cu, Zn-SOD, i.e, the protein is fully occupied by  $\text{Cu}^{2+}$  and  $\text{Zn}^{2+}$ , no vanadyl(IV) EPR spectrum is observed but a typical  $\text{Cu}^{2+}$  EPR spectrum was obtained (Figure 16). These observations indicated that the binding of  $\text{VO}^{2+}$  occurred at the copper site or zinc site in apo protein and not with unspecific negatively-charged residues in the protein. The absence of a vanadyl(IV) EPR spectrum is due to the fact that the uncomplexed  $\text{VO}^{2+}$  ion essentially exists as polymer of  $\text{VO}(\text{OH})_2$ , which is difficult to detect by EPR (Chasteen, 1981; Makinen & Mustafi, 1995).

The EPR parameters,  $g_{\parallel}$  and  $A_{\parallel}$ , can be taken as a measure of the average ligand environment on the in-plane ligand field, as reported by Chasteen (1981). Chasteen (1981) produced a plot of  $g_{\parallel}$  against  $A_{\parallel}$  for a number of vanadyl complexes of the type  $\text{VO}(\text{N}_4)$ ,  $\text{VO}(\text{O}_4)$ ,  $\text{VO}(\text{N}_2\text{O}_3)$ , and  $\text{VO}(\text{S}_2\text{O}_2)$  in aqueous frozen solutions (Figure 22). Our parameters for vanadyl-SOD (Table 11) are located in the  $\text{VO}(\text{N}_4)$  region which is evidence that the  $\text{VO}^{2+}$  ion is bound at the native copper site (4 histidine ligands). Moreover, a comparison of our parameters with the reported values for  $\text{VO}^{2+}$ -derivatives of carboxypeptidase A (with 2 histidines and 2 water ligands) and carbonic anhydrase (with 3 histidines and one water ligands), as well as the values obtained for the  $\text{VO}^{2+}$ -(imidazole)<sub>4</sub> complex, indicated that the  $\text{VO}^{2+}$  ion binds to the copper site. Furthermore, the  $A_{\parallel}$  value of vanadyl-SOD is  $163.4 \times 10^{-4} \text{ cm}^{-1}$  (Table 11) is in an  $A_{\parallel}$  range of  $120 \times 10^{-4}$  to  $180 \times 10^{-4} \text{ cm}^{-1}$  in which most biological matrices are observed (Cornman et al., 1995).

The binding constant obtained for the  $\text{VO}^{2+}$ -SOD complex  $6.8 \times 10^4 \text{ M}^{-1}$  was significantly smaller than that obtained for other  $\text{VO}^{2+}$  protein derivatives (see Table 11). The vanadyl ion prefers to coordinate to oxygen rather than to nitrogen ligands. The lower affinity of vanadyl for SOD is presumably related to its binding to four nitrogen ligands; conversely, the enhanced vanadyl binding to other metalloproteins is presumably associated with the larger number of oxygen ligands present at the vanadyl binding site.

The stability of the vanadyl-SOD was monitored by the EPR intensities of peaks (a) and (b) on Figure 17.

**Figure 22** Correlation between  $g_{\parallel}$  and  $A_{\parallel}$  values for various vanadyl(IV) complexes with equatorial ligand fields of the type  $\text{VO}(\text{O}_4)$ ,  $\text{VO}(\text{N}_2\text{O}_2)$ ,  $\text{VO}(\text{N}_4)$ , and  $\text{VO}(\text{S}_2\text{O}_2)$  in aqueous frozen (77 K) solution (adapted from Chasteen, 1981).



Exposing the vanadyl-SOD derivative to air resulted in a decrease of about 35% of the peak intensity indicating that some of vanadyl ion is oxidized. Once  $\text{VO}^{2+}$  is bound to apo-SOD, the  $\text{VO}^{2+}$  ion is therefore fairly stable to air oxidation.

### **V.2.2. Activity Assay of the Vanadyl-SOD Derivative**

We measured the activity of  $\text{VO}^{2+}$ -SOD, apo E, E-SOD, and native Cu, Zn-SOD in the presence of oxygen, as described by McCord and Fridovich (1969). The activity of the vanadyl-SOD derivative was also measured under a nitrogen atmosphere (Table 12). From a comparison of the activity of this derivative to other SOD derivatives, we conclude that the vanadyl-SOD derivative is SOD inactive. The vanadyl-carbonic anhydrase B derivative was also reported to have no esterase activity as opposed to native  $\text{Zn}^{2+}$ -containing carbonic anhydrase B (Fitzgerald & Chasteen, 1974).

### **V.2.3. Cyclic Voltammetry of the Vanadyl-SOD Derivative and of Native Cu, Zn-SOD**

Different values for the redox potentials of Cu, Zn-SOD have been published. Values of + 403 mV (St.Clair et al., 1992), +350 and +280 mV (Lawrence & Sawyer, 1979), +400 mV (Fee & DiCorleto, 1973) versus standard hydrogen electrode (SHE) at pH 7.0 were determined using either coulometric or visible spectroelectrochemical techniques, and + 320 mV, at pH 7.4 using cyclic voltammetry (Azab et al., 1992). Very

recently, a value of + 400 mV at pH 4.0 was reported by Verhagen et al. (1995) using cyclic voltammetry.

Our cyclic voltammetry studies of the vanadyl-SOD derivative (Figure 18, C) and native Cu, Zn-SOD (Figure 18, B) showed peak potential values of +425 mV and +300 mV, respectively. The reported peak value for native Cu, Zn-SOD at the same experimental pH conditions is +470 mV (Verhagen et al., 1995) (Figure 18, A). We were not able to reproduce a sharp anodic peak like the one published by Verhagen et al. (1995) (Figure 18, A). Even Verhagen et al. (1995) could not get a cathodic peak. In general, a sharp peak in the cyclic voltammogram is not common for proteins in which the active site is not located close to the protein surface; the strong adsorption of protein at the surface of the electrode and the denaturation of the protein prevent the observation of sharp peaks in the cyclic voltammogram (Armstrong, 1990).  $\text{Cu}^{2+}$  in bovine Cu, Zn-SOD is located at the bottom of a deep channel (Tainer et al., 1983). Furthermore, bovine Cu, Zn-SOD does not show direct electrochemistry due to strong adsorption of the protein on the surface of the electrode (Borsari & Azab, 1992). It is therefore not unusual to obtain a voltammogram of bovine Cu, Zn-SOD without sharp peaks. In contrast to bovine Cu, Zn-SOD, cytochromes have provided excellent demonstration of the ability of voltammetry to obtain acceptable quantitative data on protein redox equilibria due to a number of factors such as the exposure of the heme group to the solvent, and the location of  $\text{Fe}^{3+}$  at the surface of the protein (Armstrong, 1990).

We carried out cyclic voltammetry measurements with increasing scan rates (data not shown). We found that there was no significant improvement of the cyclic

voltammogram observed at higher scanning rates. Furthermore, we accurately polished the working glassy carbon electrode before each use with fine alumina (particle sizes about 0.075  $\mu\text{m}$ ), and treated it in a sonicator for a couple of minutes. We also performed experiments with increasing concentrations of protein or  $\text{Sc}^{3+}$  and did not find an improvement in the cyclic voltammogram.  $\text{Sc}^{3+}$  was used as a promoter for SOD electrochemistry as recommended by Verhagen et al. (1995).

### **V.3. Cationic Interactions with Glu-Modified Cu, Zn-SOD, Native Cu, Zn-SOD and Apo-SOD**

Fluorescence measurements were conducted to study the interactions of  $\text{Ca}^{2+}$  and  $\text{Mg}^{2+}$  with native Cu, Zn-SOD and apo-SOD using fura-2 and furaptra, respectively, as fluorophore indicators. Native Cu, Zn-SOD shows no significant interactions with  $\text{Ca}^{2+}$  (Figure 19, B) or with  $\text{Mg}^{2+}$ . Apo-SOD revealed stronger interactions with  $\text{Ca}^{2+}$  by increasing the protein concentration (Figure 20, B). The interactions of  $\text{Ca}^{2+}$  and  $\text{Mg}^{2+}$  with apo-SOD are due to the high negative charge of the apo-SOD at pH 7.4. At this pH, apo-SOD has a net negative charge of -12, whereas native Cu, Zn-SOD has a charge of -4 (Getzoff et al., 1983; Sines et al., 1990). We anticipated that the Glu-modified Cu, Zn-SOD (zero net charge) would show even lower affinity toward  $\text{Ca}^{2+}$  and  $\text{Mg}^{2+}$  relative to native Cu, Zn-SOD. Therefore, the interactions between Glu-modified Cu, Zn-SOD and  $\text{Ca}^{2+}$  or  $\text{Mg}^{2+}$  would not be observable under these experimental conditions.



$^7\text{Li}$  and  $^{23}\text{Na}$   $T_1$  relaxation measurements were conducted to investigate the interactions of sodium and lithium cations with native Cu, Zn-SOD. Tables 15-18 show that increasing the concentration of native Cu, Zn-SOD (0.20 - 2.0 mM) or of  $\text{Li}^+$  or  $\text{Na}^+$  ions did not result in significant changes in the  $T_1$  values. The viscosity of the three solutions: 9.0 mM LiCl alone, 9.0 mM LiCl with 0.50 mM native Cu, Zn-SOD and 287.5 mM LiCl with 2.0 mM native Cu, Zn-SOD were measured with a Brookfield Cone Plate viscometer, and found to be 0.79, 0.85, and 1.0 cP, respectively (Table 18). The small increase in the viscosity of the solution upon addition of protein is therefore not responsible for the small changes in the  $T_1$  values. These observations indicate that there were no significant interactions of  $\text{Li}^+$  and  $\text{Na}^+$  ions with native Cu, Zn-SOD. Therefore  $^{23}\text{Na}$  and  $^7\text{Li}$  NMR would not be good methods to study the anticipated weaker interactions of these cations with Glu-modified Cu, Zn-SOD relative to native protein.

#### V.4. CONCLUSIONS

From the studies conducted in this dissertation work, I conclude the following:

1. Glu-modified Cu, Zn-SOD can be prepared in 5.5 M  $\text{NH}_4\text{Cl}$  using a 2:1 ratio of EDC:SOD, and isolated with a high degree of purity using a FPLC system.
2. Anion interaction studies showed that the binding of azide, cyanide, phosphate, and vanadate to Glu-modified SOD was larger than for native SOD. These observations suggested that Glu-130, and Glu-131 are modified, and that these residues play critical roles in electrostatic steering of substrate toward the active site. In addition to

providing a better understanding of the enzyme mechanism, the enhanced biological activity of this derivative may have important physiological implications.

3. Native SOD shows no significant interactions with  $\text{Ca}^{2+}$ ,  $\text{Mg}^{2+}$ ,  $\text{Li}^+$ , and  $\text{Na}^+$  whereas apo SOD binds  $\text{Ca}^{2+}$  and  $\text{Mg}^{2+}$  weakly. The interactions of  $\text{Ca}^{2+}$ ,  $\text{Mg}^{2+}$ ,  $\text{Li}^+$ , and  $\text{Na}^+$  with Glu-modified Cu, Zn-SOD were not attempted because we anticipated that the interactions of these cations would be even weaker than those with native Cu, Zn-SOD. Cations at concentrations typically present in biological tissues do not interact with native Cu, Zn-SOD.
4. Vanadyl is bound to apo SOD at the  $\text{Cu}^{2+}$  site. This derivative is fairly stable to air oxidation and displays no SOD activity. The substitution of  $\text{Cu}^{2+}$  by vanadyl in native Cu, Zn-SOD provides a novel probe for the  $\text{Cu}^{2+}$  site of this enzyme which may be useful for future biophysical studies.

## REFERENCES

- Abernethy, J.L.; Steinman, H.M.; Hill, R.L.: Bovine erythrocyte superoxide dismutase. Subunit structure and sequence location of the intrasubunit disulfide bond J. Biol. Chem. **1974**, 249, 7339-7347.
- Argese, E.; Viglino, P.; Rotilio, G.; Scarpa, M.; Rigo, A.: Electrostatic control of the rate-determining step of the copper, zinc superoxide dismutase catalytic reaction. Biochemistry **1987**, 26, 3224-3228.
- Armstrong, F.A.: Probing metalloproteins by voltammetry. Struct. Bonding **1990**, 72, 137-221.
- Asmus, K.D.: Pulse radiolysis methodology. Methods Enzymol. **1984**, 105, 167-178.
- Azab, H.A.; Banci, L.; Borsari, M.; Luchinat, C.; Sola, M.; Viezzoli, M.S.: Redox chemistry of superoxide dismutase. cyclic voltammetry of wild-type enzymes and mutants on functionally relevant issues. Inorg. Chem. **1992**, 31, 4649-4655.
- Baily, D.B.; Ellis, P.D.; Fee, J.A.: Cadmium-113 nuclear magnetic resonance studies of cadmium substituted derivative of bovine superoxide dismutase. Biochemistry **1980**, 19, 591-596.
- Ballou, D.; Palmer, G.; Massey, V.: Direct demonstration of superoxide anion production during the oxidation of reduced flavin and of its catalytic decomposition by erythrocuprein. Biochem. Biophys. Res. Commun. **1969**, 36, 898-904.
- Banci, L.; Bertini, I.; Luchinat, C.; Scozzafava, A.: Nuclear relaxation in the magnetic coupled system Cu<sub>2</sub>Co<sub>2</sub>SOD. Histidine-44 is detached upon anion binding. J. Am. Chem. Soc. **1987**, 109, 2328-2334.
- Banci, L.; Bertini, I.; Luchinat, C.; Hallewell, R.A.: An investigation of superoxide dismutase Lys-143, Ile-143 and Glu-143 mutants: Cu<sub>2</sub>Co<sub>2</sub>SOD derivatives J. Am. Chem. Soc. **1988**, 110, 3629-3633.

- Banci, L.; Bertini, I.; Luchinat, C.; Scozzafava, A.: Cyanide and azide behave in a similar fashion versus cuprozinc-superoxide dismutase. J. Biol. Chem. **1989**, 264, 9742-9744.
- Banci, L.; Bertini, I.; Cabelli, D.; Hallewell, R.A.; Luchinat, C.; Viezzoli, M.S.: Investigation of copper-zinc superoxide dismutase Ser-137 and Ala-137 mutants. Inorg. Chem. **1990a**, 29, 2398-2403.
- Banci, L.; Bencini, A.; Bertini, I.; Luchinat, C.; Piccioli, M.:  $^1\text{H}$  NOE and ligand field studies of copper cobalt superoxide dismutase with anions. Inorg. Chem. **1990b**, 29, 4867-4873.
- Banci, L.; Bertini, I.; Turano, P.: An investigation of  $\text{Cu}_2\text{Zn}_2$  superoxide dismutase and its Ile-137 mutants at high pH. Eur. Biophys. J. **1991**, 19, 141-146.
- Banci, L.; Carloni, P.; La Penna, G.; Orioli, P.L.: Molecular dynamics studies on superoxide dismutase and its mutants: The structure and functional role of Arg 143. J. Am. Chem. Soc. **1992**, 114, 6994-7001.
- Banci, L.; Bertini, I.; Luchinat, C.; Viezzoli, M.S.: pH-dependence properties of SOD studies through mutants on Lys-136. Inorg. Chem. **1993a**, 32, 1403-1406.
- Banci, L.; Cabelli, D.E.; Getzoff, E.D.; Hallewell, R.A.; Viezzoli, M.S.: An essential role for the conserved Glu-133 in the anion interaction with superoxide dismutase. J. Inorg. Biochem. **1993b**, 50, 89-100.
- Banci, L.; Bertini, I.; Bruni, B.; Carloni, P.; Luchinat, C.; Mangani, S.; Orioli, P.L.; Ripniewski, W.; Wilson, K.S.: X-ray, NMR and molecular dynamics studies on reduced bovine superoxide dismutase: implications for the mechanism. Biochem. Biophys. Res. Commun. **1994a**, 202, 1088-1095.
- Banci, L.; Carloni, P.; Orioli, P.L.: Molecular dynamics studies on mutants of Cu, Zn superoxide dismutase: The functional role of charged residues in the electrostatic loop VII. Proteins **1994b**, 18, 216-230.
- Bannister, J.V.; Bannister, W.H.; Rotilio, G.: Aspects of the structure, function, and applications of superoxide dismutase. CRC Biochem. **1987**, 22, 111-180.
- Baran, E: Vanadyl(IV) complexes of nucleotides. Metal Ions in Biological Systems (Editors: Sigel, H.; Sigel, A.), Marcel Dekker, Inc., New York **1995**, 31, pp 129-146.

- Beem, K.M.; Richardson, D.C.; Rajagopalan, K.V.: Metal sites of copper-zinc superoxide dismutase. Biochemistry **1977**, 16, 1930-1936.
- Bermingham-McDonogh, O.; Mota de Freitas, D.; Kumamoto, A.; Saunders, J.E.; Blech, D. M.; Borders, C.L., Jr.; Valentine, J.S.: Reduced anion-binding affinity of Cu, Zn superoxide dismutase chemically modified at arginine. Biochem. Biophys. Res. Commun. **1982**, 108, 1376-1382.
- Bertini, I.; Borghi, E.; Luchinat, C.; Scozzafava, A.: Binding sites of anions in superoxide dismutase. J. Am. Chem. Soc. **1981**, 103, 7779-7783.
- Bertini, I.; Luchinat, C.; Monnanni, R.: Evidence of the breaking of the copper-imidazole bridge in copper cobalt-substituted superoxide dismutase upon reduction of the copper(II) center. J. Am. Chem. Soc. **1985a**, 107, 2178-2179.
- Bertini, I.; Lanini, G.; Luchinat, C.; Messori, L.; Monnanni, R.; Scozzafava, A.: Investigation of Cu<sub>2</sub>Co<sub>2</sub>SOD and its anion derivatives. <sup>1</sup>H NMR and electronic spectra. J. Am. Chem. Soc. **1985b**, 107, 4391-4396.
- Bertini, I.; Capozzi, F.; Luchinati, C.; Piccioli, M.; Viezzoli, M.S.: Assignment of active site proton in the <sup>1</sup>H NMR spectrum of reduced human Cu, Zn-SOD superoxide dismutase. Eur. J. Biochem. **1991**, 197, 691-697.
- Blackburn, N.J.; Hasnain, S.S.; Binsted, N.; Diakum, G.P.; Garner, C.D.; Knowles, P.F.: An extended-x-ray-absorption-structure study of bovine erythrocyte superoxide dismutase in aqueous solution. Direct evidence for three-co-ordinate Cu(I) in reduced enzyme. Biochem. J. **1984**, 219, 985-990.
- Blackburn, N.J.; Strange, R.W.; McFadden, L.M.; Hasnain, S.: Anion binding to bovine erythrocyte superoxide dismutase studies by x-ray absorption spectroscopy. A detailed structure analysis of the native enzyme and azido and cyano derivative using a multiple-scattering approach. J. Am. Chem. Soc. **1987**, 109, 7162-7170.
- Boden, N.; Holmes, M., C.; Knowles, P.F.: Properties of the cupric sites in bovine superoxide dismutase studies by nuclear-magnetic-relaxation measurements. Biochem. J. **1979**, 177, 303-309.
- Bogumil, R.; Hüttermann, J.; Kappl, R.; Stabler, R.; Sudfeldt, C.; Witzel, H.: Visible, EPR and electron nuclear double-resonance spectroscopic studies on the two metal-binding sites of oxovanadium(IV)-substituted D-xylose isomerase. Eur. J. Biochem. **1991**, 196, 305-312.

- Bollag, D.M.; Edelstein, S.J.: Protein Methods 1991, Wiley-Liss, New York, Chapter 3, pp 56-59.
- Bordo, D.; Djinovic, K.; Bolognesi, M.: Conserved patterns in the Cu, Zn-superoxide dismutase family. J. Biol. Chem. 1994, 238, 366-386.
- Borchelt, D.R.; Guarnieri, M.; Wong, P.C.; Lee, M.K.; Slunt, H.S.; Xu, Z.-S.; Sisodia, S.S.; Price, D.L.; Cleveland, D.W.: Superoxide dismutase 1 subunits with mutations linked to familial amyotrophic lateral sclerosis do not affect wild-type subunit function. J. Biol. Chem. 1995, 270, 3234-3238.
- Borsari, M.; Azab, H.A.: Voltammetry behaviour of bovine erythrocyte superoxide dismutase. Bioelectrochem. Bioenerg. 1992, 27, 229-233.
- Butler, A.; Danzitz, M.J.:  $^{51}\text{V}$  NMR as a probe of metal ion binding metalloproteins. J. Am. Chem. Soc. 1987, 109, 1864-1865.
- Butler, A.: The coordination and redox chemistry of vanadium in aqueous solution. Vanadium in Biological Systems (Editor: Chasteen, N.D.), Kluwer Academic Publishers, Dordrech/Boston/London, 1990, pp 25-49.
- Calabrese, L.; Rotilio, G.; Mondovi, B.: Cobalt erythrocuprein preparation and properties. Biochim. Biophys. Acta 1972, 267, 827-829.
- Cannon, J.C.; Chasteen, N.D.: Nonequivalence of the metal binding sites in vanadyl-labeled human serum transferrin. Biochemistry 1975, 14, 4573-4577.
- Carlsson, L.M.; Marklund, S.L.; Edlund, T.: The rate extracellular superoxide dismutase dimer is converted to a tetramer by exchange of a single amino acid. Proc. Natl. Acad. Sci. USA 1996, 93, 5219-5222.
- Carraway, K.L.; Koshland, D.E., Jr.: Carbodiimide modification of proteins. Methods Enzymol. 1972, 25, 616-623.
- Carrico, R.J.; Deutsch, H.F.: The presence of zinc in human cytocuprein and properties of the apoprotein. J. Biol. Chem. 1970, 245, 723-727.
- Cass, A.E.G.; Galdes, A.; Hill, H.A.O.; McCelland, C.F.; Storm, C.B.: Heavy metal binding to biological molecules. Identification of ligands by observation of  $^{199}\text{Hg}$ - $^1\text{H}$  NMR coupling. FEBS Lett. 1978, 95, 311-314.

- Chasteen, N.D.; DeKoch, R.J.; Rogers, B.L.; Hanna, M.W.: Use of the vanadyl(IV) ion as a new spectroscopic probe of metal binding of protein. Vanadyl insulin. Biochemistry **1973**, 95, 1301-1309.
- Chasteen, N.D.; Francavilla, J.: An electron paramagnetic resonance study of vanadyl(IV)-serum albumin complexes. J. Phys. Chem. **1976**, 80, 867-871.
- Chasteen, N.D.: Vanadyl (IV) EPR spin probes. Inorganic and organic aspects. Biological Magnetic Resonance (Editors: Berliner, L.J.; Reuben, J.), Plenum Press, New York, **1981**, 3, pp 53-119.
- Chasteen, N.D.: The biochemistry of vanadium. Struc. Bonding. **1983**, 53, 105-138.
- Chasteen, N.D.: Vanadyl (IV) electron nuclear double resonance/electron spin echo envelop modulation spin probes. Methods Enzymol. (Editors: Riodan, J.F.; Vallee, B.L.), Academic Press, San Diego, **1993**, pp 232-244.
- Chasteen, N.D.: Vanadium-Protein Interactions. Metal Ions in Biological Systems (Editors: Sigel, H.; Sigel, A.), Marcel Dekker, Inc., New York **1995**, 31, pp 231-247.
- Cocco, D.; Calabrese, L.; Finazzi-Agro, A.; Rotilio, G.: Electrostatic interactions in Cu, Zn-superoxide dismutase. Effects of Ca(II) and of anions not binding to the copper. Biochim. Biophys. Acta **1983**, 746, 61-64.
- Connors, K.A.: Optical absorption spectroscopy. Binding Constants Wiley & Sons, New York, **1987**, Chapter 4.
- Cornman, R.C.; Zovinka, E.P.; Boyajian, Y.D.; Geiser-Bush, K.M.; Boyle, P.D.; Singh, P.: Structural and EPR studies of vanadium complexes of deprotonated amide ligands: Effects on the  $^{51}\text{V}$  hyperfine coupling constant. Inorg. Chem. **1995**, 34, 4213-4219.
- Crans, D.C.; Shin, P.K.: Spontaneous and reversible interaction of vanadium (V) oxy anions with amine derivatives. Inorg. Chem. **1988**, 27, 1797-1806.
- Crans, D.C.; Bunch, R.L.; Theisen, L.A.: Interaction of trace level of vanadium (IV) and vanadium (V) in biological systems. J. Am. Chem. Soc. **1989a**, 111, 7597-7607.
- Crans, D.C.; Bunch, R.L.; Theisen, L.A.: Interaction of trace levels of vanadium(IV) and vanadium(V) in biological systems. J. Am. Chem. Soc. **1989b**, 111, 7597-7607.
- Crans, D.C.; Schelble, S.M.: Vanadate dimer and tetramer both inhibit glucose-6-phosphate dehydrogenase from *leuconostoc meseteroides*. Biochemistry **1990**, 29, 6698-6706.

- Crans, D.C.; Willging, E.M.; Butler, S.R.: Vanadate tetramer as the inhibition species in enzyme reaction in vitro and in vivo. J. Am. Chem. Soc. **1990**, 112, 427-432.
- Crans, D.C.; Simone, C.M.: Nonreductive interaction of vanadate with an enzyme containing a thiol group in the active site: Glycerol-3-phosphate dehydrogenase. Biochemistry **1991**, 30, 6734-6741.
- Crans, D.C.: Interaction of vanadates with Biogenic Ligands. Metal Ions in Biological Systems (Editors: Sigel, H.; Sigel, A.), Marcel Dekker, Inc., New York **1995**, 31, pp 147-209.
- Cremona, C.R.; Long, G.T.; Grammer, J.C.: Photocleavage of myosin subfragment 1 by vanadate. Biochemistry **1990**, 29, 7982-7990.
- Cudd, A.; Fridovich, I.: Electrostatic interactions in the reaction mechanism of bovine erythrocyte superoxide dismutase. J. Biol. Chem. **1982**, 257, 11443-11447.
- Cupane, A.; Leone, M.; Militello, V.; Stroppolo, M.E.; Polticelli, F.; Desideri, A.: Low-temperature optical spectroscopy of native and azide-reacted bovine Cu, Zn-SOD superoxide dismutase. A structural dynamics study. Biochemistry **1994**, 33, 15103-15109.
- DeKoch, R.J.; West, D.J.; Cannon, J.C.; Chasteen, N.D.: Kinetics and electron paramagnetic resonance spectra of vanadyl(IV) carboxypeptidase A. Biochemistry **1974**, 13, 4347-4354.
- Deng, H.-X.; Hentati, A.; Tainer, J.A.; Iqbal, Z.; Cayabyab, A.; Hung, W.-Y.; Getzoff, E.D.; Hu, P.; Herzfeldt, R.; Roos, R.P.; Warner, C.; Deng, G.; Soriano, E.; Smyth, C.; Parge, H.E.; Ahmed, A.; Roses, A.; Hallewell, R.A.; Pericak-Vance, M.A.; Siddique, T.: Amyotrophic Lateral Sclerosis and Structural defects in Cu, Zn superoxide dismutase. Science **1993**, 261, 1047-1051.
- Desideri, A.; Paci, M.; Rotilio, G.:  $^1\text{H}$  and  $^{31}\text{P}$  NMR studies of the binding of low affinity to Cu, Zn superoxide dismutase. J. Inorg. Biochem. **1988**, 33, 91-97.
- Desideri, A.; Falconi, M.; Polticelli, F.; Bolognesi, M.; Djinovic, K.; Rotilio, G.: Evolutionary conservativeness of electric field in the Cu, Zn superoxide dismutase active site. Evidence for co-ordinated mutation of charged amino acid residues. J. Mol. Biol. **1992**, 223, 337-342.
- Desvages, G.; Roustan, C.; Fattoum, A.; Pradel, L.-A.: Structure studies on yeast 3-phosphoglycerate kinase. Identification by immuno-affinity chromatography of one



residue essential for yeast 3-phosphoglycerate kinase activity. Its location in the primary structure. Eur. J. Biochem. **1980**, 105, 259-266.

Djinovic, K.; Gatti, G.; Coda, A.; Antolini, L.; Pelosi, G.; Desideri, A.; Falconi, M.; Marmocchi, F.; Rotilio, G.; Bolognesi, M.: Crystal structure of yeast Cu, Zn-SOD superoxide dismutase. Crystallographic refinement at 2.5 Å resolution. J. Mol. Biol. **1992a**, 225, 791-809.

Djinovic, K.; Coda, A.; Antolini, L.; Pelosi, G.; Desideri, A.; Falconi, M.; Rotilio, G.; Bolognesi, M.: Crystal structure solution and refinement of the semisynthetic cobalt-substituted bovine erythrocyte superoxide dismutase at 2.0 Å resolution. J. Mol. Biol. **1992b**, 226, 227-238.

Djinovic-Carugo, K.; Collyer, C.; Coda, A.; Carri, M.T.; Battistoni, A.; Bttaro, G; Polticelli, F.; Desideri, A.; Bolognesi, M.: Crystallization and preliminary crystallographic analysis of recombinant *Xenopus Laevis* Cu, Zn superoxide dismutase B. Biochem Biophys. Res. Commun. **1993**, 194, 1008-1011.

Djinovic-Carugo, K.; Polticelli, F.; Desideri, A.; Rotilio, G.; Wilson, K.S.; Bolognesi, M.: Crystallographic study of azide-inhibited bovine Cu, Zn superoxide dismutase. J. Mol. Biol. **1994**, 240, 179-183.

Eaton, S.S.; Eaton, G.R.: Biological application of EPR, ENDOR and ESEEM spectroscopy. Vanadium in Biological Systems (Editor: Chasteen, N.D.). Kluwer Academic Publishers, Dordrecht, **1990**, pp 190-222.

Ellerby, L.M.; Cabelli, D.E.; Graden, J.A.; Valentine, J.S.: Copper-zinc superoxide dismutase: Why not pH-dependent?. J. Am. Chem. Soc. **1996**, 118, 6556-6561.

Esch, F.S.; Bohlen, P.; Otsuka, A.S.; Yoshida, M.; Allison, W.S.: Inactivation of the bovine mitochondria F<sub>1</sub>-ATPase with dicyclohexyl[<sup>14</sup>C] carbodiimide leads to the modification of a specific glutamic acid residue in the β subunit. J. Biol. Chem. **1981**, 256, 9084-9089.

Evans, H.J.; Steinman, H.M.; Hill, R.L.: Bovine Erythrocyte superoxide dismutase. Isolation and characterization of tryptic, cyanogen bromide, and maleylated tryptic peptides. J. Biol. Chem. **1974**, 249, 7315-7325.

Fee, J.A.; Gaber, B.P.: Anion binding to bovine erythrocyte superoxide dismutase. Evidence for multiple binding sites with qualitatively different properties J. Biol. Chem. **1972**, 247, 60-65.

- Fee, J.A.: Studies on the reconstitution of bovine erythrocyte superoxide dismutase I. The presence of four divalent metal-binding sites on the apoprotein which are different from the native sites. Biochim. Biophys. Acta **1973a**, 295, 87-95.
- Fee, J.A.: Studies on the reconstitution of bovine erythrocyte superoxide dismutase. IV. Preparation and some properties of the enzyme in which Co(II) is substituted for Zn(II). J. Biol. Chem. **1973b**, 248, 4229-4234.
- Fee, J.A.; DiCorleto, P.E.: Observation on the oxidation-reduction potential of bovine erythrocyte superoxide dismutase. Biochemistry **1973**, 12, 4893-4899.
- Fee, J.A.; Pelsach, J.; Mims, B.: Superoxide dismutase. Examination of the metal binding sites by electron spin echo spectroscopy. J. Biol. Chem. **1981**, 256, 1910-1914.
- Fisher, C.L.; Cabelli, D.E.; Tainer, J.A.; Hallewell, R.A.; Getzoff, E.D.: The role of arginine 143 in the electrostatics and mechanism of Cu, Zn superoxide dismutase: Computational and experimental evaluation by mutational analysis. Protein **1994**, 19, 24-34.
- Fitzgerald, J.J.; Chasteen, N.D.: Electron paramagnetic resonance studies of the structure and metal ion exchange kinetics of vanadyl(IV) bovine carbonic anhydrase. Biochemistry **1974**, 13, 4338-4347.
- Fleer, E.A.; Herheu, H.M.; de Haas, G.H.: Modification of carboxylate groups in bovine pancreatic phosphate A<sub>2</sub>. Identification of aspartate as Ca<sup>2+</sup>-binding ligand. Eur. J. Biochem. **1981**, 113, 283-288.
- Forman, H.J.; Fridovich, I.: On the stability of bovine superoxide dismutase. The effects of metals. J. Biol. Chem. **1973**, 248, 2645-2649.
- Fridovich, I.: Superoxide radical and superoxide dismutases. Annu. Rev. Biochem. **1995**, 64, 97-112.
- Garner, C.D.; Collison, D.; Mabbs, F.E.: Methods for the spectroscopic characterization of vanadium centers in biological related chemical systems. Metal Ions in Biological Systems (Editors: Sigel, H.; Sigel, A.), Marcel Dekker, Inc., New York **1995**, 31, pp 617-670.
- George, G.N.; Coyle, C.L.; Hales, B.J.; Cramer, S.P.: X ray absorption of *Azotobacter vinelandii* vanadium nitrogenase. J. Am. Chem. Soc. **1988**, 110, 4057-4059.

- Getzoff, E.D.; Tainer, J.A.; Weiner, P.K.; Kollman, P.A.; Richardson, J.S.; Richardson, D.C.: Electrostatic recognition between superoxide and copper, zinc superoxide dismutase. Nature (London) **1983**, 306, 287-290.
- Getzoff, E.D.; Cabelli, D.E.; Fisher, C.L.; Parge, H.E.; Viezzoli, M.S.; Banci, L.; Hallewell, R.A.: Faster superoxide dismutase mutants designed by enhancing electrostatic guidance. Nature (London) **1992**, 358, 347-351.
- Goodon, C.C.: Inhibition of myosin ATPase by vanadate ion. Proc. Natl. Acad. Sci. U.S.A. **1979**, 76, 2620-2624.
- Grynkiewicz, G.; Poenie, M.; Tsien, R.Y.: A new generation of  $\text{Ca}^{2+}$  indicators with greatly improved fluorescence properties. J. Biol. Chem. **1985**, 260, 3440-3450.
- Hoare, D.G.; Koshland, D.C., Jr.: A procedure for the selective modification of carboxylate groups in proteins. J. Am. Chem. Soc. **1966**, 88, 2057-2058.
- Inouye, K.; Osaki, A.; Tonomura, B.: Dissociation of dimer of bovine erythrocyte Cu, Zn-superoxide dismutase and activity of the monomer subunit: Effects of urea, temperature, and enzyme concentration. J. Biochem. **1994**, 115, 507-515.
- James, T.L.; Noggle, J.H.: Na nuclear magnetic resonance relaxation studies of sodium ion interaction with soluble RNA. Proc. Natl. Acad. Sci. USA **1969**, 62, 644-649.
- Keele, B.B., Jr.; McCord, J.M.; Fridovich, I.: Superoxide dismutase from *Escherichia coli* B. A new manganese-containing enzyme. J. Biol. Chem. **1970**, 245, 6176-6181.
- Kitagawa, Y.; Tanaka, N.; Hata, R.; Kusunoki, M.; Lee, G.; Katsube, Y.; Aibara, S.; Morita, Y.: Three-dimensional structure of Cu, Zn-SOD dismutase from spinach at 2.0 Å resolution. J. Biochem. **1991**, 109, 447-485.
- Klapper, I.; Hagstrom, R.; Fine, R. Sharp, K.; Honig, B.: Focusing of electric field in the active site of Cu-Zn superoxide dismutase: Effects of ionic strength and amino acid modification. Protein **1986**, 1, 47-59.
- Klug, D.; Rabani, J.; Fridovich, I.: A direct determination of catalytic action of superoxide dismutase through the use of pulse radiolysis. J. Biol. Chem. **1972**, 247, 4839-4842.
- Kowaleski, J.; Nordenski, L.; Benetis, N.; Westund, P.O.: Theory of nuclear spin relaxation in paramagnetic systems in solution. Prog. Nucl. Mag. Reson. Spectrosc. **1985**, 17, 141-185.

- Kusthardt, U.; Hedman, B.; Hodgson, K.O.; Hahn, R.; Vilter, H.: High resolution XANES studies on vanadium containing haloperoxidase: pH-dependent and substrate binding. FEBS Lett. **1993**, 329, 5-8.
- Lawrence, G.D.; Sawyer, D.T.: Potentiometric titrations and oxidation-reduction potentials of manganese and copper-zinc superoxide dismutases. Biochemistry **1979**, 18, 3045-3050.
- Lewis, S.D.; Shafer, J.A.: Conversion of exposed aspartyl and glutamate residues in protein to asparaginylnyl and glutaminyl residues. Biochim. Biophys. Acta **1973**, 303, 284-291.
- Lowry, O.H.; Rosebrough, N.J.; Farr, A.L.; Bandall, R.J.: Protein measurement with the folin phenol reagent. J. Biol. Chem. **1951**, 193, 265-275.
- Linguist, R.N.; Lynn, J.L.; Lienhard, G.E.: Possible transition-state analogs for ribonuclease. The complex of uridine with oxovanadate(IV) ion and vanadate(V) ion. J. Am. Chem. Soc. **1973**, 95, 8762-8768.
- Lundblad, R.L.: The modification of carboxylate groups. Chemical Reagents for Protein Modification **1991**, CRC Press, Boca Raton, Florida, 2nd. Edn., pp 267-286.
- Mach, H.; Dong, Z.; Middaugh, C.R.; Lewis, R.V.: Conformational stability of Cu, Zn-superoxide dismutase, the apoprotein, and its zinc-substituted derivative: Second-derivative spectroscopy of phenylalanine and tyrosine residues. Arch. Biochem. Biophys. **1991**, 287, 41-47.
- Makinen, M.W.; Mustafi, D.: The vanadyl ion: Molecular structure of coordinating ligands by electron paramagnetic resonance and electron nuclear double resonance spectroscopy. Metal Ions in Biological Systems (Editors: Sigel, H.; Sigel, A.), Marcel Dekker, Inc., New York **1995**, 31, pp 89-127.
- Malinowski, P.D.; Fridovich, I.: Chemical modification of arginine at the active site of the bovine erythrocyte superoxide dismutase. Biochemistry **1979a**, 18, 5909-5917.
- Malinowski, D.P.; Fridovich, I.: Subunit association and side-chain reactivities of bovine erythrocyte superoxide dismutase in denaturing solvents. Biochemistry **1979b**, 18, 5055-5060.
- Mann, T.; Keilin, D.: Haemocuprein and heptacuprein, copper-protein compound of blood and liver in mammals. Proc. Roy. Soc. (London) Ser. B **1938**, 126, 303-315.

- Marmocchi, F.; Mavelli, I.; Rigo, A.; Stevanato, R.; Bossa, F.; Rotilio, G.: Succinylated copper, zinc superoxide dismutase. A novel approach to the problem of active subunits. Biochemistry **1982**, 21, 2853-2856.
- Marmocchi, F.; Argese, E.; Rigo, A.; Mavelli, I.; Rossi, L.; Rotilio, G.: A comparative study of bovine, porcine and yeast superoxide dismutase. Mol. Cell. Biochem. **1983**, 51, 161-164.
- Marklund, S.: Spectrophotometric study of spontaneous disproportionation of superoxide anion radical and sensitive direct assay for superoxide dismutase. J. Biol. Chem. **1976**, 251, 7504-7507.
- Matsuo, M.; Huagn, C.-H.; Huanng, L.C.: Modification and identification of glutamate residues at the arginine recognition site in the catalytic subunit of adenosine 3':5'-cyclic monophosphate-dependent protein kinase of rabbit skeletal muscle. Biochem. J. **1980**, 187, 371-379.
- McAdam, M.E.; Fielden, E.M.; Lavelle, F.; Calabrese, L.; Cocco, D.; Rotilio, G.: The involvement of the bridging imidazolate in the catalytic mechanism of bovine superoxide dismutase. Biochem. J. **1977a**, 167, 271-274.
- McAdam, M.E.: A consideration of the effects of added solute on the activity of bovine superoxide dismutase. Biochem. J. **1977b**, 161, 697-699.
- McCord, J.M.; Fridovich, I.: Superoxide dismutase. An enzymatic function for erythrocuprein (hemocuprein). J. Biol. Chem. **1969**, 244, 6049-6055.
- Mei, G.; Rosato, N.; Silivia, N., Jr, Ruch, R.; Gratton, E.; Sanini, I.; Finazzi-Agro, A.: Denaturation of human Cu/Zn superoxide dismutase by guanidine hydrochloride: A dynamic fluorescence study. Biochemistry **1992**, 31, 7224-7230.
- Ming, L.-J.; Valentine, J.S.: Preparation and characterization of  $\text{Cu}_2\text{Ni}_2$  and  $\text{Ag}_2\text{Ni}_2$  superoxide dismutase. Two new metal-substituted derivatives. J. Am. Chem. Soc. **1987**, 109, 4426-4428.
- Ming, L.-J.; Banci, L.; Luchinat, C.; Bertini, I.; Valentine, J.S.: NMR study of cobalt(II)-substituted yeast and human copper-zinc superoxide dismutase. Inorg. Chem. **1988**, 27, 728-733.
- Ming, L.-J.; Valentine, J.S.: NMR studies of nickel(II)-substituted derivative of bovine copper-zinc superoxide dismutase with nickel(II) bound in the copper site. J. Am. Chem. Soc. **1990a**, 112, 6374-6383.

- Ming, L.-J.; Valentine, J.S.: NMR studies of cobalt(II)-substituted derivative of bovine copper-zinc superoxide dismutase. Effects of pH, phosphate, and metal migration. J. Am. Chem. Soc. **1990b**, 112, 4256-4264.
- Morgenstren-Badaran, I.; Cocco, D.; Desideri, A.; Rotilio, G.; Jordano, J.; Dupre, N.: Magnetic susceptibility studies of the native cupro-zinc superoxide dismutase and its cobalt substituted derivatives. Antiferromagnetic coupling in the imidazolate-bridged copper(II)-cobalt(II) pair. J. Am. Chem. Soc. **1986**, 108, 300-302.
- Morpurgo, L.; Giovagnoli, C.; Rotilio, G.: Studies of the metal sites of copper protein. V. A model compound for the copper site of superoxide dismutase. Biochim. Biophys. Acta **1973**, 322, 204-210.
- Mota de Freitas, D.; Valentine, J.S.: Phosphate is an inhibitor of copper-zinc superoxide dismutase. Biochemistry **1984**, 23, 2079-2082.
- Mota de Freitas, D.; Luchinat, C.; Banci, L.; Bertini, I.; Valentine, J.S.:  $^{31}\text{P}$  NMR study of the interaction of inorganic phosphate with bovine copper-zinc superoxide dismutase. Inorg. Chem. **1987**, 26, 2788-2791.
- Mota de Freitas, D.; Ming, L.-J.; Ramasamy, R.; Valentine, J.S.:  $^{35}\text{Cl}$  and  $^1\text{H}$  NMR study of anion binding to reduced bovine copper-zinc superoxide dismutase. Inorg. Chem. **1990**, 29, 3512-3518.
- Mulks, C.K.; Kirste, B.; Willigen, H.V.: ENDOR study of  $\text{VO}^{2+}$ -Imidazole complexes in frozen aqueous solution. J. Am. Chem. Soc. **1982**, 104, 5906-5911.
- Nieves, J.; Kim, L.; Puett, D.; Echegoyen, L.: Electron spin resonance of calmodulin-vanadyl complexes. Biochemistry **1987**, 26, 4523-4527.
- Ogihara, N.L.; Parge, H.E.; Hart, P.J.; Weiss, M.S.; Goto, J.J.; Crane, B.R.; Tsang, J.; Slater, K.; Roe, J.A.; Valentine, J.S.; Eisenberg, D.; Tainer, J.A.: Unusual trigonal-planar copper configuration revealed in the atomic structure of yeast copper-zinc superoxide dismutase. Biochemistry **1996**, 35, 2316-2321.
- Omar, A.B.; Flores, S.C.; McCord, J.M.: Superoxide dismutase: Pharmacological developments and applications. Advanc. Pharma. **1992**, 23, 109-161.
- O'Neill, P.; Daves, S.; Fielden, E.M.; Calabrese, L.; Capo, C.; Marmocchi, F.; Natoli, G.; Rotilio, G.: The effects of pH and various salts upon the activity of a series of superoxide dismutase. Biochem. J. **1988**, 251, 41-46.

- Paci, M.; Desideri, A.; Rotilio, G.: Cyanide binding to Cu, Zn superoxide dismutase. An NMR study for Co(II) derivative. J. Biol. Chem. **1988**, 263(1), 162-166.
- Pantoliano, M.W.; McDonnell, P.J.; Valentine, J.S.: Reversible loss of metal ions from the zinc bind site of copper-zinc superoxide dismutase. The low pH transition. J. Am. Chem. Soc. **1979**, 101, 6454-6456.
- Pantoliano, M.W.; Valentine, J.S.; Mammone, R.J.; Scholler, D.M.: pH dependence of metal ion binding to the native zinc site of bovine erythrocuprein (superoxide dismutase). J. Am. Chem. Soc. **1982**, 104, 1717-1723.
- Parge, H.E.; Hallewell, R.A.; Tainer, J.: Atomic structure of wild-type and thermostable mutant recombinant human Cu, Zn-SOD superoxide dismutase. Proc. Natl. Acad. Sci. U.S.A. **1992**, 89, 6109-6113.
- Pho, D.B.; Roustan, C.; Tot, A.N.T.; Pradel, L.-A.: Evidence for glutamyl residue in yeast hexokinase. Biochemistry **1977**, 16, 4533-4537.
- Polticelli, F.; Bottaro, G.; Battistoni, A.; Carri, M.T.; Djinovic-Carugo, K.; Bolognesi, M.; O'Neill, P.; Rotilio, G.; Desideri, A.: Modulation of the catalytic rate of Cu, Zn-SOD superoxide dismutase in single and double mutants of conserved positively and negatively charged residues. Biochemistry **1995**, 34, 6043-6049.
- QUANTA96: Computational results obtained using software programs from Molecular Simulations distance calculations were done with the QUANTA96 and graphical displays and printed out from the QUANTA96 molecular modeling system.
- Rabizadeh, S.; Gralla, E.B.; Borchelt, D.R.; Gwinn, R.; Valentine, J.S.; Sisodia, S.; Wong, P.; Lee, M.; Hahn, H.; Bredesen, D.E.: Mutations associated with amyotrophic lateral sclerosis convert superoxide dismutase from an antiapoptotic to a proapoptotic gene: Studies in yeast and neural cells. Proc. Natl. Acad. Sci. USA **1995**, 92, 3024-3028.
- Raju, B.; Murphy, E.; Levy, L.A.; Hall, R.D.; London, R.E.: A fluorescence indicator for measuring cytosolic free magnesium. Am. J. Physiol. **1989**, 256, C540-C548.
- Rehder, D.: Bio;ogical applications of <sup>51</sup>V NMR spectroscopy. Vanadium in Biological systems (Editor: Chasteen, N.D.), Kluwer Academic Publishers, Dordrech/Boston/London, **1990**, pp 173-197.
- Rehder, D.; Holst, H.; Pribsch, W.; Vilter, H.: Vanadate dependent bromo/iodoperoxidase from *Ascophyllum nodisum* also contains unspecific low-affinity binding sites for

vanadate(V): A  $^{51}\text{V}$  NMR investigation, including the model peptides Phe-Glu and Glu-Tyr. J. Inorg. Biochem. **1991**, 41, 171-185.

Rehder, D.; Structure and function of vanadium compounds in living organisms. BioMetals **1992**, 5, 3-12.

Roe, J.A.; Butler, A.; Scholler, D.M.; Valentine, J.S.: Differential scanning calorimetry of Cu, Zn superoxide dismutase, the apoprotein and its zinc-substituted derivatives. Biochemistry **1988**, 27, 950-958.

Roe, J.A.; Peoples, R.; Scholler, D.M.; Valentine, J.S.: Silver-binding properties of bovine cuprozinc superoxide dismutase and the overall stability of selected metal-ion derivatives. J. Am. Chem. Soc. **1990**, 112, 1538-1545.

Rong, Q.; Espanol, M.; Mota de Freitas, D.; Geraldles, C.F.G.C.:  $^7\text{Li}$  NMR relaxations studiey of  $\text{Li}^+$  binding in human erythrocyte. Biochemistry **1993**, 32, 13490-13498.

Rosen, D.R.; Siddique, T.; Patterson, D.; Figlewicz, D.A.; Sapp, P.; Hentati, A.; Donaidson, D.; Goto, J.; O'Regan, J.P.; Deng, H.-X.; Rahmani, Z.; Krizus, A.; McKenna-Yasek, D.; Annarueber, C.; Gaston, S.M.; Berger, R.; Tanzi, R.E.; Halperin, J.J.; Herzfeldt, B.; Bergh, R.V.D.; Hung, W.-Y.; Bird, T.; Deng, G.; Mulder, D.W.; Smyth, C.; Laing, N.G.; Soriamo, E.; Pericak-Vance, M.A.; Haines, J.; Roulleau, G.A.; Gusella, J.S.; Horvitz, H.R.; Brown, R.H., Jr.: Mutation in Cu/Zn superoxide dismutase gene are associated with familial amyotrophic lateral sclerosis. Nature (London) **1993**, 362, 59-62.

Rotilio, G.; Bray, R.C.; Fielden, E.M.: A pulse radiolysis study of superoxide dismutase. Biochim. Biophys. Acta **1972a**, 268, 605-609.

Rotilio, G.; Morpurgo, L.; Giovgnoli, C.; Calabrese, L.; Mondovi, B.: Studies of the metal site of copper protein. Symmetry of copper in bovine superoxide dismutase and its functional significance. Biochemistry **1972b**, 11, 2187-2192.

Rotilio, G.; Calabrese, L.; Mondovi, B.; Blumber, W.E.: Electron paramagnetic resonance studies of cobalt-copper bovine superoxide dismutase. J. Biol. Chem. **1974**, 249, 3157-3160.

Rypniewski, W.R.; Magani, S.; Bruni, B.; Orioli, P.L.; Casati, M.; Wilson, K.S.: Crystal structure of reduced bovine erythrocyte superoxide dismutase at 1.9 Å resolution. J. Biol. Chem. **1995**, 251, 282-296.



- Sakurai, H.; Nishida, M.; Kida, K.; Koyama, M.; Tada, J.: Determination and characterization of vanadium ion in serum albumins. Inorg. Chim. Acta **1987**, 138, 149-153.
- Salin, M.L.; Wilson, W.W.: Porcine superoxide dismutase. Isolation and characterization of a relatively basic cuperozinc enzyme. Mol. Cell. Biochem. **1981**, 36, 157-161.
- Saponja, J.A.; Vogel, H.J.: Metal-ion binding properties of the transferrins: A vanadium-51 NMR study. J. Inorg. Biochem. **1996**, 62, 253-270.
- Segel, I.H. Enzyme Kinetics Wiley & Sons, Wiley Classic Library Edition, **1993**, pp 218-225.
- Selbin, J.: The chemistry of oxovanadium(IV). Chem. Rev. **1965**, 65, 153-175.
- Selbin, J.: Oxovanadium(IV) complexes. Coord. Chem. Rev. **1966**, 1, 293-314.
- Shah V.K.; Brill, W.J.: Isolation of an iron-molybdenum cofactor from nitrogenase. Proc. Natl. Acad. Sci. USA **1977**, 74, 3249-3253.
- Sines, J.J.; Allison, S.A.; McCammon, J.A.: Point charge distribution and electrostatic steering in enzyme/ substrate encounter: Brownian dynamics of modified copper/ zinc superoxide dismutases. Biochemistry **1990**, 29, 9403-9412.
- St.Clair, C.S.; Gray, H.B.; Valentine, J.S.: Spectroelectrochemistry of copper-zinc superoxide dismutase. Inorg. Chem. **1992**, 31, 925-927.
- Steinman, H.M.; Naik, V.R.; Abernethy, J.L.; Hill, R.L.: Bovine erythrocyte superoxide dismutase. complete amino acid sequence. J. Biol. Chem. **1974**, 249, 7326-7338.
- Stellwagen, E.; Wilgus, H. Biochemistry of Thermophily Friedman S.M., Ed., Academic Press, New York, **1978**, pp 223-232.
- Tainer, J.A.; Getzoff, E.D.; Beem, K.M.; Richardson, J.S.; Richardson, D.C.: Determination and analysis of the 2 Å structure of copper, zinc superoxide dismutase. J. Mol. Biol. **1982**, 160, 181-217.
- Tainer, J.A.; Getzoff, E.D.; Richardson, J.S.; Richardson, D.C.: Structure and mechanism of copper, zinc superoxide dismutase. Nature (London) **1983**, 306, 284-286.

- Valentine, J.S.; Pantoliano, M.W.; McDonnell, P.J.; Burger, A.R.; Lippard, S.J.: pH-dependent migration of copper(II) to vacant zinc-binding site of zinc-free bovine erythrocyte superoxide dismutase. Proc. Natl. Acad. Sci. USA **1979**, 76, 4245-4249.
- Valentine, J.S.; Pantoliano, M.W.: Protein-metal ion interactions in cuprozinc protein (superoxide dismutase). Copper Proteins (Editor: Spiro, T.G.), Wiley, New York, **1981**, pp 291-358.
- Valentine, J.S.; Mota de Freitas, D.: Copper-zinc superoxide dismutase. A unique biological "Ligand" for bioinorganic studies. J. Chem. Educ. **1985**, 62, 990-997.
- Valentine, J.S.; Mota de Freitas, D.: NMR studies of the anion binding sites of oxidized and reduced bovine copper-zinc superoxide dismutase in superoxide and superoxide dismutase chemistry. Biology and Medicine (Editor: Rolilio, G.), Elsevier, Amsterdam, **1986**, 149-154.
- VanEtten, R.L.; Waymack, P.P.; Rehkop, D.M.: Transition metal inhibition of enzyme-catalyzed phosphate ester displacement reactions. J. Am. Chem. Soc. **1974**, 96, 6782-6785.
- Verhagen, M.; Meussen, E.; Hagen, W.: On the reduction potentials of Fe and Cu-Zn containing superoxide dismutase. Biochim. Biophys. Acta **1995**, 1244, 99-103.
- Wang, T.-T.; Young, N.M.: Modification of aspartate acid residues to induce trypsin cleavage. Anal. Biochem. **1978**, 91, 696-699.
- Wever, R.; Kustin, K.: Vanadium: A biologically relevant element. Advanc. Inorg. Chem. **1990**, 35, 81-115.
- Wittenkeller, L.; Abraha, A.; Ramasamy, R.; Mota de Freitas, D.; Theisen, L.; Crans, D.C.: Vanadate interaction with bovine Cu, Zn-superoxide dismutase as probed by <sup>51</sup>V NMR spectroscopy. J. Am. Chem. Soc. **1991**, 113, 7872-7881.
- Wittmann-Liebold, B. Methods in Protein sequencing analysis. (Editor: Elzinga, M.), Humana Press, Clifton, New Jersey, **1982**, pp 27-63.
- Yamada, H.; Imoto, T.; Fujita, K.; Okazaki, K.; Motomura, M.: Selective modification of aspartic acid-101 in lysozyme by carbodiimide reaction. Biochemistry **1981**, 20, 4836-4842.
- Yost, F.J., Jr.; Fridovich, I.: An iron-containing superoxide dismutase from Escherichia coli. J. Biol. Chem. **1973**, 248, 4905-4908.

## **VITA**

### **HANAN A. HASAN QASEER**

The author was born in Irbid, Jordan from Lebanese parents. She obtained a Bachelor of Science degree in Chemistry from Yarmouk University (Jordan) in 1983 and a Master of Science degree from the same school in 1986. She was supported by a Ministry of Education Scholarship, Jordan from 1979 until 1983. She received two golden watches awards from King Hussein (King of Jordan) for her superiority in Chemistry in 1983 and 1986. She worked as an instructor in the Department of Chemistry from 1983 until 1992. She was awarded a graduate assistantship in the Fall of 1992 by the Graduate School and the Department of Chemistry, Loyola University of Chicago. She was supported by a research assistantship from January 1995 until August 1995 by a grant awarded to Professor Duarte Mota de Freitas. She will join the department of chemistry at Mu'tah University in 1997 as an assistant professor of chemistry.

## DISSERTATION APPROVAL SHEET

The dissertation submitted by Hanan A. Hasan has been read and approved by the following committee:

Duarte Mota de Freitas, Ph.D., Director  
Professor, Chemistry  
Loyola University Chicago

Patrick M. Henry, Ph.D.  
Professor, Chemistry  
Loyola University Chicago

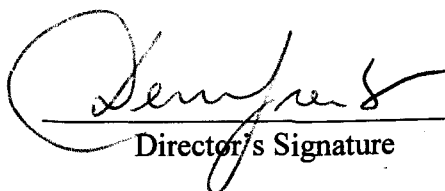
David S. Crumrine, Ph.D.  
Associate Professor, Chemistry  
Loyola University Chicago

Mir Shamsuddin, Ph.D.  
Associate Professor, Medicine  
Northwestern University

The final copies have been examined by the director of the committee and the signature which appears below verifies the fact that any necessary changes have been incorporated and that the dissertation is now given final approval by the committee with reference to content and form.

The dissertation is, therefore, accepted in partial fulfillment of the requirements for the degree of doctor of philosophy.

12/31/96  
Date

  
Director's Signature